Title	Spatial and temporal changes in the plankton community in the western Arctic Ocean
Author(s)	Matsuno, Kohei
Citation	Memoirs of the Faculty of Fisheries Sciences, Hokkaido University, 56(2): 65-107
Issue Date	2014-12
DOI	10.14943/mem.fish.56.2.65
Doc URL	http://hdl.handle.net/2115/57515
Right	
Type	bulletin (article)
Additional Information	
File Information	mem.fish.56.2.65.pdf

DOI 10.14943/mem.fish.56.2.65

Spatial and temporal changes in the plankton community in the western Arctic Ocean

Kohei MATSUNO[1)2)]

(2014年4月18日受付，2014年6月2日受理)

Table of contents

[1)] *Laboratory of Marine Biology (Plankton Laboratory), Division of Marine Bioresource and Environmental Science, Graduate School of Fisheries Science, Hokkaido University, 3-1-1 Minato-cho, Hakodate, Hokkaido, 041-8611, Japan (e-mail: k.matsuno@fish.hokudai.ac.jp)*
(北海道大学大学院水産科学研究院海洋生物資源科学部門海洋生物学分野浮遊生物学領域)

[2)] *Present address: Arctic Environmental Research Center, National Institute of Polar Research, 10-3 Midori-cho, Tachikawa, Tokyo, 190-8518, Japan*
(現所属: 国立極地研究所北極観測センター)

Key words: Arctic Ocean, Copepods, Mesozooplankton, Microplankton, Pacific water, Sea ice, Spatial distribution

1. Preface

The Arctic Ocean covers approximately 14×10^6 km^2 and is a semi-closed sea surrounded by Eurasia, North America and Greenland (Fig. 1a). The Arctic Ocean is covered by sea ice from autumn to spring, and the ice-covered area varies seasonally. Every year, the area covered by sea ice is the smallest in September. The average ice-cover area in September has decreased annually from 7.5×10^6 km^2 in the 1980s to 6.8×10^6 km^2 in the 1990s and 5.7×10^6 km^2 in the 2000s (Fig. 1b). In 2012, the ice-covered area was the lowest ever recorded, 3.7×10^6 km^2, which is only 50% of the ice-covered area during the 1980s.

The reduction of the area of sea ice in the Arctic Ocean has been remarkable in the Pacific sector (western Arctic Ocean) (Fig. 1c) (Shimada et al., 2001, 2006; Stroeve et al., 2007; Comiso et al., 2008; Markus et al., 2009). It is thought that the reduction is related to increased inflow of warm Pacific Water (Shimada et al., 2006; Woodgate et al., 2010). This reduction of sea ice is thought to have had large effects on the structure of marine ecosystems (Grebmeier et al., 2006; Hunt and Drinkwater, 2007). Studies of marine ecosystem structure, especially in the western Arctic Ocean, are urgently needed for evaluation of the effects of sea ice reduction on marine ecosystems.

The western Arctic Ocean has a shallow shelf (～50 m depth, Chukchi Sea) and a deep basin (> 3,000 m depth, Canada Basin) (Fig. 1a). On the shelf, Pacific Water flows through the Bering Strait into the western Arctic Ocean (Coachman and Aagaard, 1966). Because the Pacific Water contains high nutrients, this inflow is important in terms of the nutrient supply to the Arctic Ocean (Springer and McRoy, 1993). Pacific Water also transports Pacific zooplankton. Because Pacific fauna are entirely different from Arctic fauna, the zooplankton community in the shelf shows large spatial variability (Hopcroft et al., 2010; Matsuno et al., 2011, 2012a). The continuous inflow of the eutrophic Pacific Water causes high primary production on the shelf and a large material flux to the seafloor, resulting in the abundant benthic community there (Grebmeier et al., 1989).

In contrast to the shelf, the basin is oligotrophic. The large amount of low-salinity ice-melt water forms a strong halocline, which prevents nutrients from reaching the surface layer. Because the Pacific Water is very dense, it is found below the sea-ice melt water in the basin (Codispoti et al., 2005) and forms a small Chl. *a* peak (< 1 μg chl. *a* L^{-1}) near 50 m depth (Hill and Cota, 2005). Because the primary production is low, the zooplankton standing stock is low in the basin (Lane et al., 2008; Matsuno et al., 2012b). Anticyclonic eddies sometimes form around the Barrow Canyon and transport nutrients northward. Primary production in the eddies is reported to be high (Nishino et al., 2011a). Thus, in the western Arctic Ocean, the hydrography and marine ecosystem structure greatly varies between the shelf and basin. Accurate evaluation of the effect of the reduction of sea ice on the plankton community requires studies in different parts of the Arctic Ocean.

The effects of drastic reductions in sea ice are expected to be first observed in short-lived plankton in the Arctic Ocean. Thus, information about the plankton community in the western Arctic Ocean is required for estimating possible future changes in the Arctic marine ecosystem. However,

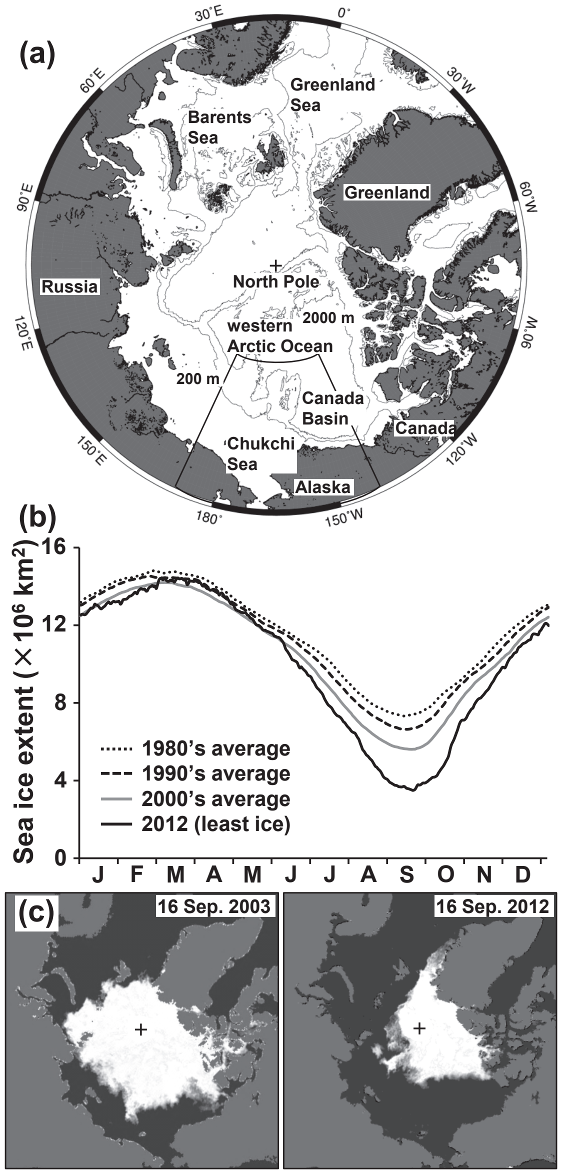

Fig. 1. Map of the Arctic Ocean (a). The lower box in (a) indicates the location of the western Arctic Ocean, which was treated in this study. Seasonal changes in the Arctic sea ice extent during 1980–2012 (b). Data on decadal averages (1980's, 1990's and 2000's) and 2012 are shown in (b). The horizontal distribution of the sea ice extent on the same date (16 September) of 2003 (left) and 2012 (right) (c). The data of (b) and (c) are provided by JAXA.

because of the seasonal ice coverage, shipboard observation is limited to a few months each year. Our knowledge of the plankton community in this region is mainly based on snap–shot studies conducted only in summer. Little information is available on seasonal and interannual changes. It should also be noted that snap–shot studies have generally examined either only phytoplankton or zooplankton; few studies have been performed on the entire plankton community (both phytoplankton and zooplankton).

In this study, I describe the spatial, interannual and seasonal changes in microplankton and mesozooplankton communities in the western Arctic Ocean. Individual chapters examine the horizontal distribution of the microplankton community (Chapter 2), the horizontal distribution of the mesozooplankton community (Chapter 3), interannual changes in the mesozooplankton community (Chapter 4) and seasonal changes in the mesozooplankton community (Chapter 5). Based on these results, in Chapter 6, I discuss the effects of recent environmental changes in the ocean on the plankton community in the Arctic Ocean.

2. Horizontal distribution of microplankton community structure in the western Arctic Ocean during late summer of 2010

2–1. Introduction

Recently, a drastic decrease of the sea–ice coverage area has been observed in the Arctic Ocean during summer and attributed to the increased inflow of the Pacific Summer Water (PSW) through the Bering Strait (Shimada et al., 2006; Woodgate et al., 2010). Because the PSW flows into the western Arctic Ocean, sea ice reduction in the Arctic Ocean has been greatest in this region (Shimada et al., 2001, 2006). Reduction of sea ice in the Arctic Ocean is expected to affect the marine ecosystem structure (Grebmeier et al., 2006; Hunt and Drinkwater, 2007).

In marine ecosystems, members of the microplankton community include both primary producers and consumers, and they are composed of autotrophs (diatoms), heterotrophs (ciliates) and mixotrophs (some species in the dinoflagellates). In the western Arctic Ocean, diatoms usually form a short–term pulse bloom (peaks exceeding 8 μg chl. *a* L^{-1}) during late spring to summer (Springer and McRoy, 1993). The dinoflagellates include autotrophic, heterotrophic and mixotrophic species (Gaines and Elbrächter, 1987). Because of the strong stratification in the Chukchi Sea during summer, photosynthetic dinoflagellates are dominant in the surface layer (Sergeeva et al., 2010). Ciliates are heterotrophic organisms, grazing bacteria and small phytoplankton (e.g., nano–sized pennate diatoms) (Capriulo and Carpenter, 1983; Gast, 1985; Paranjape, 1987), and they are preyed upon by mesozooplankton, so they have an important role in the microbial loop (Pomeroy, 1974). The growth rates of ciliates are determined not only by food but also by temperature. Especially in the Arctic Ocean, temperature is well known to be a main factor controlling the growth rates of ciliates (Hansen and Jensen, 2000). Despite their importance, little information is available for the microplankton community in the western Arctic Ocean. Previous studies on the microplankton community in this region have covered limited areas, such as small regions of the shelf or shelf break, and information on species compositions is scarce (Springer and McRoy, 1993; Codispoti et al., 2005; Sergeeva et al., 2010).

In the present chapter, I discuss my investigation the species composition, cell density and horizontal distribution of microplankton (diatoms, dinoflagellates and ciliates) in the western Arctic Ocean during late summer. Microplankton assemblages were clustered based on 59 stations covering the shelf, shelf break, slope and basin. The horizontal distribution of microplankton in the western Arctic Ocean is discussed based on the parameters governing their distribution.

2–2. Materials and Methods

2–2–1. Field sampling

CTD (Sea–Bird Electronics Inc., SBE 911 Plus) casts were made at 59 stations (located at 65°46′–78°52′N, 177°43′E–151°15′W) in the western Arctic Ocean from 4 September to 13 October 2010 on R/V *Mirai*, Japan Agency for Marine–Earth Science and Technology (JAMSTEC) (Fig. 2). Water samples (1 L) were collected from the layer of maximum chlorophyll fluorescence (4.5–65 m) with rosette Niskin bottles mounted on the CTD frame. Samples were fixed and preserved with 1% glutaraldehyde immediately after the collections.

For nutrient and chlorophyll *a* (Chl. *a*) measurements, seawater samples were collected from five to eight depths (maximum chlorophyll fluorescence layer and 5, 10, 20, 30, 50, 75, 100 m, depending on bottom depth). Nutrients (nitrate, nitrite, ammonium, phosphate and silicate) were analysed using an autoanalyser (Bran+Luebbe GmbH, TRAACS–800) on board, and Chl. *a* was also measured using the Welschmeyer method and a fluorometer (Turner Designs, Inc., 10–AU–005). Both nutrients and Chl. *a* data were provided by JAMSTEC.

2–2–2. Microscopic analysis

In the land laboratory, the water samples were concentrated to 20 mL using a siphon. Subsamples (100–500 μL) were mounted on a slide glass, and cell counts and species identification on diatoms and ciliates were made under an inverted microscope with 40–600× magnification. Cells larger than 10 μm are treated in this chapter. Species identification was made to the lowest possible level (species or genus). For species identification, I referred to Hasle and Syvertsen (1997) and Hoppenrath et al. (2009) for diatoms and to Maeda (1997) and Taniguchi (1997) for ciliates. For dinoflagellate observation, some of the subsamples were stained with calcofluor (1 mg mL^{-1}), and examined under an epifluorescence microscope with UV light excitation (Fritz and Trimer, 1985). Species identification of dinoflagellates followed Fukuyo et al. (1997) and Hoppenrath et al. (2009). For other taxa (silicoflagellates, golden algae and radiolaria), species identification followed Throndsen (1997) and Toriumi (1997). For all taxa, cell counts were made twice and were recounted if the two counts differed by more than 20%. Using the mean value, the cell density (cells L^{-1}) of each species was calculated.

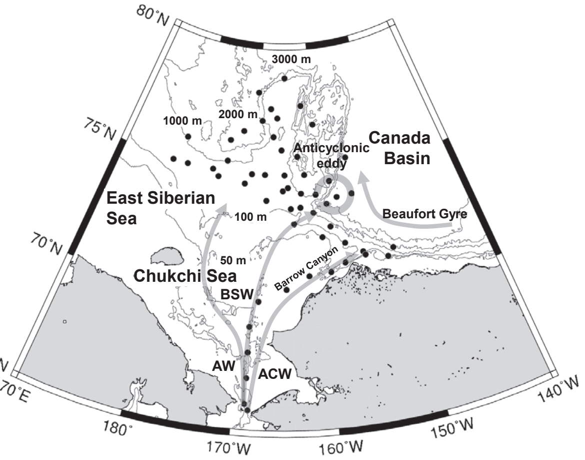

Fig. 2. Location of sampling stations in the western Arctic Ocean during 4 September–13 October 2010. The arrows indicate approximate positions of the current flow. The clockwise arrow indicates the anticyclonic eddy reported by Nishino et al. (2011a). ACW: Alaskan Coastal Water, AW: Anadyr Water, BSW: Bering Shelf Water.

2–2–3. Data analysis

Cell density (X: cells L^{-1}) for each species was logarithmically transformed ($Log_{10}[X+1]$) prior to further analysis to reduce any bias in abundances. Similarities between samples were examined using the Bray–Curtis method (Bray and Curtis, 1957). To group the samples, similarity indices were coupled with hierarchical agglomerative clustering with a complete linkage method (Unweighted Pair Group Method using Arithmetic mean, UPGMA; Field et al., 1982). Non–metric Multi–Dimensional Scaling (NMDS) ordination was conducted to delineate the sample groups on a two–dimensional map. All analyses were carried out using PRIMER v6 (PRIMER–E Ltd.).

Multiple regression analyses ($Y = aX_1 + bX_2 + c$, where Y is the environmental variable and X_1 and X_2 are axes 1 and 2 of NMDS, respectively) were performed to clarify which environmental parameters (latitude, longitude, depth, temperature, salinity, dissolved inorganic nitrogen [DIN], phosphate, silicate and Chl. *a*) had significant relationships with the microplankton groupings. Correlation analyses were also made between cell density (for total microplankton, diatoms, dinoflagellates and ciliates) and hydrographic parameters. To evaluate the characterised microplankton species in each group, tests by one–way ANOVA and Fisher's PLSD were performed based on the cell density data of the most five abundant species of each taxon. These statistical analyses were conducted using StatView v5 (SAS Institute Inc.).

2–3. Results

2–3–1. Abundance

Total microplankton cell densities at each station ranged between 416 and 142,624 cells L^{-1}. Diatoms ranged in density from 0 to 138,640 cells L^{-1} and composed 0–98% of the

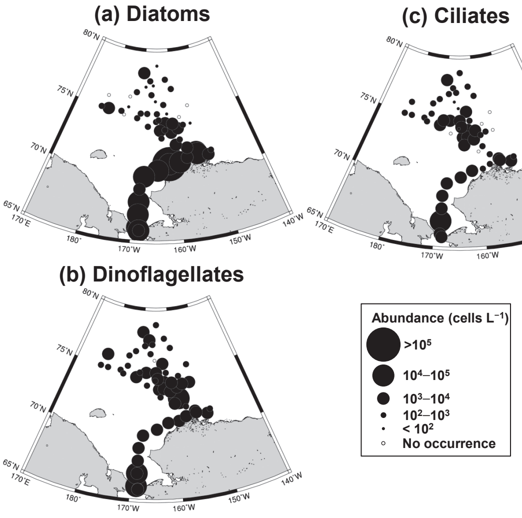

Fig. 3. Spatial changes in the cell density of the diatoms (a), dinoflagellates (b) and ciliates (c) in the western Arctic Ocean during 4 September–13 October 2010.

microplankton abundance (Fig. 3a). Dinoflagellates ranged in density from 0 to 16,460 cells L^{-1} and composed 0–100% of the total microplankton abundance (Fig. 3b). Ciliates ranged in density from 0 to 10,933 cells L^{-1} and composed 0–88% of the total microplankton abundance (Fig. 3c). The horizontal distribution of diatoms had a clear regional pattern; abundance was higher in the Chukchi Sea, especially around the Bering Strait and Barrow Canyon (Fig. 3a). Horizontal distribution patterns of dinoflagellates and ciliates were similar, and they were greater around the Bering Strait and around an anticyclonic eddy (Nishino et al., 2011a) (Fig. 3b, c).

In the present chapter, 134 microplankton species were identified. These include 37 species in 17 genera of centric diatoms, 9 species in 9 genera of pennate diatoms, 50 species in 13 genera of dinoflagellates, 32 species in 21 genera of ciliates, 4 species in 2 genera of silicoflagellates, and 1 species each of golden algae and radiolaria (Table 1). The dominant groups in terms of abundance were pennate diatoms (*Pseudo-nitzchia* spp. (grand mean: 3,052 cells L^{-1}), *Cylindrotheca closterium* (1,169 cells L^{-1}) and *Thalassionema nitzschioides* (742 cells L^{-1})) and centric diatoms (*Leptocylindrus minimus* (858 cells L^{-1}), *Proboscia alata* (782 cells L^{-1}) and *Chaetoceros socialis* (622 cells L^{-1})) (Table 1). Other abundant taxa included the dinoflagellates *Gymnodinium* spp. (532 cells L^{-1}), *Prorocentrum minimum* (492 cells L^{-1}) and *Prorocentrum balticum* (477 cells L^{-1}), and the ciliate *Strombidium* spp. (507 cells L^{-1}).

2–3–2. Community structure

Cluster analysis based on cell density classified the microplankton community into five groups (A–E) at 62% and 76% dissimilarity levels (Fig. 4a). Cell density was significantly greater in group B (mean: 31,036 cells L^{-1}) than in other groups, by a factor of 10 (705–3,657 cells L^{-1}) (one-way ANOVA, $p < 0.0001$). The proportions of the three dominant taxa (diatoms, dinoflagellates and ciliates) varied among groups; the dominant taxa were ciliates in group A (36% of total cells), diatoms in group B (78%), ciliates in group C (59%), and dinoflagellates in group D (94%) (Fig. 4b). Group E had the lowest cell density (705 cells L^{-1}). Each group was also clearly separated in the NMDS plot (Fig. 4c). Various environmental parameters including latitude, longitude, sampling depth, temperature, salinity, DIN, phosphate and Chl. *a* had significant relationships with the NMDS ordination ($r^2 = 0.12$–0.61, $p < 0.05$) (Fig. 4c).

The horizontal distributions of each group were well separated, and they varied with sea area. Group A, which occurred at the most stations (25 stations), was observed from the East Siberian Sea to the Canada Basin (Fig. 5). Group B occurred at 22 stations on the southern Chukchi Sea shelf. The other three groups (C–E), including a few stations, were observed in the areas between groups A and B (Fig. 5).

To show the characterised species for each group, intergroup comparisons of abundance were made for the top five abundant species of each taxon. No characterised species were recognised in groups A and E (Table 2). Cell densities of most of the species were greatest in group B, and significantly greater abundances were detected in group B than in other groups for the diatom *Th. nitzschioides*, and the ciliates *Tintinnidium mucicola* and *Tintinnopsis* spp. Groups C and D were characterised by significantly greater abundances of the ciliate *Strombidium* spp. and the dinoflagellate *P. minimum*, respectively (Table 2).

2–4. Discussion

2–4–1. Abundance

As a comparable study on microplankton abundance, Sukhanova et al. (2009) reported that phytoplankton cell density in the Chukchi Sea during spring to summer was 0.13–1.3×10^6 cells L^{-1} and was greater in summer than in spring due to the dominance of centric diatoms. Niemi et al. (2011) studied microplankton abundance under sea ice in a coastal area of the Beaufort Sea during winter. The winter microplankton community had a low cell density (320 cells L^{-1}) and was dominated by heterotrophic dinoflagellates and ciliates (Niemi et al., 2011). The mean microplankton density in the present study (1.4×10^5 cells L^{-1}) was similar to the summer values reported by Sukhanova et al. (2009); however, the dominant taxon in the present study was pennate diatoms. These results suggest that there is a large seasonal species succession in the microplankton assemblages in the western Arctic Ocean. During summer, the highest cell density was composed of centric diatoms (Sukhanova et al., 2009). After the bloom, the microplankton decreased in abundance, and the dominant species changed from diatoms

Table 1. List of microplankton (diatoms, dinoflagellates, ciliates and others) species identified in the western Arctic Ocean during 4 September–13 October 2010. Values in the parentheses indicate grand mean abundance (cells L^{-1}) through the whole stations.

Centric diatoms

Asteromphalus hookeri (1)
Attheya longicornis (7)
Attheya septentrionalis (28)
Chaetoceros affinis (9)
Chaetoceros atlanticus (34)
Chaetoceros compressus (93)
Chaetoceros concavicornis (44)
Chaetoceros constrictus (36)
Chaetoceros convolutus (147)
Chaetoceros danicus (12)
Chaetoceros debilis (201)
Chaetoceros decipiens (42)
Chaetoceros diadema (188)
Chaetoceros didymus (246)
Chaetoceros furcellatus (201)
Chaetoceros simplex (6)
Chaetoceros socialis (622)
Chaetoceros tenuissimus (52)
Chaetoceros teres (3)
Chaetoceros spp. (56)
Chaetoceros spp. (resting spore) (205)
Coscinodiscus centralis (2)
Dactyliosolen fragilissimus (1)
Eucampia groenlandica (63)
Leptocylindrus danicus (174)
Leptocylindrus minimus (858)
Melosira arctica (33)
Odontella aurita (5)
Planktoniella muriformis (5)
Proboscia alata (782)
Rhizosolenia borealis (32)
Rhizosolenia setigera (11)
Roperia tesselata (3)
Thalassiosira constricta (187)
Thalassiosira hyalina (126)
Thalassiosira gravida (26)
Thalassiosira nordenskioeldii (414)

Pennate diatoms

Cylindrotheca closterium (1,169)
Fragilaria striatula (47)
Fragilariopsis spp. (133)
Navicula spp. (66)
Pauliella taeniata (5)
Pleurosigma spp. (17)
Pseudo-nitzchia spp. (3,052)
Thalassionema nitzschioides (742)
Thalassiothrix longissima (50)

Dinoflagellates

Alexandrium tamarense (84)
Alexandrium spp. (9)
Alexandrium spp. (cyst) (5)
Ceratium arcticum (18)
Ceratium fusus (3)
Ceratium horridum (35)
Ceratium lineatum (6)
Ceratium pentagonum (16)
Ceratium tripos (34)
Dinophysis acuta (3)
Dinophysis lenticula (14)
Dinophysis norvegica (37)
Gonyaulax polygramma (3)
Gonyaulax turbynei (25)
Gonyaulax verior (14)
Gonyaulax spp. (40)
Gonyaulax scrippsae (3)
Gonyaulax spp. (cyst) (14)
Gymnodinium breve (2)
Gymnodinium spp. (532)
Gyrodinium spp. (1)
Heterocapsa niei (1)
Heterocapsa spp. (2)
Oxytoxum scolopax (54)
Oxytoxum sp. 1 (172)
Oxytoxum sp. 2 (145)
Prorocentrum balticum (477)
Prorocentrum compressum (40)
Prorocentrum dentatum (106)
Prorocentrum minimum (492)
Protoperidinium avellanum (1)
Protoperidinium bipes (83)
Protoperidinium crassipes (3)
Protoperidinium depressum (1)
Protoperidinium leonis (4)
Protoperidinium marukawai (16)
Protoperidinium minutum (6)
Protoperidinium mite (16)
Protoperidinium monovelum (3)
Protoperidinium pellucidum (25)
Protoperidinium punctulatum (40)
Protoperidinium pyriforme (1)
Protoperidinium subinerme (2)
Protoperidinium spp. (14)
Protoperidinium spp. (cyst) (15)
Pyrophacus steinii (7)
Scripsiella crystallina (5)
Scripsiella precaria (1)
Cysts (19)

Silicoflagelates

Dictyocha pseudofibula var. *complexa* (1)
Dictyocha spp. (11)
Distephanus speculum var. *regularis* (3)
Distephanus spp. (3)

Chrysophyte

Dinobryon balticum (256)

Oligotrich ciliates

Laboera strobila (2)
Leegaardiella spp. (51)
Lohmanniella spp. (24)
Parastrombidium spp. (2)
Strobilidium spp. (139)
Strombidium spp. (507)
Tontonia appendiculariformis (4)
Tontonia gracillima (24)
Tontonia spp. (4)

Tintinnid ciliates

Acanthostomella conicoides (3)
Acanthostomella norvegica (14)
Acanthostomella spp. (3)
Ascampbelliella spp. (1)
Canthariella pyramidata (5)
Codonellopsis frigida (1)
Codonellopsis morchella (7)
Codonellopsis schabi (3)
Favella azorica (163)
Favella spp. (2)
Leprotintinnus spp. (7)
Ormosella trachelium (1)
Parafavella jorgenseni (47)
Ptychocylis obtusa (7)
Salpingacantha perca (1)
Stenosemella nivalis (13)
Stenosemella ventricosa (2)
Stenosemella spp. (2)
Tintinnidium mucicola (150)
Tintinnopsis spp. (206)
Unidentified (5)

Radiolaria (2)

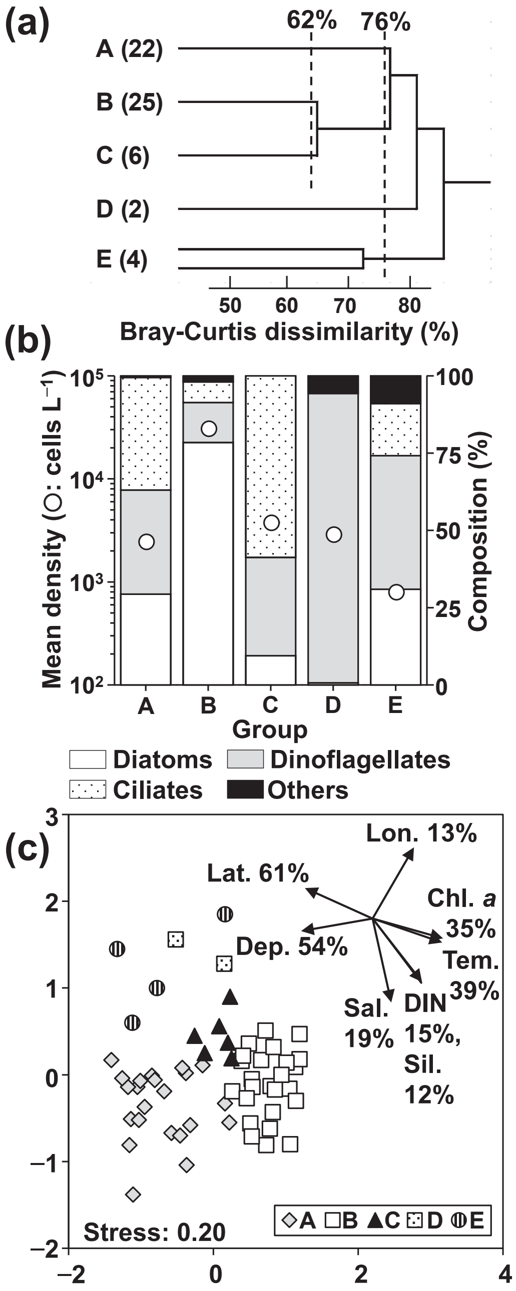

Fig. 4. Dendrogram that shows the results of the Bray–Curtis dissimilarity based on the microplankton abundance and composition (a). Five groups (A–E) were recognised at a 62% and 76% dissimilarity. The numbers in the parentheses indicate the number of stations that were included. The mean cell density and taxonomic composition of each group (b). Non-metric multidimensional scaling plots of each group (c). For various environmental parameters, their directions and coefficients of determination (%) are shown. Chl. *a*: chlorophyll *a*, Dep.: sampling depth, DIN: dissolved inorganic nitrogen, Lat.: latitude, Lon.: longitude, Sal.: salinity, Sil.: silicate, Tem.: temperature.

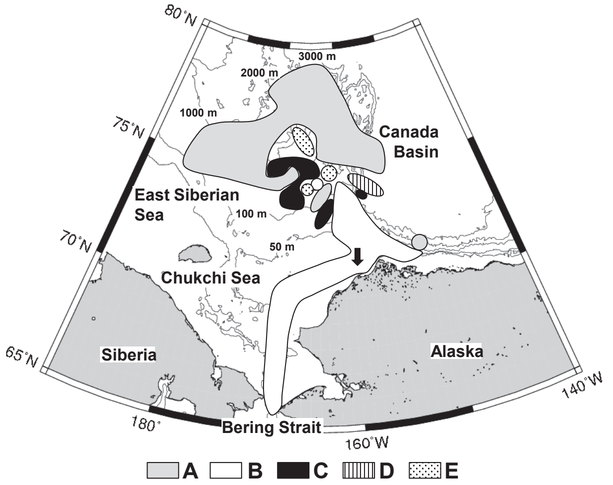

Fig. 5. Spatial distribution of microplankton assemblages identified by Bray–Curtis dissimilarity on microplankton abundance (cf. Fig. 4a). The solid arrow ingroup B indicates Barrow Canyon station, where the peak of chlorophyll *a* was anomalously high and deep (cf. Fig. 6).

to dinoflagellates and ciliates from summer to winter (Niemi et al., 2011). Because species successions have also been observed in the diatoms from centric to pennate diatoms (Sukhanova et al., 2009; Sergeeva et al., 2010), this may explain why the pennate diatoms dominated in this study period (late summer).

Correlation analysis between environmental parameters and the abundance of each microplankton taxon showed a clear taxon–specific pattern (Table 3). Diatoms had positive correlations with salinity, nutrients and Chl. *a*, while dinoflagellates and ciliates showed no correlation with these parameters and had only negative and positive correlations with sampling depth and temperature, respectively (Table 3). These taxon–specific correlations with environmental parameters are likely due to the differences in nutritional modes (i.e., autotrophs, heterotrophs and mixotrophs) of each taxon.

Most diatoms are autotrophs. Their growth requires nutrients and suitable light conditions. Diatoms were abundant around the Bering Strait and Barrow Canyon (Fig. 3a). In the Bering Strait, high primary production is supported by nutrients supplied by the continuous inflow of Pacific Water (Springer and McRoy, 1993). In Barrow Canyon, a nutrient–rich upwelling current from the Canada Basin to the euphotic zone supports high primary production (Hill and Cota, 2005; Hill et al., 2005) and high cell density (Sukhanova et al., 2009; Sergeeva et al., 2010). Thus, the predominance of diatoms in the Bering Strait and Barrow Canyon was presumably caused by the nutrient input to these regions.

Dinoflagellates include photosynthetic, heterotrophic and mixotrophic species (Gaines and Elbrächter, 1987). Because dinoflagellates can swim, they can grow faster in lower nutri-

Table 2. Comparison in abundances of dominated microplankton species in the five groups (A–E) of the western Arctic Ocean during 4 September–13 October 2010. The five groups were identified from Bray–Curtis dissimilarity based on microplankton abundance (cf. Fig. 4a). Values are mean abundance and standard deviation. Differences between groups were tested by one–way ANOVA and post–hoc test by Fisher's PLSD. Any groups not connected by the underlines are significantly different ($p < 0.05$). Numbers in the parentheses indicate the number of stations included in each group. NS: not significant, *: $p < 0.05$, **: $p < 0.01$.

Species	Abundance (cells L^{-1})					one–way ANOVA	Fisher's PLSD
	A (22)	B (25)	C (6)	D (2)	E (4)		
Diatoms							
Leptocylindrus minimus	0	2,025±9,040	0	0	0	NS	
Proboscia alata	161±625	1,695±4,212	33±39	0	0	NS	
Cylindrotheca closterium	9±43	2,733±5,138	73±85	0	0	NS	
Pseudo–nitzchia spp.	14±64	7,188±23,485	13±21	0	0	NS	
Thalassionema nitzschioides	35±80	1,668±2,816	160±110	0	80±86	*	A D C B
Dinoflagellates							
Gymnodinium spp.	258±275	937±1,297	347±165	0	60±120	NS	
Prorocentrum balticum	49±116	991±1,942	83±76	870±1,146	10±20	NS	
Prorocentrum minimum	36±63	988±1,578	80±72	1,530±2,022	0	*	A C B D
Oxytoxum sp. 1	130±123	250±467	67±106	190±71	60±77	NS	
Oxytoxum sp. 2	175±184	174±263	53±41	0	15±30	NS	
Ciliates							
Favella azorica	155±476	248±771	0	0	0	NS	
Strobilidium spp.	158±236	189±337	0	0	0	NS	
Strombidium spp.	305±363	436±631	2,000±2,879	0	70±89	**	E A B C
Tintinnidium mucicola	23±68	333±491	0	0	0	*	A B
Tintinnopsis spp.	4±17	457±676	107±155	0	0	*	A C B

ent concentrations than diatoms by performing diel vertical migration (Margalef, 1979). Because of the strong stratification in the Chukchi Sea during summer, dinoflagellates dominate in the surface layer (Sergeeva et al., 2010).

Ciliates are heterotrophic and graze on bacteria and small phytoplankton (< 5 µm) (Capriulo and Carpenter, 1983; Gast, 1985; Paranjape, 1987). In the Arctic Ocean, temperature is a main factor controlling the growth rates of both dinoflagellates and ciliates (Hansen and Jensen, 2000). Strongly positive correlations were confirmed between temperature and cell densities of dinoflagellates and ciliates in the present study (Table 3), which is consistent with the findings of previous studies.

Taxon–specific relationships between abundances and environmental parameters (Table 3), and horizontal distribution patterns (Fig. 3) would be related with nutritional types of microplankton. The growth of autotrophic diatoms is expected to be greater in regions with nutrient inputs, such as the Bering Strait and Barrow Canyon (Springer and McRoy, 1993; Hill et al., 2005). Higher temperatures probably enhance the growth of mixotrophic dinoflagellates and heterotrophic ciliates (Hansen and Jensen, 2000). The optimal environmental conditions for microplankton varied with taxa in the western Arctic Ocean during late summer (Table 3). This taxon–specific growth would govern the taxon–specific horizontal distribution of the microplankton community (Fig. 3).

2–4–2. Community structure

Based on the data of microplankton cell densities, five community groups were recognised. Cell densities, proportions of the three taxa (diatoms, dinoflagellates and ciliates) (Fig. 4b), and the characteristic species all varied between groups (Table 2). The horizontal distributions of each group were distinct: the large groups (A and B) occurred at the basin and shelf, respectively, and the three small groups (C–E) occurred between the two large groups (Fig. 5). Vertical profiles of hydrographic parameters (temperature, salinity, DIN and Chl. *a*) are summarised in Fig. 6 for each group.

Group A was widely distributed from the East Siberian Sea to the Canada Basin (Fig. 5), and no characteristic species were identified (Table 2). The hydrography where group A occurred was characterised by low temperature, low nutrients, and a low Chl. *a* peak in the subsurface layer (mean: 48 m) (Fig. 6). The relatively high proportion of ciliates (36%) (Fig. 4b) suggests the dominance of microbial loop organisms (Pomeroy, 1974). Thus, the basin of the western Arctic Ocean during late summer was oligotrophic, and the microplankton were dominated by organisms involved in the microbial loop.

Group B was observed on the Chukchi Sea shelf, and it had

Table 3. Matrix of correlation coefficient (r) between abundance of each microplankton taxon and environmental parameters. NS: not significant, *: $p < 0.05$, **: $p < 0.01$, ***: $p < 0.001$.

Environmental parameters	Diatoms	Dinoflagellates	Ciliates	Total microplankton
Sampling depth (m)	NS	−0.525***	−0.486***	−0.335**
Temperature (°C)	NS	0.647***	0.413***	0.321*
Salinity	0.374**	NS	NS	0.366**
DIN (μM)	0.422***	NS	NS	0.400**
Silicic acid (μM)	0.410***	NS	NS	0.379**
Phosphate (μM)	0.304*	NS	NS	NS
N: P ratio	0.335**	NS	NS	0.333*
Chlorophyll a (μg L^{-1})	0.573***	0.375*	NS	0.567***

the highest cell density and a predominance of diatoms. This area was characterised by higher temperature, salinity, nutrients and Chl. *a*, which peaked at the surface layer (mean: 20 m) (Fig. 6). All of these physical characteristics were caused by the warm, saline and nutrient-rich Pacific Water that flowed through the Bering Strait. Characteristic species of group B were the diatom *Th. nitzschioides* and tintinnid ciliates (Table 3). *Th. nitzschioides* is a cosmopolitan species common in cold water, particularly in the polar regions (Degerlund and Eilertsen, 2010). Tintinnid ciliates usually attach detritus and biogenic particles on their lorica and are abundant in neritic zones (Taniguchi, 1997). On the Chukchi Sea shelf, the diatom *Th. nitzschioides* could grow faster under the high nutrient concentrations caused by the inflow of Pacific Water, and the high level of biogenic particles in this region may provide suitable conditions for the growth of tintinnid ciliates. An anomalously high Chl. *a* concentration was detected at 50 m depth in the Barrow Canyon (Fig. 6). In the Barrow Canyon, because of ice melt, low-salinity water is present at the surface, and high-saline Pacific Water usually sinks below the low-salinity water (Codispoti et al., 2005). Diatoms transported with the sinking Pacific Water presumably utilise the high nutrients in relatively deep layers and form the subsurface Chl. *a* peak (Hill and Cota, 2005; Hill et al., 2005; Sergeeva et al., 2010).

Group C was dominated by ciliates, and the representative species was *Strombidium* spp. (Fig. 4b, Table 3). The oligotrich *Strombidium* spp. are small (20–30 μm in this study) and graze on bacteria and small phytoplankton (Capriulo and Carpenter, 1983; Gast, 1985; Paranjape, 1987). Temperature is generally a main factor controlling the growth rate of ciliates, and ciliates tend to grow faster than dinoflagellates, especially at low temperatures (Hansen and Jensen, 2000). Group C occurred near group B, which was characterised by high cell density. Group C occurred in water that was colder and more oligotrophic than group B did (Fig. 6). These facts suggest that the abundant small pennate diatoms and nanophytoplankton on the Chukchi Sea shelf (group B) were transported to the shelf break and grazed actively by oligotrich ciliates (group C).

Group D occurred north of the anticyclonic eddy (Figs. 2, 5) and was dominated by dinoflagellates (Fig. 4b); the representative species was *P. minimum* (Table 2). According to Nishino et al. (2011a), an anticyclonic eddy (100 km in diameter) was formed on the Chukchi Sea slope due to an increase in the volume of Alaskan Coastal Water (ACW) along the Barrow Canyon. Because this anticyclonic eddy temporally retained Pacific Water from shelf to basin, the area where group D occurred was less affected by Pacific Water and was low in salinity and nutrients. The oligotrophic conditions may have caused the predominance of dinoflagellates in group D.

Group E had the lowest cell density (Fig. 4b), and the hydrography in the area where it was collected was similar to that of group C (Fig. 6). Groups C and E occurred close to each other and in similar hydrographic conditions, but they showed different microplankton cell density and species composition. As mentioned above, group C was abundant and dominated by the oligotrich ciliates *Strombidium* spp., while group E was characterised by fewer ciliates (Table 2, Fig. 4b). Because group E occurred north of group C (Fig. 5), group E was farther from the nutrient input of the Pacific Water. It also indicates that the microplankton in group E were probably grazed by mesozooplankton such as copepods for a longer time. During summers in the Arctic Basin, it is reported that copepods consume 36% of primary production and prefer mobile microzooplankton to microphytoplankton as food (Campbell et al., 2009). Because group E is expected to have suffered grazing pressure for a longer time, the abundance of mobile heterotrophic ciliates was lower than in group C.

In conclusion, the horizontal distribution of microplankton in the western Arctic Ocean during late summer varied greatly by region. On the shelf, the predominance of diatoms was attributed to the continuous inflow of nutrient-rich Pacific Water. However, in the basin, the effects of the Pacific Water were diminished, and the microbial loop became dominant. On the continental slope between these two regions, the horizontal distribution of microplankton tended to show greater spatial differences. This is presumably related to the

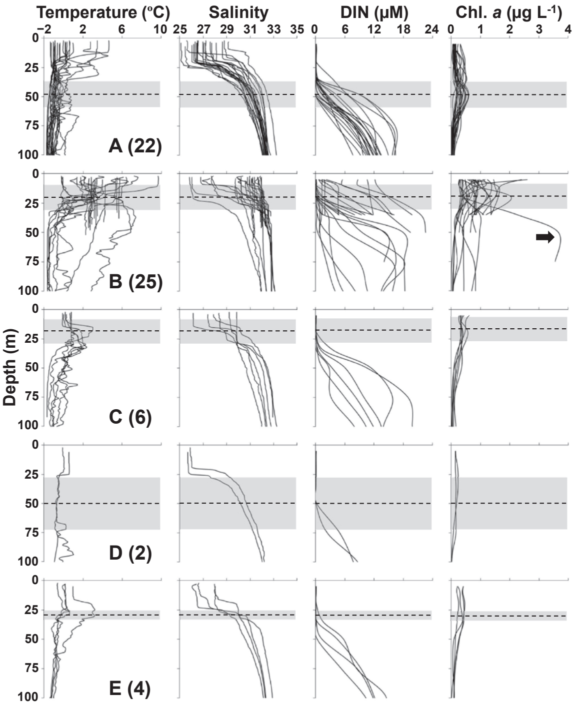

Fig. 6. Vertical profiles of hydrographic parameters at each group. Horizontal dashed lines and shades indicate the means and standard deviations of the sampling depths, respectively. The arrow in the chlorophyll *a* panel of group B indicates an anomalously high peak at a deep layer (50 m) in the Barrow Canyon station (cf. Fig. 5).

complex physical oceanography structures in this region, such as anticyclonic eddies.

3. Spatial and annual changes in mesozooplankton community structure in the western Arctic Ocean during the summers of 2008 and 2010

3-1. Introduction

Recently, a drastic reduction in the area of sea ice has been observed in the Arctic Ocean during summer. This reduction is considered to be caused by an increase in the amount of warm Pacific Summer Water (PSW) entering the Arctic Ocean through the Bering Sea Strait (Shimada et al., 2006; Woodgate et al., 2010). Because PSW flows through the Pacific sector in the Arctic Ocean (western Arctic Ocean, Fig. 7), sea ice reduction in the Arctic Ocean has been greatest in this region: e.g., Chukchi Sea, East Siberian Sea, Canada Basin and Mendeleyev Ridge (Shimada et al., 2001, 2006; Stroeve et al., 2007; Comiso et al., 2008; Markus et al., 2009). This reduction of sea ice is expected to induce changes in the marine ecosystem structure in the Arctic Ocean (Grebmeier et al., 2006; Hunt and Drinkwater, 2007). To evaluate the effects of sea ice reduction on marine ecosystems, studies on the plankton community in the western Arctic Ocean are needed.

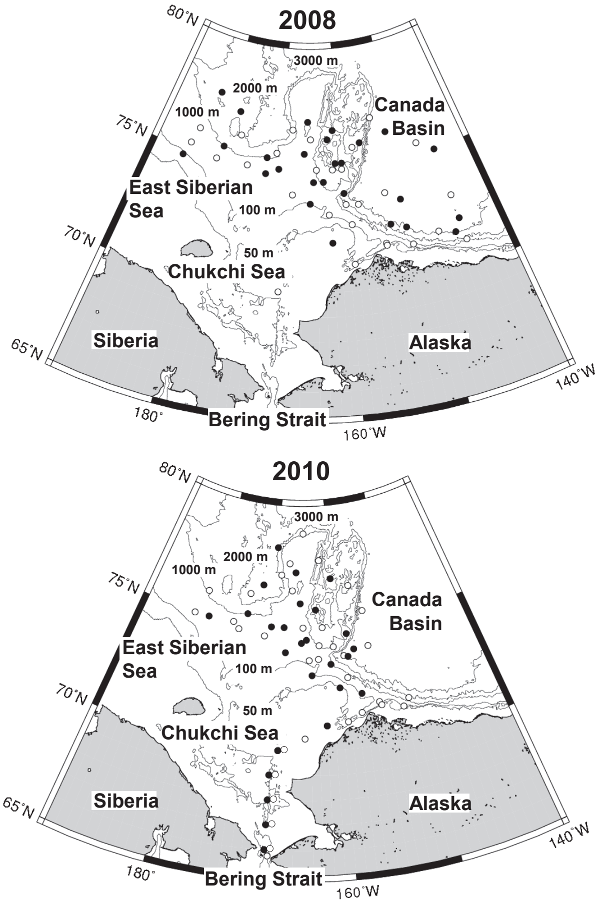

Fig. 7. Location of the sampling stations in the western Arctic Ocean during August-October 2008 and 2010. The open and solid symbols denote stations at which the samplings were conducted day and night, respectively.

Melting of the sea ice in the western Arctic Ocean during late spring to summer allows the sunlight to reach phytoplankton, resulting in short-term phytoplankton blooms (peaks exceeding 8 mg Chl. *a* L^{-1}) (Springer and McRoy, 1993; Hill and Cota, 2005). After these blooms, a subsurface maximum of phytoplankton occurs at approximately 20-40 m depth, supported by the inflow of dense, high-nutrient Pacific Water under the low-nutrient ice-melt water (salinity < 30) (Cota et al., 1996; Codispoti et al., 2005). According to Nishino et al. (2011b), the high chlorophyll *a* area varied due to meanders and the strength of the Beaufort Gyre, which are related to the decrease of sea ice. Thus, the phytoplankton standing stock in the western Arctic Ocean shows large seasonal and spatial variability (Springer and McRoy, 1993; Codispoti et al., 2005).

Zooplankton are a secondary producer in marine ecosystems and an important food for pelagic fishes and whales in the western Arctic Ocean (Lowry et al., 2004; Wassmann et al., 2006; Ashjian et al., 2010). In terms of zooplankton biomass, Arctic copepods, especially *Calanus glacialis* Jaschnov, *Calanus hyperboreus* Krøyer, *Metridia longa* (Lubbock) and *Pseudocalanus* spp., are dominant (Ashjian et al., 2003; Campbell et al., 2009; Matsuno et al., 2012b). However, in the southern Chukchi Sea, large Pacific copepods (e.g., *Calanus marshallae* Frost, *Neocalanus cristatus* (Krøyer), *Neocalanus flemingeri* Miller, *Neocalanus plumchrus* (Marukawa), *Eucalanus bungii* Giesbrecht and *Metridia pacifica* Brodsky) dominate in biomass because of the Pacific Water inflow. Thus, the zooplankton community greatly varies spatially according to the distribution of water masses (Springer et al., 1989; Lane et al., 2008; Hopcroft et al., 2010; Matsuno et al., 2011). While knowledge of the horizontal distribution of zooplankton has been increasing, the research areas of most studies have been limited, and information is scarce for the horizontal distribution covering broader areas from shelf to basin.

In the present chapter, I evaluate the horizontal distribution of zooplankton abundance, biomass, community and population structures, as well as the species diversity from shelf to basin in the western Arctic Ocean during the summers of 2008 and 2010. Small copepods (*Pseudocalanus* spp.) and large copepods (*C. glacialis*, *C. hyperboreus* and *M. longa*) were analysed down to the species and copepodid stages level, respectively. Based on these results, I will discuss what parameters govern the horizontal distribution of zooplankton in the western Arctic Ocean. Via comparison with the results from 2008 and 2010, I evaluate the inter-annual variability in zooplankton community and discuss possible causes.

3-2. Materials and Methods

3-2-1. Field sampling

A total of 117 zooplankton samplings were conducted by the R/V *Mirai* in the Chukchi Sea, Canada Basin and Mendeleyev Ridge (65°46′-78°52′N, 174°45′E-145°00′W) from 26 August to 8 October, 2008 ($n = 54$) and 2 September to 16 October, 2010 ($n = 63$) (Fig. 7). Zooplankton samples were collected during both day and night by vertical hauls with a NORPAC net (mouth diameter 45 cm, mesh size 0.335 mm) between the surface and 150 m depth (at stations where the bottom was deeper than 150 m) or between the surface and 5 m above the bottom (at stations where the bottom was shallower than 150 m). The volume of water filtered through the net was estimated using a flow-meter mounted in the mouth of the net. Zooplankton samples were fixed with 5% buffered formalin immediately on board. Accompanying the zooplankton sampling, temperature and salinity were measured by CTD (Sea-Bird Electronics Inc., SBE 911 Plus) casts. Sea-water samples were collected from 4-9 discrete depths (5, 10, 20, 30, 50, 75, 100, 125 and 150 m) between 5 and 150 m (at stations where the bottom was deeper than 150 m) or 10 m above the bottom (at stations where the bottom was shallower than 150 m) using Niskin bottles mounted on the CTD. Water samples were analysed for nitrate, nitrite, ammonia, and phosphate using an autoanalyser (Bran+Luebbe GmbH, TRAACS-800) on board. Chlorophyll *a* (Chl. *a*) concentration was also measured using a fluorometre (Turner Designs, Inc., 10-AU-005). All hydrographic data (temperature, salinity, nutrient and Chl. *a*) were provided by JAMSTEC.

3-2-2. Samples and data analysis

In the land laboratory, zooplankton samples were split using a Motoda box splitter (Motoda, 1959). One aliquot was weighed for wet mass (WM), with a precision of 0.01 g using an electronic balance (Mettler PM4000). The remaining aliquots were used for identification and enumeration under a dissecting microscope. Identification of calanoid copepods was made to the species and copepodid stage level. Species identification followed mainly Brodsky (1967) and Frost (1989) for *Pseudocalanus* spp. (*P. acuspes*, *P. major*, *P. mimus*, *P. minutus* and *P. newmani*), Frost (1974) for *Calanus* spp. (*C. glacialis* and *Calanus marshallae*), and Miller (1988) for *Neocalanus* spp. For *Pseudocalanus* spp., species identification was made for late copepodid stages (C5F/M and C6F/M), and early copepodid stages (C1-C4) were treated as *Pseudocalanus* spp. For large copepods (e.g., *C. glacialis*, *C. hyperboreus* and *M. longa*), the Mean Copepodid Stage (*MCS*) was calculated from the following equation:

$$MCS = \frac{\sum_{i=1}^{6} i \times Ai}{\sum_{i=1}^{6} Ai} \qquad (1)$$

where i (1-6 indicates C1-C6) is the copepodid stage, and Ai (ind. m^{-2}) is the abundance of the ith copepodid stage (cf. Marin, 1987).

Samplings were conducted during both day and night, and the day and night sampling stations were distributed evenly (day:night = 28:26 for 2008 and 36:27 for 2010) (Fig. 7). No significant differences were detected between day and night data for most species and copepodid stages (total zooplankton abundance and biomass by U-test, $p = 0.13$-0.27 [2008], $p = 0.44$-0.61 [2010], *M. longa* abundance by U-test, $p = 0.43$ [2008], 0.67 [2010]). Therefore, I made no day-night conversions for abundance or biomass data.

Abundance data (X: ind. m^{-2}) for each species were log-transformed ($\log_{10}[X+1]$) prior to analysis to reduce the bias of abundance. Similarities between samples were examined using the Bray-Curtis index (Bray and Curtis, 1957). To group the samples, the similarity indices were coupled with hierarchical agglomerative clustering using a complete linkage method (Unweighted Pair Group Method using Arithmetic mean: UPGMA) (Field et al., 1982). Nonmetric Multi-Dimensional Scaling (NMDS) ordination was carried out to delineate the sample groups on a two-dimensional map. All analyses were performed using PRIMER v6 software (PRIMER-E Ltd.). Multiple-regression analysis was carried out between NMDS plots and hydrographic data (latitude, longitude, depth, integrated mean temperature, integrated mean salinity and integrated chlorophyll *a* of the net-towed water column). A species diversity index (H') in each group was calculated using the following equation:

$$H' = -\sum ni/N \times \ln ni/N \qquad (2)$$

where ni is the abundance (ind. m^{-2}) of the ith species, and N is the abundance (ind. m^{-2}) of total calanoid copepods in the group (Shannon and Weaver, 1949). Inter-regional differences in the abundance of all copepods and *MCS* of large copepods were tested by one-way ANOVA and an ex post facto test by Fisher's Protected Least Significant Difference test (PLSD). These statistical analyses were performed using StatView v5 software (SAS Institute Inc.).

3-3. Results

3-3-1. Abundance and biomass

Throughout the study area, zooplankton abundance and biomass ranged from 0.03 to 2.74×10^5 ind. m^{-2} and 3 to 678 g WM m^{-2}, respectively (Fig. 8). The abundance and biomass were greater on the Chukchi Sea shelf in both 2008 and 2010 (Fig. 8). Copepods composed 8 to 95% of zooplankton abundance and were the dominant taxa. In the present chapter, 38 species of calanoid copepods in 25 genera were identified (Table 4). The most abundant calanoid copepods were *Pseudocalanus* spp., *C. glacialis* and *M. longa*. Among the 38 calanoid copepod species, five (*C. marshallae*, *E. bungii*, *M. pacifica*, *N. cristatus* and *N. flemingeri*) were Pacific species.

Results of the cluster analysis based on the copepod abundance classified the copepod communities into four groups at 30% and 36% dissimilarity levels (Fig. 9a). Each group was also clearly separated in the NMDS plot (Fig. 9b). For the ordination of NMDS plots, several environmental parameters (i.e., Chl. *a*, depth, latitude, temperature and salinity) were significant (r^2 = 0.16–0.61) (Fig. 9b). The horizontal distribution of each group was well separated and varied with depth. Based on location depth, the groups were named (with increasing depth): Shelf (n = 27 stations), Shelf break (41), Slope (28) and Basin (21) (Fig. 10). The horizontal distribution of each group was well separated in 2010, while the distributions of the Shelf break and Slope groups were intricately mixed in 2008 (Fig. 10). Species diversity (H') in the Basin was 2.07, while the other groups had higher species diversity (2.38–2.49) (Fig. 9c).

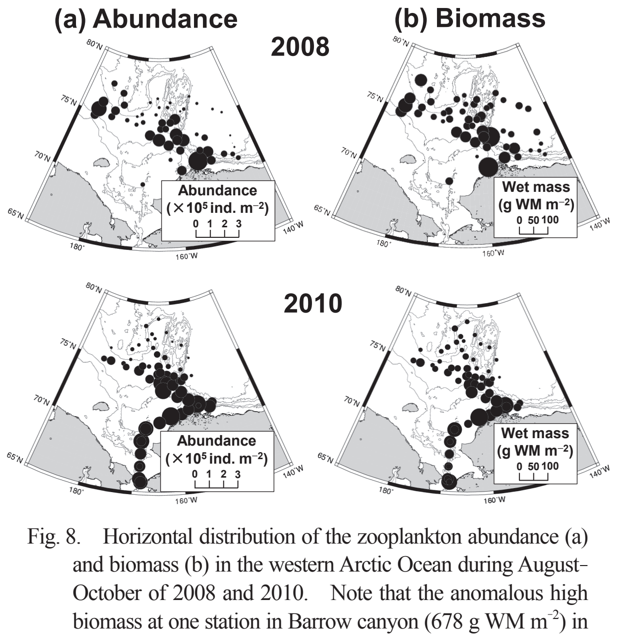

Fig. 8. Horizontal distribution of the zooplankton abundance (a) and biomass (b) in the western Arctic Ocean during August–October of 2008 and 2010. Note that the anomalous high biomass at one station in Barrow canyon (678 g WM m^{-2}) in 2008 is omitted from (b).

3-3-2. Community structure

The results of inter-group comparisons of zooplankton abundance evaluated by one-way ANOVA are shown in Table 4. Total zooplankton values from the Slope and Basin (0.06–0.16×10^5 ind. m^{-2}) were lower than those on the Shelf and Shelf break (0.64–0.88×10^5 ind. m^{-2}) (Table 4). This spatial variability was due to the lower abundance of the numerically dominant copepods (*Pseudocalanus* spp.) and other zooplankton (especially barnacle larvae, bivalvia larvae and Polychaetes) in the Slope and Basin regions.

The characteristic species for each group were as follows: Shelf, Pacific copepods (*C. marshallae*, *E. bungii*, *M. pacifica* and *N. cristatus*), neritic copepods (*C. abdominalis* and *Pseudocalanus* spp.), barnacle larvae (*Balanus* spp.), bivalvia larvae, Chaetognatha, *Clione limacine*, Echinodermata larva, Eubrachyura zoea, Euphausiacea and Polychaeta; Shelf break, *C. glacialis*, *C. hyperboreus*, Cyclopoida, *M. longa*, *Microcalanus pygmaeus*, Appendicularia, Hydromedusa, Isopoda and *Limacina helicina*; Slope, *Heterorhabdus norvegicus*, *Paraeuchaeta glacialis*, *Spinocalanus longicornis*, *Temorites brevis* and Ostracoda; Basin, *Scaphocalanus magnus* (Table 4).

The results of the inter-regional comparison of the *MCS* for the large Arctic copepods (*C. glacialis*, *C. hyperboreus* and *M. longa*) are shown in Table 5. In both 2008 and 2010, the *MCS* of *C. glacialis* was highest in the Basin and lowest at the Shelf break. The high *MCS* value for *C. hyperboreus* on the Shelf was due to the occurrence of one individual in a late copepodid stage (C5 or C6F). In both 2008 and 2010, the *MCS* values of *C. hyperboreus* in the Slope and Basin regions were higher than at the Shelf break. The *MCS* of *M. longa* was greater in the Basin than in the Shelf in both years (Table 5).

3-3-3. Hydrography in each region

Vertical profiles of temperature, salinity, dissolved inorganic nitrogen (DIN) and chlorophyll *a* (Chl. *a*) in the four clustered groups are summarised in Fig. 11. Pacific Water, which is the main source of nutrients, is characterised by high temperature and high salinity (Shimada et al., 2001,

Table 4. Comparison of mesozooplankton abundances in the four regions identified by Bray-Curtis dissimilarity based on mesozooplankton abundance (cf. Fig. 9) in the western Arctic Ocean during August-October of 2008 and 2010. Values are mean abundance in each region. Differences between regions were tested by one-way ANOVA and post-hoc test by Fisher's PLSD. Any regions not connected by the underlines are significantly different ($p < 0.05$). Numbers in the parentheses indicate number of stations included in each region. *: $p < 0.05$, **: $p < 0.01$, ***: $p < 0.001$ NS: not significant.

Species	Abundance (ind. m^{-2})				one-way ANOVA	Fisher's PLSD			
	Shelf (27)	Shelfbreak (41)	Slope (28)	Basin (21)					
Acartia hadsonica	76	27	8	0	NS				
Acartia longiremis	1,649	1,106	93	415	***	Slope	Basin	Shelfbreak	Shelf
Aetideopsis multiserrata	0	48	0	0	NS				
Aetideopsis rostrata	0	10	0	0	NS				
Calanus glacialis	6,957	8,201	2,176	957	***	Basin	Slope	Shelf	Shelfbreak
Calanus hyperboreus	3	213	132	198	**	Shelf	Slope	Basin	Shelfbreak
Calanus marshallae	211	0	4	0	***			Slope	Shelf
Centropages abdominalis	1,637	189	15	0	***		Slope	Shelfbreak	Shelf
Chiridius obtusifrons	2	59	8	15	NS				
Cyclopoida	2,892	5,875	3,075	2,180	**	Basin	Shelf	Slope	Shelfbreak
Epilabidocera amphitrites	19	0	0	0	NS				
Eucalanus bungii	1,105	13	3	1	**	Basin	Slope	Shelfbreak	Shelf
Eurytemora herdmani	9	8	1	0	NS				
Gaidius brevispinus	0	27	0	1	NS				
Gaidius tenuispinus	0	5	1	3	NS				
Heterorhabdus norvegicus	0	19	36	34	***		Shelfbreak	Basin	Slope
Lucicutia anomala	0	0	1	0	NS				
Metridia longa	60	2,924	1,013	579	***	Shelf	Basin	Slope	Shelfbreak
Metridia pacifica	3,153	30	4	3	***	Basin	Slope	Shelfbreak	Shelf
Microcalanus pygmaeus	105	919	759	695	***	Shelf	Basin	Slope	Shelfbreak
Neocalanus cristatus	16	1	1	0	*		Slope	Shelfbreak	Shelf
Neocalanus flemingeri	17	28	1	0	NS				
Neocalanus plumchrus	38	3	1	1	***	Slope	Basin	Shelfbreak	Shelf
Oncaea spp.	9	17	0	0	NS				
Paraeuchaeta glacialis	0	110	134	131	***	Shelf	Shelfbreak	Basin	Slope
Pseudocalanus acuspes	11,998	6,427	610	7	***	Basin	Slope	Shelfbreak	Shelf
Pseudocalanus major	1,236	779	77	9	*	Basin	Slope	Shelfbreak	Shelf
Pseudocalanus mimus	2,065	1,243	89	3	***	Basin	Slope	Shelfbreak	Shelf
Pseudocalanus minutus	4,977	1,556	129	37	***	Basin	Slope	Shelfbreak	Shelf
Pseudocalanus newmani	9,237	7,846	763	4	***	Basin	Slope	Shelfbreak	Shelf
Pseudocalanus spp. (C1-C4)	14,919	11,932	2,893	49	***	Basin	Slope	Shelfbreak	Shelf
Racovitzanus antarcticus	0	1	1	0	NS				
Scaphocalanus magnus	0	1	3	7	**		Shelfbreak	Slope	Basin
Scolecithricella minor	17	34	49	40	NS				
Spinocalanus longicornis	0	1	14	8	*		Shelfbreak	Basin	Slope
Temorites brevis	0	19	43	11	*		Basin	Shelfbreak	Slope
Tortanus discaudatus	0	4	1	0	NS				
Undinella oblonga	0	2	0	0	NS				
Amphipoda	25	17	28	25	NS				
Appendicularia	1,494	3,018	625	80	***	Basin	Slope	Shelf	Shelfbreak
Balanus spp.	6,983	4,094	1,337	69	***	Basin	Slope	Shelfbreak	Shelf
Bivalvia larva	4,338	94	4	1	***	Basin	Slope	Shelfbreak	Shelf
Chaetognatha	1,238	1,115	318	205	***	Basin	Slope	Shelfbreak	Shelf
Clione limacina	100	29	5	1	***	Basin	Slope	Shelfbreak	Shelf
Echinodermata larva	1,295	1,061	15	0	***		Slope	Shelfbreak	Shelf
Eubrachyura zoea	7	1	0	1	*		Basin	Shelfbreak	Shelf
Euphausiacea	272	96	7	0	***		Slope	Shelfbreak	Shelf
Evadne spp.	14	18	2	0	NS				
Hydrozoa	2,371	2,587	1,283	206	***	Basin	Slope	Shelf	Shelfbreak
Isopoda	6	23	9	4	*	Basin	Shelf	Slope	Shelfbreak
Limacina helicina	553	697	309	53	***	Basin	Slope	Shelf	Shelfbreak
Ostracoda	2	61	152	134	***	Shelf	Shelfbreak	Basin	Slope
Podon spp.	34	15	2	0	NS				
Polychaeta	6,551	1,045	134	18	***	Basin	Slope	Shelfbreak	Shelf
Total copeods	62,408	49,677	12,137	5,386	***	Basin	Slope	Shelfbreak	Shelf
Total zooplankton	87,690	63,647	16,364	6,183	***	Basin	Slope	Shelfbreak	Shelf

2006). From the Shelf to the Basin, the surface temperature and salinity gradually decreased because of the dilution of the Pacific Water with ice-melt water. Chlorophyll *a* was also high on the Shelf under the conditions of inflow of nutrient-rich Pacific Water, and there was a sub-surface peak at approximately 50 m depth in the Basin.

3-4. Discussion

3-4-1. Spatial changes

The Shelf group was dominated by Pacific copepods transported by Pacific Water through the Bering Strait (Table 4). The highest latitude at which Pacific copepods occurred in this study was 78°16′N. According to Johnson (1963), the Pacific copepods *N. cristatus* and *E. bungii* occurred on the Chukchi Abyssal Plain (85°06′N, 168°40′W) in 1953. Therefore, the occurrence of the Pacific copepods observed in this study was in the previously reported area. Among the Pacific copepods, *Neocalanus* spp. have a 1- or 2-year generation length. They feed on phytoplankton near the surface layer, accumulate lipids in the body, migrate down to the depths, and reproduce there (Miller et al., 1984). The Arctic copepod *C. hyperboreus* has a similar life-cycle pattern, though its generation length is longer (mostly 3 years), with large regional variability (1-5 years) (Falk-Petersen et al., 2009). They begin diapause from stage C3 and diapause several times over several years. These multiple diapauses are considered to occur during the short high-primary-production season in the Arctic Ocean. Although Pacific copepods also diapause in deep layers, their shorter generation lengths and limited resting stages may prevent them from completing their life cycle in the Arctic Ocean. Thus, over the past 50 years, the transported Pacific copepods are thought to have undergone an abortive migration to the Arctic Ocean.

For the Shelf group, zooplankton abundance was the highest, due to the large numbers of *Pseudocalanus* spp. and benthic larvae (Fig. 9c, Table 4). In the western Arctic Ocean, the *Pseudocalanus* spp. included two species that diapause (*P. acuspes* and *P. minutus* (Norrbin, 1994, 1996; Richter, 1995; Renz and Hirche, 2006; Renz et al., 2007)), one that does not (*P. newmani* (McLaren et al., 1989)), and two species that may or may not diapause (*P. major* and *P. mimus*). All five *Pseudocalanus* species showed greater abundance on the Shelf than in the Basin (Table 4). The most remarkable gradient from the Shelf to the Basin was in phytoplankton abundance and primary production (Fig. 11). These findings suggest that the food supply is an important factor in the abundance of *Pseudocalanus*. A similar response (magnitude of reproduction being related with phytoplankton stock) has been reported for benthic larvae (barnacle, bivalvia and Polychaeta larvae) (von Oertzen, 1972; Clare et al., 1984; Clare and Walker, 1986; Ambrose and Renaud, 1997). Thus, the dominant taxa/species on the

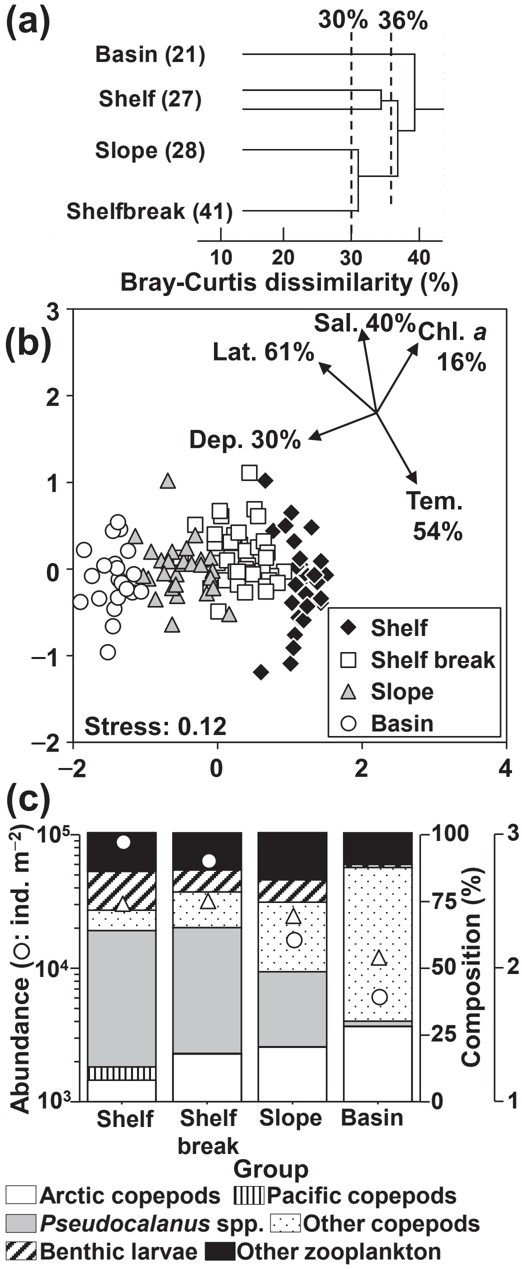

Fig. 9. Dendrogram that shows the results of Bray-Curtis dissimilarity on mesozooplankton assemblages (a). Four groups were identified at 30% and 36% dissimilarity. The numbers in the parentheses indicate the number of stations included. Non-metric multidimensional scaling (NMDS) plots of each group (b). For environmental parameters that have a significant relationship with NMDS plots; their directions and coefficients of determination (%) are shown. Chl. *a*: integrated chlorophyll *a*, Dep.: bottom depth, Lat.: latitude, Sal.: integrated mean salinity, Tem.: integrated mean temperature. The mean abundance and taxonomic composition of each group (c). Arctic Copepoda are included, namely, *C. glacialis*, *C. hyperboreus* and *M. longa*. Pacific Copepoda are included, namely, *C. marshallae*, *E. bungii*, *M. pacifica*, *N. cristatus*, *N. flemingeri* and *N. plumchrus*. Benthic larvae are included, namely, *Balanus* spp., Bivalvia larva, Echinodermata larva and Eubrachyura zoea.

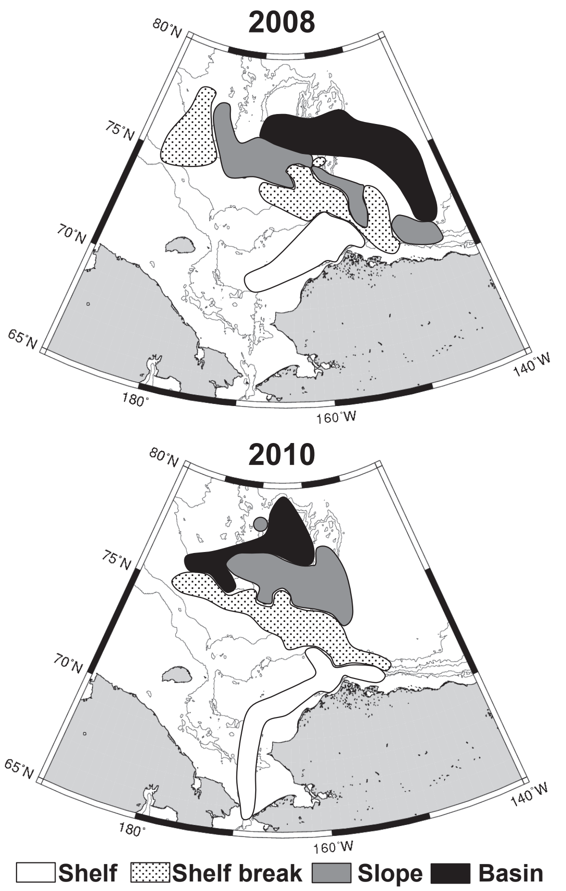

Fig. 10. Horizontal distribution of the four groups (Shelf, Shelf break, Slope and Basin) identified from the Bray–Curtis similarity based on mesozooplankton abundances (cf. Fig. 9) in the western Arctic Ocean during September–October of 2008 and 2010.

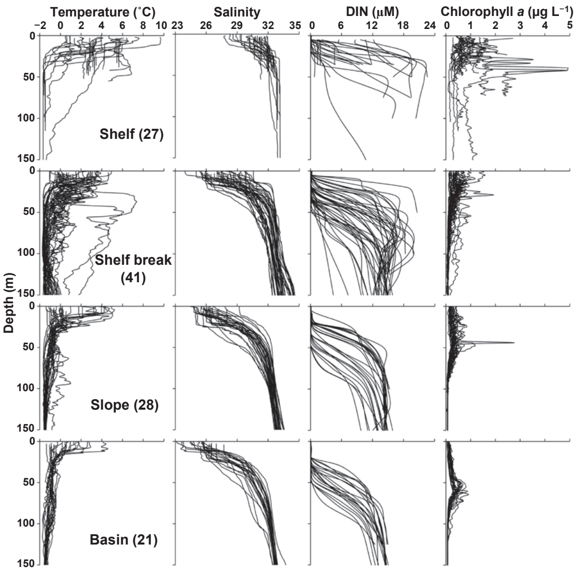

Fig. 11. Vertical profiles of the temperature and salinity and of chlorophyll *a* at four regions in the western Arctic Ocean during August–October of 2008 and 2010: Shelf (upper), Shelf break (middle–upper), Slope (middle–lower) and Basin (lower). The four regions were identified from the cluster analysis based on the mesozooplankton abundance and using a Bray–Curtis similarity (see Fig. 9). The number of included stations in each region are shown in parentheses.

Shelf (*Pseudocalanus* spp. and benthos larvae) is attributed to the high phytoplankton standing stock there.

The Shelf break group was characterised by the dominance of the early copepodid stages of large Arctic copepods (*C. glacialis*, *C. hyperboreus*, *M. longa*) (Tables 4 and 5). *Calanus* spp. diapause in deep–sea layers (> 200 m) (Falk–Petersen et al., 2009), and *M. longa* perform diel vertical migration (Båmstedt and Ervik, 1984; Grønvik and Hopkins, 1984). These facts suggest that they require deep water to complete their life cycles. The dominance of large Arctic copepods on the Shelf break is supported by the sufficient depth and also the fairly abundant phytoplankton stock (Fig. 11). *Pseudocalanus* spp. were also abundant at the Shelf break (Fig. 9c), which induced secondary greater abundance on the Shelf break region in the Arctic Ocean. At the Shelf break, various gelatinous zooplankton (Hydrozoa and Appendicularia) were also abundant (Table 4). Hydrozoa prey upon small copepods (e.g., Cyclopoida and *Acartia* spp.) (Sullivan et al., 1994) and reproduce in summer (Pertsova et al., 2006). Appendicularia graze on nano/pico–sized phytoplankton (Acuña et al., 1996, 1999) and have a short generation length (1–3 weeks) (Paffenhöfer, 1973). The dominance of these taxa in the Shelf break region might have been caused by their reproduction under the sufficient food condition before the sampling period.

In the Slope group, both large Arctic copepods and *Pseudocalanus* spp. were less abundant (Table 4). Because their population size may be determined by the magnitude of the primary production, the remarkable decrease of these species on the Slope may be attributed to low primary production on the Slope caused by the reduction in the nutrient–rich Pacific Water. In fact, Chl. *a* in the Slope and Basin regions had a subsurface peak at approximately 50 m depth (Fig. 11). The characteristic species on the Slope were deep–sea copepods (*H. norvegicus*, *P. glacialis*, *S. longicornis* and *T. brevis*) and ostracods (Table 4). Because of the deep depths on the Slope (mean 1,708 m), these species/taxa are considered to be abundant there.

The Basin had the lowest *Pseudocalanus* spp. abundance, the lowest zooplankton abundance (Fig. 9c), and the lowest species diversity. The low species diversity is thought to have been caused by the predominance of Cyclopoida, which accounted for 40% of the copepods and 35% of the total zooplankton in this region (Table 4).

Cyclopoida are small copepods whose regional variability in abundance was less remarkable (2.7 times = 5,875/2,180 ind. m^{-2}, cf. Table 4). This variability is comparable to those of *Pseudocalanus* spp., which showed ca. 300–fold differ-

Table 5. Regional comparison of mean copepodid stage of *C. glacialis*, *C. hyperboreus* and *M. longa* in the western Arctic Ocean during August–October of 2008 and 2010. Differences between regions were tested by one-way ANOVA and post-hoc test by Fisher's PLSD. Any regions not connected by the underlines are significantly different ($p < 0.05$). Values are mean copepodid stage±1sd. Numbers in the parentheses indicate number of stations included in each region. *: $p < 0.05$, **: $p < 0.01$, ***: $p < 0.0001$.

Species		Mean copepodid stage				one-way ANOVA	Fisher's PLSD			
	Year	Shelf (27)	Shelfbreak (41)	Slope (28)	Basin (21)					
C. glacialis										
	2008	3.55	3.49	3.59	4.65	***	Shelfbreak	Shelf	Slope	Basin
	2010	4.30	3.68	4.12	4.42	**	Shelfbreak	Slope	Shelf	Basin
C. hyperboreus										
	2008	5.00	4.46	4.77	5.29	**	Shelfbreak	Slope	Shelf	Basin
	2010	6.00	4.12	5.21	5.05	*	Shelfbreak	Basin	Slope	Shelf
M. longa										
	2008	4.01	4.20	4.80	5.54	***	Shelf	Shelfbreak	Slope	Basin
	2010	3.48	4.19	4.87	5.60	***	Shelf	Shelfbreak	Slope	Basin

ences in abundance with region (= 14,919/49 ind. m^{-2}, cf. Table 4). These differences in abundance among the small copepods may have been caused by differences in feeding between the two taxa. *Pseudocalanus* spp. are herbivorous (Corkett and McLaren, 1978), while Cyclopoida are coprophagous (feeding on faecal pellets of zooplankton) (Svensen and Nejstgaard, 2003; Poulsen and Kiørboe, 2006). Because of this feeding pattern, Cyclopoida are considered to be abundant at the Shelf break, where the large Arctic copepods were abundant and presumably egested large faecal pellets on which Cyclopoida could feed.

In the present study, calanoid species were identified, but cyclopoid species were not. The identification of cyclopoid species might change the results on species diversity in this study. Because the regional pattern of Cyclopoida varied with that of *Pseudocalanus* spp., the major factor determining population size is suggested to vary between the two taxa. In the future, detailed analysis (species identification and population structure) of cyclopoid copepods is required, using nets with smaller mesh sizes in the Arctic Ocean.

3–4–2. Annual changes

Annual changes in the horizontal distribution of zooplankton showed clear separations by depth in 2010 but a meandering and complicated boundary between the Shelf break and Slope groups in 2008 (Fig. 10).

Differences in hydrographic conditions between 2008 and 2010 were thought to be caused mainly by the ice coverage area. The area in 2008 (mean 5.0×10^6 km^2) was lower than in 2010 (mean 5.5×10^6 km^2) during the sampling period, and the reduction was greatest in the western Arctic Ocean (http://www.ijis.iarc.uaf.edu/seaice/extent/plot-/csv). As mentioned above, high primary production in the shelf region may be caused by the inflow of the nutrient-rich Pacific Water, and the decrease of primary production along Shelf to Basin is attributed to the dilution of the Pacific Water. The horizontal distribution of zooplankton in the western Arctic Ocean is governed by the amount of primary production (Matsuno et al., 2012b). From this point of view, the clear separation of zooplankton in 2010 related with latitude and depth is considered to be a normal feature of summer in the western Arctic Ocean.

The sea ice reduction in the Canada Basin in 2008 was greater than that in 2010 (http://www.ijis.iarc.uaf.edu/cgi-bin/seaice-monitor.cgi?lang=j), which caused the meander to change and increased the inflow of the Beaufort Gyre (Nishino et al., 2011b). The meander and the increased strength of the Beaufort Gyre in 2008 may have caused the complex distribution of the Shelf break and Slope groups that year (Fig. 10).

In conclusion, the horizontal distribution of zooplankton in the western Arctic Ocean in the summer was mainly governed by the Pacific Water inflow. Annual changes in sea-ice reduction may be affected by the physical characteristics of the Beaufort Gyre. Such physical oceanography may also induce annual changes in the horizontal distribution of zooplankton.

4. Year-to-year changes of the mesozooplankton community and biomass size spectra in the Chukchi Sea during summers of 1991, 1992 and 2007, 2008

4–1. Introduction

The Chukchi Sea is located in the Arctic Ocean, close to the Bering Strait, which connects the Arctic Ocean to the North Pacific. Its seafloor is mostly a shallow shelf (depth < 50 m), and recent observations have shown that the most drastic reduction of sea ice within the Arctic Ocean (Shimada et al., 2001, 2006) has occurred here. It is believed that the large sea–ice reduction in the Chukchi Sea has been due to the increased inflow of the warm Pacific Water passing through the Bering Strait (Shimada et al., 2006). Based on satellite observations from 1991 to 2007, both the volume and temperature of the Pacific Water that passed through the Bering Strait were highest in 2007, when the extent of sea ice was the lowest (Woodgate et al., 2010). The summer sea surface temperature in the Chukchi Sea is normally 4–6°C, but it reached 12°C in 2007 (Vanin, 2010). This anomalously high temperature in 2007 is considered to have been caused by the early sea ice reduction (Markus et al., 2009) and intensive solar heating caused by a stationary presence of anticyclonic circulation over the Chukchi Sea in that year (Mizobata et al., 2010; Vanin, 2010). Such drastic changes in recent hydrography in this region are considered to have had a substantial effect on the marine ecosystem, especially plankton (Grebmeier et al., 2006; Hunt and Drinkwater, 2007).

In the Chukchi Sea, zooplankton are important secondary producers and form a vital link between phytoplankton and fishes or marine mammals (Lowry et al., 2004; Wassmann et al., 2006). The southern Chukchi Sea has high primary production enhanced by the inflow of nutrient–rich Pacific Water (Sambrotto et al., 1984; Springer and McRoy, 1993). Because the Pacific Water also transports zooplankton from the Bering Sea, this inflow has a significant effect on the spatial distribution of zooplankton biomass and species composition (Springer et al., 1989; Hopcroft et al., 2010; Matsuno et al., 2011).

The zooplankton community in the Chukchi Sea is dominated by both Arctic (*Calanus glacialis*) and Pacific (*Eucalanus bungii* and *Metridia pacifica*) copepods (Springer et al., 1989; Matsuno et al., 2011); small barnacle larvae (*Balanus crenatus*) can also became abundant after a phytoplankton bloom (Barnes, 1957; Crisp, 1962). Zooplankton community structure in the southern Chukchi Sea varies geographically and is governed by water masses (Springer et al., 1989; Hopcroft et al., 2010). Although most of the studies of zooplankton in the western Arctic Ocean have treated large geographic areas, such as the Beaufort Sea (e.g., Thibault et al., 1999; Ashjian et al., 2005; Darnis et al., 2008), few studies have been conducted in the Chukchi Sea, especially near the Lisburne Peninsula. It is expected that the zooplankton community in the western Arctic Ocean changed after 2007, when the drastic decrease of sea ice area was observed, but no studies have compared the zooplankton community structure between the 1990s (extended sea–ice coverage) and in recent years (reduced sea–ice coverage).

The zooplankton size spectrum is an important factor for evaluating marine ecosystem structure (Sheldon et al., 1972; Kerr, 1974), as are the growth rate and metabolic activity of zooplankton (Platt and Denman, 1977, 1978), but size measurements on zooplankton by microscopic observation are time–consuming and difficult to do accurately. To overcome these problems, an Optical Plankton Counter (OPC) instrument (Herman, 1988), which can measure zooplankton size and number quickly and accurately, has been used in various marine ecosystems (Herman, 1992; Huntley et al., 1995; Nogueira et al., 2004; Baird et al., 2008). Specifically, Normalised Biomass Size Spectra (NBSS) analysis (Platt and Denman, 1978) on zooplankton size spectrum data by OPC measurement was been used to evaluate marine ecosystems around the world (Nogueira et al., 2004; Herman and Harvey, 2006; Basedow et al., 2010). NBSS analysis can evaluate whether bottom–up or top–down controls are dominant in each marine ecosystem (Suthers et al., 2006; Moore and Suthers, 2006; Finlay et al., 2007). Thus, the combination of OPC and NBSS analyses may help us evaluate the characteristics of zooplankton in the Chukchi Sea. However, few studies have been made on zooplankton size spectra in this region.

In the present chapter, I examine year–to–year changes in the zooplankton community and zooplankton size spectra in the Chukchi Sea in 1991 and 1992 (years with extended sea ice area) and in 2007 and 2008 (years with reduced sea ice area). Based on the whole–year zooplankton abundance data, zooplankton community clustering and year–to–year changes in abundance, biomass and community structure were evaluated. Year–to–year changes in stage composition of large copepods were also revealed. The NBSS analysis was performed on each clustered group. Based on NBSS data, I evaluated zooplankton productivity in summer in the Chukchi Sea and clarified the ecosystem characteristics of the Chukchi Sea through comparison with other oceans. The effects of sea–ice reduction on the zooplankton community in the western Arctic Ocean are also discussed.

4–2. Materials and Methods

4–2–1. Field sampling

A total of 120 zooplankton samplings were conducted by the T/S *Oshoro–Maru*, Hokkaido University, in the Chukchi Sea (66°00′–71°11′N 162°02′–168°58′W) during 24–31 July 1991 (*n* = 27), 24–31 July 1992 (*n* = 34), 5–13 August 2007 (*n* = 31) and 7–13 July 2008 (*n* = 28) (Fig. 12). Samples were collected during day or night by vertical tows with a NORPAC net (mouth diameter 45 cm, mesh size 0.335 mm) from 5 m above the bottom (depths of most stations were approximately 50 m). The volume of water filtered was estimated by reading a flow–meter (Rigosha Co. Ltd.) mounted on the net ring. The volume filtered ranged from 2.1 to 10.1 m^3 (mean±sd: 5.5±1.6 m^3). This large range of filtered volumes was caused by the large differences in net towing depth (25–63 m, mean 45 m), which was determined by the water depth at each station. Once on board, samples were immediately preserved with 5% v/v borax–buffered formalin. At each sampling station, temperature and salinity were mea-

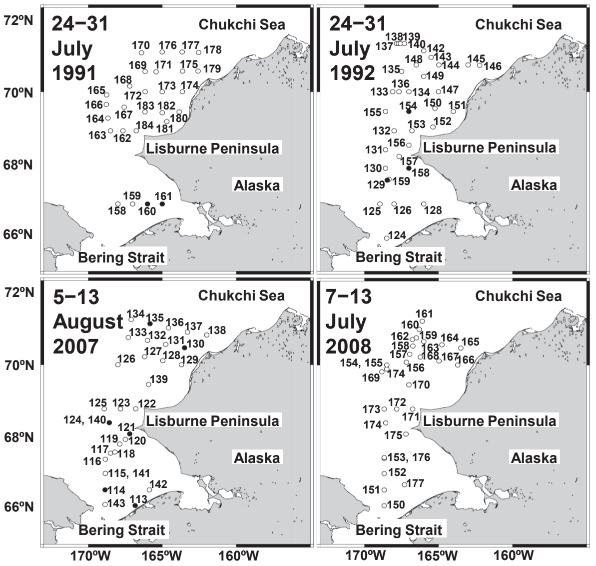

Fig. 12. Location of the sampling stations in the Chukchi Sea during July–August of 1991, 1992, 2007 and 2008. The open and solid symbols denote stations at which the samplings were conducted during the day and night, respectively.

sured by CTD (Neil Brown, Mark 3B [1991 and 1992] or Sea–Bird Electronics Inc., SBE 911 Plus [2007 and 2008]) casts. These hydrographic data have been published elsewhere (Hokkaido University, 1992, 1993, 2008, 2009).

4–2–2. Microscopic analysis

In the land laboratory, zooplankton samples were split using a Motoda box splitter (Motoda, 1959), and half of the aliquots were weighed for wet mass (WM) with a precision of 0.01 g using an electronic balance (Mettler PM4000). Zooplankton in the remaining aliquots were identified and counted under a dissecting microscope. Calanoid copepods were identified to species and copepodid stage level. Identification of copepods mainly followed Brodsky (1967), but identification of *C. marshallae* and *Pseudocalanus* spp. (*P. acuspes*, *P. major*, *P. mimus*, *P. minutus* and *P. newmani*) followed Frost (1974, 1989). Identification of *Pseudocalanus* species late copepodid stages (C5F/M and C6F/M) was made at the species level, but early copepodid stages (C1–C4) were treated as *Pseudocalanus* spp. because of the difficulty in species–level identification. Because of the large mesh size used (335 μm), there may be some underestimations of smaller zooplankton forms (*Pseudocalanus* spp. C1–C4 and Cyclopoida). The early copepodid stages of large copepods (e.g., *C. glacialis*, *E. bungii* and *M. pacifica*) were sampled quantitatively, and their Mean Copepodid Stage (*MCS*) was calculated using the following equation:

$$MCS = \frac{\sum_{i=1}^{6} i \times Ai}{\sum_{i=1}^{6} Ai} \qquad (3)$$

where i (1–6 indicate C1–C6) is the copepodid stage for a species, and Ai (ind. m^{-2}) is the abundance of the copepodid stage (cf. Marin, 1987).

4–2–3. Cluster analysis

Zooplankton samplings were conducted during July and August (Arctic summer), and daytime sampling accounted for 91% of the sampling stations (Fig. 12), so I made no day–night conversions on the abundance or biomass data. Abundance data (X: ind. m^{-2}) for each species were transformed to $\log_{10}(X+1)$ prior to cluster analysis to reduce the bias of the abundant species. Similarities between samples were examined using the Bray–Curtis index (Bray and Curtis, 1957) according to the differences in species composition. For grouping the samples, the similarity indices were coupled with hierarchical agglomerative clustering with a complete linkage method (Unweighted Pair Group Method using Arithmetic mean: UPGMA) (Field et al., 1982). Nonmetric Multi–Dimensional Scaling (NMDS) ordination was performed to delineate the sample groups on a two–dimensional map. All of these analyses were performed using PRIMER v6. Multiple–regression analysis was performed for dependent hydrographic variables (latitude, longitude, depth, integrated mean temperature and salinity) and two–dimensional NMDS as independent variables. A species diversity index (H') was calculated for each group using the following equation:

$$H' = -\sum n/Ni \times \ln n/Ni \qquad (4)$$

where n is the abundance (ind. m^{-2}) of the ith species, and Ni is the total zooplankton abundance (ind. m^{-2}) in the group (Shannon and Weaver, 1949). This calculation was made for all zooplankton taxa (not limited to copepods) because zooplankton taxa other than copepods (e.g., barnacle larvae) dominated at some stations. Inter–group differences in abundance of each copepod and zooplankton taxon, and the *MCS* values of large copepods were tested with one–way ANOVA. If the ANOVA identified statistically significant differences ($p < 0.05$), an ex post facto test with Fisher's Protected Least Significant Difference test (PLSD) was performed to clarify the interaction between groups.

4–2–4. OPC analysis

In the land laboratory, 1/8–1/2 of the aliquots of the zooplankton samples, separated using a Motoda box splitter (Motoda, 1959), were used for OPC measurement (OPC–1L: Focal Technologies Corp.). The OPC can measure the number of particles in 4,096 size categories between 0.250 and 20 mm ESD with a precision of 0.001–0.021 mm. Because I collected samples with vertical hauls of a NORPAC net, large plankton such as giant jellyfish (Brodeur et al., 2008) and euphausiids (Ashjian et al., 2010) were not quantitatively collected. Because of this, OPC analysis treated only mesozooplankton in the size range of 0.25–5.0 mm ESD, which is collected with the mesh size I used. Measurements of size number were made using an adequate flow rate (10 L min^{-1}) and particle density (< 10 counts sec^{-1}) according to the procedures of Mullin et al. (2000) and Yokoi et al. (2008). In addition to whole-sample measurements, OPC measurements were made for individuals (i.e., each copepodid stage of the dominant copepods (*Calanus glacialis* and *Pseudocalanus* spp.) and barnacle larvae (*Balanus crenatus*), sorted from the samples).

Based on the OPC data, NBSS was calculated following the procedure of Suthers et al. (2006). Zooplankton biovolume (B: mm^3 m^{-3}) was calculated in each of the 48 size classes. To calculate the X axis of NBSS ($\log_{10}$ zooplankton biovolume [mm^3 ind.$^{-1}$]), B was divided by the abundance of each size class (ind. m^{-3}) and converted to $\log_{10}$. To calculate the Y axis of NBSS ($\log_{10}$ normalised biovolume [mm^3 m^{-3}] / Δbiovolume [mm^3]), B was divided by interval of biovolume between a consecutive size class (Δbiovolume [mm^3]), and converted to $\log_{10}$. Based on these data, the NBSS linear model: $Y = aX + b$, where a and b are the slope and intercept of the NBSS, respectively (Platt and Denman, 1978), was calculated for each group.

4–3. Results

4–3–1. Hydrography

Throughout the study area, sea surface and bottom temperatures ranged from −0.9 to 14.0°C and −1.7 to 8.0°C, respectively (Fig. 13a). In 1991, 1992 and 2008, sea surface temperatures ranged from −0.9 to 9.6°C (mean: 4.8°C), but in 2007, they were 3.9 to 14.0°C (mean: 9.7°C), substantially higher than in the other years (one-way ANOVA, $p < 0.0001$). Sea surface and bottom salinities ranged from 25.3 to 32.9 and 30.7 to 33.5, respectively (Fig. 13b). Sea surface salinities in 1991, 1992 and 2008 ranged from 25.3 to 32.8, but in 2007, they ranged from 30.0 to 32.9 and were significantly higher than in the other years (one-way ANOVA, $p < 0.0001$), although bottom salinity did not show interannual variability (Fig. 13b).

The water masses in the Chukchi Sea during summer were separated into three water masses based on salinity: Surface Mixed Layer Water (SMLW, salinity < 30), Eastern Chukchi Summer Water (ECSW, salinity of 31–32) and Western Chukchi Summer Water (WCSW, salinity > 32) (Shimada et al. 2001). Based on sea surface temperature and surface salinity, all stations in 2007 belonged to ECSW, and all stations in the other years belonged to SMLW (Fig. 13). The surface salinities were significantly lower in 1991 and 1992 than in 2007 and 2008 (one-way ANOVA, $p < 0.0001$).

4–3–2. Zooplankton abundance and biomass

Zooplankton abundance ranged from 4,000 to 316,000 ind. m^{-2} (mean: 70,000) (Fig. 14a). Abundance in 1991, 1992 and 2008 was greatest for north of the Lisburne Peninsula, while in 2007, it was greatest south of the Peninsula (Fig. 14a). Zooplankton biomass ranged from 0.07 to 286 g WM m^{-2} (mean: 36 g WM m^{-2}). The geographic distribution of biomass was not parallel with abundance except for south of the Lisburne Peninsula in 2007 (Fig. 14b).

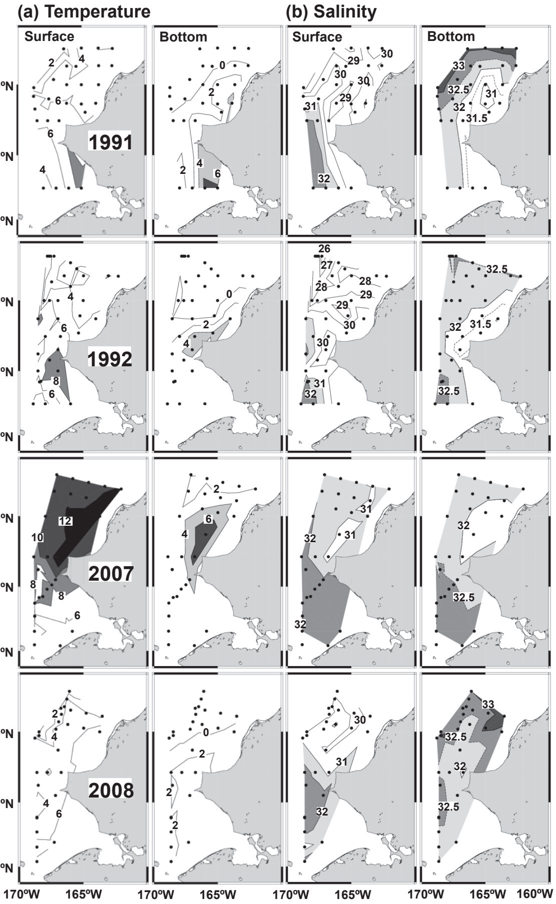

Fig. 13. Temperature (a) and salinity (b) of the sea surface (left) and bottom (right) of the stations in the Chukchi Sea during July–August of 1991, 1992, 2007 and 2008.

During the four years of analysis, 22 species of calanoid copepods belonging to 13 genera were identified (Table 6). Among these species, 6 species belonging to 4 genera were Pacific copepods: *C. marshallae*, *E. bungii*, *M. pacifica*, *N. cristatus*, *N. flemingeri* and *N. plumchrus* (Springer et al., 1989).

4–3–3. Year-to-year changes in zooplankton

Statistical analyses of year-to-year changes in zooplankton abundance showed significant differences for 21 taxa/species (Table 6). The abundance of total copepods was the highest in 2007, while that of total zooplankton was the highest in 2008. Significantly abundant taxa/species in each year were the Appendicularia in 1991, the Arctic copepod *C. glacialis* in 1992, various copepods (*Acartia tumida* Willey, *Centropages abdominalis* Sato, Cyclopoida, *E. bungii*, *M. pacifica*, *Microcalanus pygmaeus* (Sars), *N. cristatus*, *P. minutus* and *Scolecithricella minor* (Brady)), Echinodermata larvae and Polychaeta in 2007, and several copepods (*Eurytemora herdmani* Thompson and Scott, *N. plumchrus* and *Tortanus discaudatus* (Thompson and Scott)), barnacle larvae (*B.*

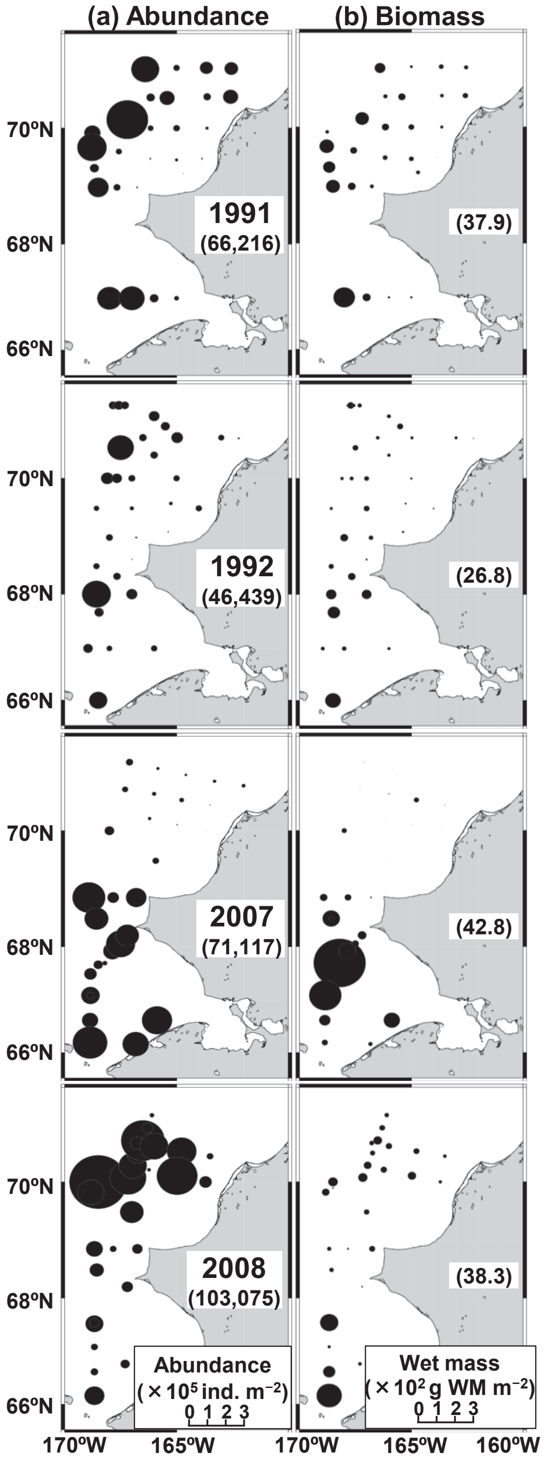

Fig. 14. Horizontal distribution of the abundance (a) and biomass (b) of mesozooplankton in the Chukchi Sea during July–August of 1991, 1992, 2007 and 2008, as analysed by OPC.

crenatus), Eubrachyura zoeae and *Limacina helicina* (Phipps) in 2008. Since Pacific copepods were dominant in 2007, total copepod abundance was the greatest that year. Although barnacle larvae were dominant in 2008, total zooplankton abundance was also the highest (Table 6).

Year-to-year changes in the *MCS* of the large copepod *C. glacialis*, *E. bungii* and *M. pacifica* were tested by one-way ANOVA. The *MCS* of *C. glacialis* and *M. pacifica* in 2007 was significantly higher (because of domination by the late copepodid stage and faster growth) than in other years (Table 7).

4-3-4. Zooplankton community

Based on the taxon abundance, zooplankton communities were classified into six groups (A–F) by cluster analysis with 28% and 34% dissimilarities (Fig. 15a). The number of stations where each group was found varied between 3 and 60, and groups C and F were considered to be out-groups because few stations (3–4 stations) belonged to either group (Fig. 15a). Environmental parameters significantly affecting cluster analysis were latitude, longitude, sea surface temperature, sea surface salinity and bottom salinity, with 24–37% coefficient of determinations (r^2) (Fig. 15b). Mean abundances of groups A, B and D ranged from 76,800 to 101,030 ind. m^{-2}, but those of groups C, E and F were lower (5,744 to 30,283 ind. m^{-2}) (Fig. 15c). For groups B, C and E, barnacle larvae dominated, and species diversities were low. Groups A, D and F had few barnacle larvae and many Pacific copepods (groups A, D) or Arctic copepods (group F) (Fig. 15c). The species diversity of groups A and D was high because of the occurrence of both Pacific and Arctic copepods.

The distribution of each group was well separated both geographically and interannually (Fig. 16). Group B was observed offshore north of the Lisburne Peninsula, and group E was observed inshore in the same region (Fig. 16). Group A was observed south of the Peninsula in 1991 and 1992 but north of it in 2007 and 2008. Group D, which was dominated by Pacific copepods, occurred only south of the Peninsula in 2007.

The geographic distribution of zooplankton was similar in 1991 and 1992 (Fig. 16). However, in 2007, the entire distribution area shifted northward, while group D, characterised by the dominance of Pacific copepods, occurred south of the Lisburne Peninsula. In 2008, the geographic distribution of groups was similar to that in 1991 and 1992, but group A, which was found south of the Lisburne Peninsula in 1991 and 1992, also occurred north of the Peninsula (Fig. 16).

The slope of NBSS for each group ranged from −0.61 to −1.09 (Table 8). Results for mean NBSS for each group are shown in Fig. 17. The slopes showed significant inter-group differences ($p < 0.0001$, one-way ANOVA). The slope of NBSS was steeper in the following order: D > A, B > C > E > F (Fig. 17).

4-4. Discussion

4-4-1. Year-to-year changes

Year-to-year characteristics of hydrographic environment, zooplankton biomass, community structure, species diversity

Table 6. Year to year comparison of zooplankton abundances in the Chukchi Sea during July–August of 1991, 1992, 2007 and 2008. Values are mean abundances in each year. Differences between years were tested by one-way ANOVA and post-hoc test by Fisher's PLSD. Any years not connected by the underlines are significantly different ($p < 0.05$). Numbers in the parentheses indicate number of stations in each year. *: $p < 0.05$, **: $p < 0.01$, NS: not significant.

Species	Abundance (ind. m^{-2})				one-way ANOVA	Fisher's PLSD			
	91 (27)	92 (34)	07 (31)	08 (28)					
Acartia hudsonica	13	31	64	37	NS				
Acartia longiremis	181	255	247	277	NS				
Acartia tumida	0	0	31	0	*				07
Calanus marshallae	11	50	40	11	NS				
Calanus glacialis	2,019	5,565	1,038	1,266	**	07	08	91	92
Centropages abdominalis	403	5	6,665	199	**	92	08	91	07
Cyclopoida	358	1,144	1,210	202	*	08	91	92	07
Eucalanus bungii	540	560	5,305	159	**	08	91	92	07
Eurytemora herdmani	0	2	3	15	*		92	07	08
Epilabidocera amphitrites	0	0	5	0	NS				
Gaidius brevispinus	0	1	0	0	NS				
Metridia pacifica	33	972	4,906	96	**	91	08	92	07
Microcalanus pygmaeus	7	18	412	41	*	91	92	08	07
Neocalanus cristatus	6	5	44	34	**	92	91	08	07
Neocalanus flemingeri	49	72	34	42	NS				
Neocalanus plumchrus	51	83	163	271	**	91	92	07	08
Pseudocalanus spp. (C1–C4)	2,562	3,068	2,877	4,186	NS				
Pseudocalanus acuspes	1,488	1,279	2,363	1,987	NS				
Pseudocalanus major	1,222	306	449	502	NS				
Pseudocalanus mimus	662	311	474	614	NS				
Pseudocalanus minutus	1,182	2,239	3,481	2,011	*	91	08	92	07
Pseudocalanus newmani	2,091	3,498	3,853	1,671	NS				
Scolecithricella minor	0	6	80	23	*		92	08	07
Tortanus discaudatus	0	0	0	17	*				08
Amphipoda	3	5	36	1	NS				
Appendicularia	9,461	2,808	5,129	2,107	**	08	92	07	91
Balanus crenatus (nauplius and cypris larva)	39,625	19,114	20,029	79,899	**	92	07	91	08
Bivalvia larva	0	0	495	48	NS				
Chaetognatha	958	581	1,060	721	NS				
Clione limacina	12	170	50	110	NS				
Echinoidea larva	0	0	1,420	14	**			08	07
Eubrachyura zoea	49	96	29	221	**	07	91	92	08
Euphausiacea	1,475	1,237	967	1,958	NS				
Evadne spp.	56	2	190	2	NS				
Hydrozoa	500	922	2,171	1,422	NS				
Isopoda	14	76	27	123	NS				
Limacina helicina	24	29	9	84	*	07	91	92	08
Polychaeta	1,161	1,930	5,763	2,703	*	91	92	08	07
Total copepods	12,878	19,470	33,744	13,661	**	91	08	92	07
Total zooplankton	66,216	46,439	71,117	103,075	**	92	91	07	08

Table 7. Year to year comparison on mean copepodid stage of *C. glacialis*, *E. bungii* and *M. pacifica* in the Chukchi Sea during July-August of 1991, 1992, 2007 and 2008. Differences between years were tested by one-way ANOVA and post-hoc test by Fisher's PLSD. Any years not connected by the underlines are significantly different ($p < 0.05$). Values are mean copepodid stage±sd. Numbers in the parentheses indicate number of stations in each year. *: $p < 0.05$, **: $p < 0.01$.

Species	Mean copepodid stage				one-way ANOVA	Fisher's PLSD			
	91 (27)	92 (34)	07 (31)	08 (28)					
C. glacialis	3.32±0.63	3.61±0.81	4.34±0.52	2.92±0.69	**	08	91	92	07
E. bungii	3.44±2.32	3.85±1.39	2.91±0.90	3.85±1.22	NS				
M. pacifica	1.94±0.81	3.14±0.93	4.42±0.51	3.25±1.43	**	91	92	08	07

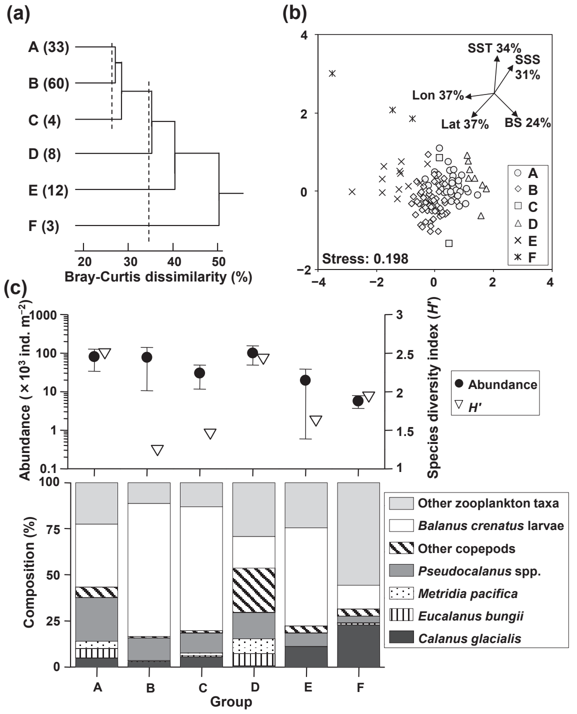

Fig. 15. Results of cluster analysis based on mesozooplankton biovolume size spectra in the Chukchi Sea (a). Six groups (A-F) were identified at a 28% and 34% Bray-Curtis dissimilarity connected with UPGMA. Numbers in the parentheses in (a) indicate the number of stations that each group contains. The NMDS plots of each group (b). The arrows and percentages in (b) indicate the directions of the environmental parameters and the coefficient of determination (r^2), respectively. BS: bottom salinity, Lat: latitude, Lon: longitude, SSS: sea surface salinity, SST: sea surface temperature. The mean biomass and size composition (ESD in mm) of each group (c).

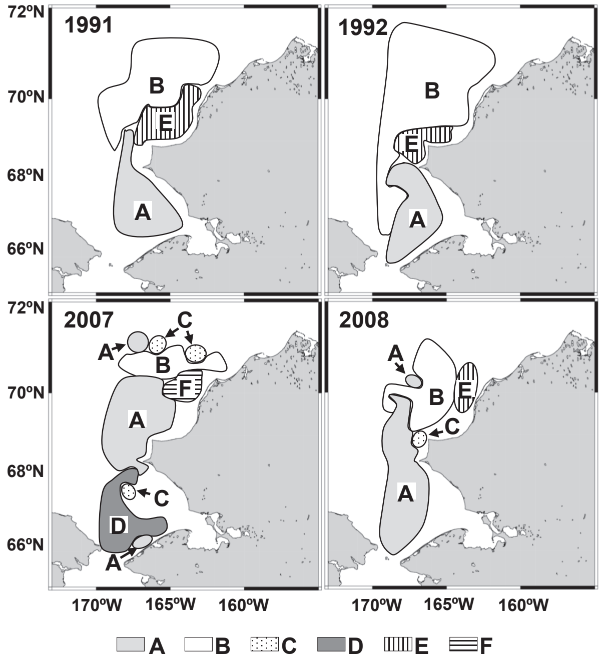

Fig. 16. Horizontal distributions of each group identified from Bray-Curtis similarity based on the zooplankton abundance (cf. Fig. 15a) in the Chukchi Sea during July-August of 1991, 1992, 2007 and 2008.

and growth of large copepods in each year are summarised in Table 9.

The years 1991 and 1992 showed similar characteristics, such as the presence of fresh and cold ice-melt water of the surface, low zooplankton biomass and low species diversity due to the dominance of small Arctic copepods and their slower development under the low temperature condition. Zooplankton in 1991 was characterised by the dominance of Appendicularia (mainly *Oikopleura vanhoeffeni*), which is occurs around the ice edge area of the Arctic Ocean (Acuña et al. 1999). The dominance of Appendicularia may have been related to the strong presence of ice-melt water.

Water mass formation in 2007 differed greatly from that in the other years. Warm and saline ECSW from the Pacific predominated throughout the stations. Zooplankton biomass was high south of the Lisburne Peninsula due to the dominance of large Pacific copepods transported by the ECSW. Zooplankton species diversity was also high in 2007, when the zooplankton comprised a mixture of Arctic and Pacific species. Warm temperature is the primary cause of faster development of copepods (cf. Corkett and McLaren, 1978). In 2007, large copepods (*C. glacialis* and *M. longa*) developed significantly faster than in other years. Because the population structure of *E. bungii* in 2007 was dominated by nauplii and early copepodid stages, which may reflect reproduction, this species had no significant year-to-year dif-

Table 8. Comparison on the slope (a) of NBSS ($Y = aX+b$) on mesozooplankton community from various locations. Numbers in the parentheses indicate range of slope.

Location/Region	Unit	Size range (mm)	Slope	References
Gulf of St. Lawrence (Open Water)	Biovolume	0.25–2	−0.47	Herman and Harvey, (2006)
Barents Srea	Biovolume	0.25–14	−0.63 (−0.44〜−0.91)	Basedow et al., (2010)
Tasman Sea	Biovolume	0.11–3.3	−0.69 (−0.59〜−0.78)	Baird et al., (2008)
Gulf of St. Lawrence (Estuay)	Biovolume	0.25–2	−0.90	Herman and Harvey, (2006)
Coral Sea	Biovolume	0.11–3.3	−0.97 (−0.94〜−0.99)	Baird et al., (2008)
South West Coral Sea	Wet mass	0.25–2.5	−1.00 (−0.49〜−1.31)	Suthers et al., (2006)
North Iberian Shelf	Carbon	0.25–17	−1.11 (−0.90〜−1.21)	Nogueira et al., (2004)
North Pacific Ocean	Carbon	0.18–4.0	−1.13	Rodriguez and Mullin, (1986)
Northwest Atlantic Ocean	Carbon	0.07–8.0	−1.14 (−1.09〜−1.17)	Quinones et al., (2003)
California Current	Carbon	0.20–3.3	−1.43 (−0.53〜−1.96)	Huntley et al., (1995)
Australian Estuary	Wet mass	0.25–1.6	−1.89 (−0.72〜−3.06)	Moore and Suthers, (2006)
Chukchi Sea (A: south in all years)	Biovolume	0.25–5	−0.96 (−0.62〜−1.13)	Chapter 4 in this study
Chukchi Sea (B: norh in all years)	Biovolume	0.25–5	−0.96 (−0.64〜−1.30)	Chapter 4 in this study
Chukchi Sea (C: interspersion in 2007/2008)	Biovolume	0.25–5	−0.87 (−0.64〜−1.24)	Chapter 4 in this study
Chukchi Sea (D: south in 2007)	Biovolume	0.25–5	−1.09 (−0.89〜−1.23)	Chapter 4 in this study
Chukchi Sea (E: shore in 1991/1992/2008)	Biovolume	0.25–5	−0.74 (−0.55〜−1.10)	Chapter 4 in this study
Chukchi Sea (F: shore in 2007)	Biovolume	0.25–5	−0.61 (−0.48〜−0.71)	Chapter 4 in this study

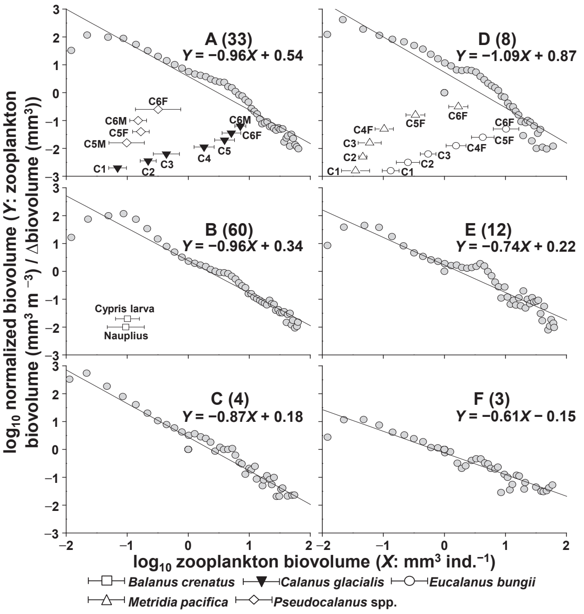

Fig. 17. Mean normalised biomass size spectra (NBSS) of four groups identified from cluster analysis on the mesozooplankton biovolume size spectra (cf. Fig. 15a) in the Chukchi Sea during July–August of 1991, 1992, 2007 and 2008. The numbers in the parentheses indicate the number of stations that belong to each group. For the dominant zooplankton species in each group (cf. Fig. 15c), the mean (symbols) and standard deviation (bars) data on each developmental stage are shown in the panel.

ferences in *MCS*.

In 2008, zooplankton characteristics were similar to those in 1991 and 1992, but the hydrography was characterised by high saline water in the surface layer, in contrast to the ice melt water in 1991–1992. In 2008, zooplankton biomass was low, but its abundance was the highest of the four years due to the dominance of small barnacle larvae (*B. crenatus*) (Table 6). Because of the predominance of barnacle larvae, species diversity was low. The moderate temperatures may have induced ordinary developmental rates of large copepods in that year.

Of the four years studied, 2007 was the most distinctive. According to Woodgate et al. (2010), the volume and temperature of inflowing PSW were the greatest and warmest from 1991 to 2007. The high volume of PSW may have induced high advection of large Pacific copepods and led to the high zooplankton biomass and high species diversity observed in that year. Higher temperatures may have led to faster development of large copepods in that year, which was observed in both a Pacific copepod (*M. pacifica*) and an Arctic copepod (*C. glacialis*). Therefore, the increase of inflow of the warm PSW is considered to have had a positive effect on the zooplankton community in terms of biomass and development of large copepods.

Comparison between 1991 and 1992 (much sea ice) and 2007–2008 (reduced sea ice) showed a remarkable northward shift in the distribution of zooplankton communities (Fig. 16). This northward shift may have been related to differences in the formation of water masses. The greatest differences in the hydrographic environment between 1991–1992 and 2007–2008 were in the presence (1991–1992) or absence (2007–2008) of sea ice melt water and in the salinity of surface layer, which was low in 1991–1992 and high in 2007–2008 (Fig. 13).

Table 9. Summary of the year-to-year comparisons in hydrography, zooplankton (biomass, community and diversity) and development of large copepods in the Chukchi Sea during July-August of 1991, 1992, 2007 and 2008. Values in the parentheses indicate mean±sd for sea surface salinity (SSS), temperature (SST) and biomass, and mean for *H′*. ECSW: Eastern Chukchi Summer Water.

Year	Hydrography (SSS, SST)	Zooplankton				Development of large copepods (cf. Table 7)
		Biomass (g WM m^{-2})	Community	Diversity (*H′*)	Slope of NBSS	
1991	Ice melt water (30.0±1.3, 5.2±1.7)	Low (38±26)	Arctic	Low (1.61)	Flat (−0.87±0.15)	Slow
1992	Ice melt water (29.4±1.9, 5.2±2.1)	Low (27±18)	Arctic	Low (2.18)	Flat (−0.90±0.12)	Slow
2007	ECSW (31.9±0.7, 9.7±2.6)	High (43±60)	Pacific+Arctic	High (2.56)	Steep (−0.91±0.20)	Fast
2008	High saline water (30.9±1.1, 4.3±1.9)	Low (38±27)	Arctic (*Balanus* larvae dominant)	Low (1.13)	Steep (−1.06±0.11)	Slow

The Arctic copepod *C. glacialis* was relatively abundant in 1991-1992 and less so in 2007-2008. The zooplankton community was dominated by Pacific copepods in 2007 and by barnacle larvae in 2008 (Table 6). The dominance of barnacle larvae in 2008 suggests that the larvae were released earlier from their benthic adult form than in 1991-1992.

Concerning the release timing of barnacle larvae from benthic adults, laboratory rearing studies have shown that food concentration (phytoplankton) is a key factor for release timing (Clare et al., 1984; Clare and Walker, 1986). Field studies also indicate that the onset of the phytoplankton bloom is a key factor stimulating the release of barnacle larvae (Barnes, 1957; Crisp, 1962). Because the sea surface salinity was higher in 2007-2008 than in 1991-1992 (Fig. 13b), the timing of sea-ice reduction was considered to have occurred earlier in 2007-2008 (Markus et al., 2009). This earlier sea ice reduction in 2007-2008 may have induced the earlier phytoplankton bloom in these years because of the earlier release from the light limitation on the photosynthesis. The earlier onset of the phytoplankton bloom in 2008 is considered to have been a cause of the dominance of the barnacle larvae in that year. Early sea ice reduction and onset of phytoplankton bloom also occurred in 2007, but the greater inflow of PSW that year forced the barnacle distribution area north (Fig. 16), leading to a lower abundance of barnacle larvae in 2007 than 2008.

4-4-2. Normalised biomass size spectrum

NBSS analysis based on the zooplankton biovolume size spectra is used to evaluate marine ecosystem structures from world-wide oceans (Herman and Harvey, 2006; Baird et al., 2008; Basedow et al., 2010). The slope of NBSS is an important index to assess marine ecosystem structure and its productivity (Rodriguez and Mullin, 1986; Splures and Munawar, 1986). Sheldon et al. (1972) reported that the slope of NBSS in a stable marine ecosystem is −1, and slopes higher and lower than −1 indicate that the ecosystems have high and low productivity, respectively (cf. Rodriguez and Mullin, 1986; Splures and Munawar, 1986). Slopes of NBSS in each group were in the order of D > A, B > C > E > F; the slope of group D was greater than −1, while those of the other groups were less than −1 (Table 8). The high NBSS slopes observed for group D (−1.09) indicate that that group was highly productive. The slopes of groups A and B (−0.96) were moderate, and the low NBSS slopes of the other groups (C, E and F) suggest that those groups were low in productivity. The high slopes of the top three groups were due to *Metridia pacifica* and *E. bungii* in group D, *Pseudocalanus* spp. and *C. glacialis* in group A, and barnacle larvae in group B (Table 6, Fig. 17).

Comparisons of the slopes of NBSS between the present study and previous studies from world-wide oceans are shown in Table 8. The slope of group D (−1.09) was close to the values from the North Pacific Ocean (−1.13) and the Atlantic Ocean (−1.14), whereas those of groups A and B (−0.96) were similar to those in coral seas (−0.97 to −1.00). Because the area south of the Lisburne Peninsula was occupied by group A throughout the four years (Fig. 16), the zooplankton community in this area is considered to have highly a productive ecosystem, due to continuous inflow of Pacific Water. In 2007, significantly higher production is observed in group D, south of the Lisburne Peninsula, with a mixture of Pacific and Arctic communities.

4-4-3. Future prospects in the Chukchi Sea

Year-to-year comparisons in this chapter revealed significant differences in zooplankton abundance, biomass and community structure (Table 9). As global temperature increases, a highly relevant issue in recent years, a large reduction of ice cover area and increased inflow of the PSW are expected to occur. Because PSW contains higher nutrient levels than Arctic water (Springer and McRoy, 1993; Cota et al., 1996), an increase of the inflow of the PSW is expected to induce the expansion of the high primary production area in the Chukchi Sea. Thus, in terms of primary production, global warming may have a positive function in this area.

From the viewpoint of zooplankton production, increased inflow of PSW induced the dominance of the large Pacific copepods, and thus may have positively affected productivity. However, the increased inflow of PSW caused changes in the marine ecosystem structure in the Chukchi Sea (loss of characteristic Arctic species in part of the region), which is considered a negative effect of global warming.

The zooplankton fauna is completely different between the Pacific and Arctic Oceans. The PSW contains various Pacific copepods, such as *E. bungii*, *M. pacifica*, *N. cristatus*, *N. flemingeri* and *N. plumchrus* (Springer et al., 1989). *Eucalanus bungii*, the dominant copepod in the PSW, has a diapause phase during autumn and winter and has a flexible generation length of 1–3 years (Miller et al., 1984; Tsuda et al., 2004; Shoden et al., 2005). Because the family Eucalanidae is a minor component of the North Atlantic and Arctic Oceans, the ecological niche that *E. bungii* occupies in the PSW is considered to be underutilised in these oceans. If this assumption is correct and the Pacific copepods colonise the Arctic Ocean, they may increase their population by utilising this vacant ecological niche. In the future Chukchi Sea, reduction of the ice–covered area may accelerate changes in the marine ecosystem structure. Therefore, a critical and continuous monitoring of the zooplankton community structure in this area is required.

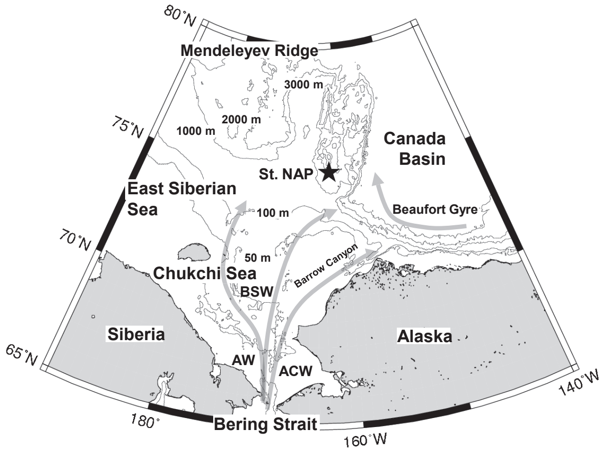

Fig. 18. Location of St. NAP (Northwind Abyssal Plain) in the western Arctic Ocean where the sediment trap was moored at 180 m during October 2010 to September 2011. ACW: Alaskan Coastal Water, AW: Anadyr Water, BSW: Bering Shelf Water.

5. Seasonal changes in mesozooplankton swimmers collected by sediment trap moored in the western Arctic Ocean

5–1. Introduction

Recently, a drastic reduction in the sea ice cover area has been observed in the Arctic Ocean during the summer. This reduction is considered to have been caused by an increased flow of warm Pacific Summer Water (PSW) from the Bering Sea Strait into the Arctic Ocean (Shimada et al., 2006; Woodgate et al., 2010). The Pacific sector of the Arctic Ocean comprises both shallow (Chukchi Sea and East Siberian Sea) and deep (Canada Basin and Mendeleyev Ridge) areas (Fig. 18). Sea ice reduction in this region has been the greatest in the Arctic Ocean (Shimada et al., 2001, 2006; Stroeve et al., 2007; Comiso et al., 2008; Markus et al., 2009), and this reduction in the sea ice is expected to alter the marine ecosystem structure in the Arctic Ocean (Grebmeier et al., 2006; Hunt and Drinkwater, 2007; Grebmeier, 2012). To evaluate the effects of sea ice reduction in the western Arctic Ocean, studies on plankton communities are necessary.

The zooplankton community in the western Arctic Ocean has been studied based on net samples (Springer et al., 1989; Hopcroft et al., 2010; Matsuno et al., 2011, 2012b). However, seasonal sea ice coverage in this area prevents the collection of net samples in the winter, and most of the studies were conducted only in the summer. To evaluate the seasonal changes in the zooplankton community, analysis on zooplankton swimmers collected by moored sediment trap is a powerful tool (cf. Forbes et al., 1992). Because the mass of zooplankton flux sometimes exceeds the passive particle flux and occasionally reaches more than tenfold of the passive flux, zooplankton flux could have an important role in the carbon cycle (Sampei et al., 2009, 2012). Because of their importance, seasonal changes in the zooplankton community collected by sediment trap have been studied in several areas of the Arctic Ocean, especially in the Beaufort Sea (Forbes et al., 1992; Ota et al., 2008; Makabe et al., 2010). According to Makabe et al. (2010), seasonal changes in the Arctic zooplankton community are related to the sea ice concentration, temperature and salinity. This relationship arises partly because large copepods migrate to the surface when the sea ice melts (Conover and Huntley, 1991); they graze on phytoplankton in the ice–edge bloom (Springer and McRoy, 1993) and then reproduce. The reproduction seasons of dominant copepods vary with the species and areas within the Arctic Ocean (Falk–Petersen et al., 2009). Despite their importance, few studies have examined zooplankton swimmers that are collected by sediment trap moored in the western Arctic Ocean, which prevents the accurate evaluation of the life cycle of Arctic copepods in this region.

In the present chapter, I analysed zooplankton swimmers that were collected by sediment traps that rotated at 13– to 15–day intervals moored at 180 m in the Northwind Abyssal Plain during October 2010 through September 2011. Through this analysis, seasonal changes in the zooplankton community structure and the population structure of the dominant copepods were evaluated. Lipid accumulation and gonad maturation of adult females (C6F) from the dominant copepods were analysed to evaluate their life cycle patterns. Seasonal occurrence of the Pacific copepods and carcasses of the Arctic copepods were also noted, and their possible causes were discussed.

5-2. Materials and Methods

5-2-1. Field sampling

Samples were collected by sediment trap (SMD26 S-6000, open mouth area 0.5 m^2, Nichiyu Giken Kogyo, Co. Ltd.) that were rotated at 13-15 day intervals and moored at 180 m at St. NAP (Northwind Abyssal Plain, 75°00′N, 162°00′W) during 4 October 2010 to 28 September 2011 (Fig. 18). The end of the trap rope was fixed to the sea bottom. The sample caps were filled with 5% buffered formalin before the sediment trap was deployed. After the trap was retrieved, the 26 samples were gently filtered with 1 mm mesh, and the remaining fraction (> 1 mm size) on the mesh was treated as zooplankton swimmers. The total mass flux data (mg dry mass m^{-2} day^{-1}) of a < 1 mm size fraction were provided by JAMSTEC. Time-series data on weekly averaged percentage ice coverage around St. NAP (74.5-75.5N, 161.5-162.5W) during the mooring period were calculated from the sea ice concentration data set (http://iridl.ldeo.columbia.edu/SOUR-CES/.IGOSS/.nmc/.Reyn_SmithOIv2/, cf. Reynolds et al., 2002). For the sea ice coverage data of the whole Arctic Ocean, the data were downloaded from the AMSER-E data set (http://www.ijis.iarc.uaf.edu/seaice/extent/plot.csv).

5-2-2. Analysis of zooplankton swimmers

For zooplankton swimmer samples, identification and enumeration of zooplankton was made under a dissecting microscope. Species identification of copepods followed mainly Brodsky (1967) and Frost (1989) for *Pseudocalanus* spp. (*P. minutus* and *P. newmani*), Frost (1974) for *Calanus* spp. (*C. glacialis* and *Calanus marshallae*), and Miller (1988) for *Neocalanus* spp. Identification of the four dominant calanoid copepods (*Calanus hyperboreus*, *Metridia longa*, *Heterorhabdus norvegicus* and *Paraeuchaeta glacialis*) was made to the copepodid stage level. For *C. hyperboreus*, *M. longa* and *P. glacialis*, the copepodid stage 6 females (C6Fs) contain a large oil sac in the prosome. To analyse the amount of oil, the oil length relative to the prosome length (PL) was scored into three groups: I (the lipid length is 0-4% of PL), II (4-40% of PL) and III (> 40% of PL). For the same three species, gonad maturation of the C6F was also scored into three groups: I (immature), II (small oocytes in ovary or oviduct) and III (large eggs or distended opaque in oviduct). For this gonad maturation index, I referred to those used previously for *C. hyperboreus* (Hirche and Niehoff, 1996) and *M. longa* (Tande and Grønvik, 1983). Of the four dominant copepods, only *H. norvegicus* was not analysed for lipid accumulation and gonad maturation, which was because of the difficulty in observation. *Heterorhabdus norvegicus* accumulate lipids in many small oil droplets, and the low transparency of the prosome prevents observation of their gonads. Species identification was also made for amphipods, the second most abundant taxon, following Vinogradov et al. (1996).

The flux (F, ind. m^{-2} day^{-1}) of the zooplankton swimmers was calculated from the following equation:

$$F = N \times \frac{1}{0.5} \times \frac{1}{d} \tag{5}$$

where N is the number of individuals (ind.), 0.5 is the mouth area (m^2) of the sediment trap, and d is the sampling interval (days). For the dominant copepods (*C. hyperboreus*, *M. longa*, *H. norvegicus* and *P. glacialis*), the Mean Copepodid Stage (*MCS*) was calculated from the following equation (Marin, 1987):

$$MCS = \frac{\sum_{i=1}^{6} i \times Fi}{\sum_{i=1}^{6} Fi} \tag{6}$$

where i (1-6 indicates C1-C6) is the copepodid stage, and Fi (ind. m^{-2} day^{-1}) is the flux of the ith copepodid stage.

5-2-3. Data analysis

Zooplankton flux data (F: ind. m^{-2} day^{-1}) for each species was log transformed ($\log_{10}[X+1]$) prior to analysis, to reduce the bias of the flux. Similarities between the samples were examined using the Bray-Curtis index (Bray and Curtis, 1957). To group the samples, the similarity indices were coupled with hierarchical agglomerative clustering using a complete linkage method (Unweighted Pair Group Method using Arithmetic mean: UPGMA) (Field et al., 1982). All of these analyses were conducted using PRIMER v6 software (PRIMER-E Ltd.). Inter-group differences in the flux of all of the zooplankton swimmers were tested by one-way ANOVA and an ex post facto test by Fisher's Protected Least Significant Difference test (PLSD). These statistical analyses were conducted using StatView v5 software (SAS Institute Inc.).

5-3. Results

5-3-1. Hydrography

The sea-ice area during the sampling period had the range 4.5-13.9×10^6 km^2 and was lowest in September (Fig. 19). Sea ice around the sediment-trap site showed clear seasonal changes, with a decrease from early July, complete melting (sea ice concentration: 0%) in September, a rapid increase during October, and 100% coverage during November to June. The total mass flux (< 1 mm size range) had the range 0.1-215.9 (mg DM m^{-2} day^{-1}) and peaked during November-December. During July to September, appendicularian houses were abundant in the > 1 mm size fraction (Fig. 19).

5-3-2. Zooplankton community

Based on the zooplankton flux, cluster analysis classified the zooplankton swimmer communities into three groups (A-C) at the 47% and 55% dissimilarity levels (Fig. 20a). The occurrences of each group showed distinct seasonality. Group A (n = 8) was observed from July through October, group B (n = 6) from November through January, and group C (n = 9) from March to June (Fig. 20b). The zoo-

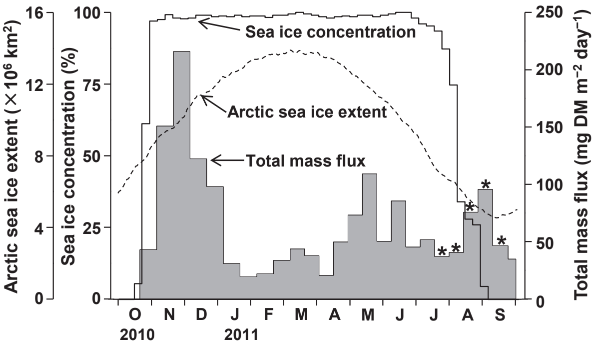

Fig. 19. Seasonal changes in the Arctic sea ice extent (http://www.ijis.iarc.uaf.edu/sea-ice/extent/plot.csv), the sea ice concentration during the sampling period (http://iridl.ldeo.columbia.edu/SOURCES/.IGOSS/.nmc/.Reyn_SmithOIv2/, the data from Reynolds et al., 2002) and the total mass flux (< 1 mm size fraction) collected by a sediment trap moored at 180 m of St. NAP during 4 October 2010 to 28 September 2011. *: Samples with abundant appendicularian houses in a > 1 mm size fraction.

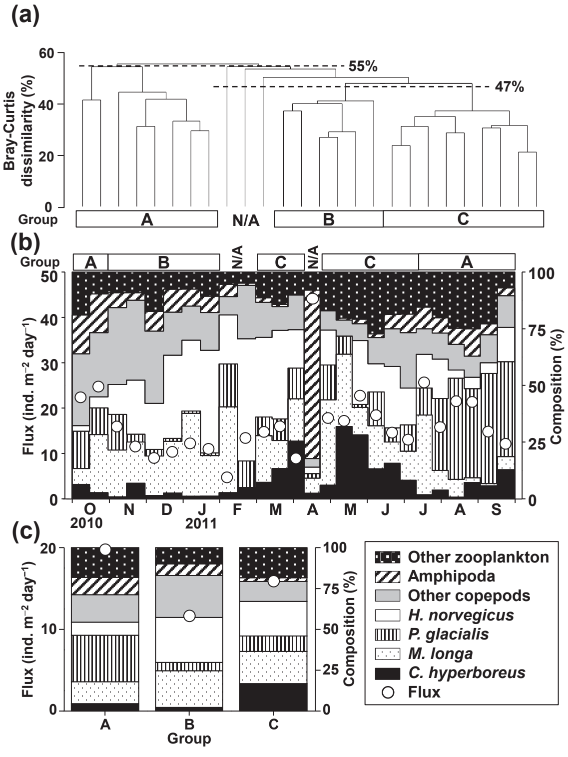

Fig. 20. Results of cluster analysis based on the flux of zooplankton swimmers. Twenty-six samples were clustered into three groups from the Bray-Curtis dissimilarity (a). Seasonal changes in the zooplankton swimmer flux, species composition and clustered groups collected by a sediment trap moored at 180 m of St. NAP during 4 October 2010 to 28 September 2011 (b). The mean zooplankton flux and species composition of each group (c).

plankton flux ranged from 5 to 44 ind. m^{-2} day^{-1} and was highest during July to October (Fig. 20b). The zooplankton flux was highest in A, lower in C, and lower in B (Fig. 20c). Copepods comprised 18 to 94% of the zooplankton flux and were the dominant taxon; amphipods were the second most dominant group (0–74%) (Fig. 20b). The characteristic species of each group were as follows: A, the mesopelagic copepods *Gaidius brevispinus* and *Paraeuchaeta glacialis*, the amphipod *Themisto libellula* and barnacle larvae; B, the amphipod *Mimonectes* sp.; and C, the inter-zonal copepod *Calanus hyperboreus* and Polychaeta (Table 10).

5–3–3. Copepod population structure

The population structures of the four dominant copepods (*C. hyperboreus*, *M. longa*, *H. norvegicus* and *P. glacialis*) varied with the species. Throughout the year, *C. hyperboreus* was predominated by C6F (Fig. 21a). The population structure of *M. longa* and *P. glacialis* showed seasonal changes; both were dominated by C6F from January through May, and early copepodid stages (C1–C4) occurred during June–October (Fig. 21b, c). *Heterorhabdus norvegicus* showed a different seasonal pattern; it was dominated by C5 during November–February; the composition of C6F/M increased during March–May, and the C1 and C2 stages occurred in June–July (Fig. 21d).

Lipid accumulation in C6Fs of the dominant copepods (excluding *H. norvegicus*) also showed species-specific seasonal patterns. Most *C. hyperboreus* contained more lipids (stage III) during December–January than during February–October (Fig. 22a). For *M. longa*, full-lipid individuals dominated during October–December, their composition gradually decreased during March to June, and all specimens had no oil sacs in July (Fig. 22b). The lipid accumulation of *P. glacialis* showed little seasonal change (Fig. 22c).

Gonad maturation of C6Fs of the dominant copepods (excluding *H. norvegicus*) showed more distinct seasonality. For *C. hyperboreus*, mature individuals were observed only during February–April (Fig. 22d). Mature *M. longa* was observed only during March to June (Fig. 22e), with the lipid accumulation decreased (Fig. 22b). Most *P. glacialis* matured during August–December (Fig. 22f), when eggs carrying *P. glacialis* C6Fs were also observed.

5–3–4. Other zooplankton fluxes

The Pacific copepod *Neocalanus cristatus* occurred (0–0.92 ind. m^{-2} day^{-1}) throughout the year and was higher during August–September when the sea ice was reduced (Fig. 23a). All *N. cristatus* were stage C5, and the lipid accumulation varied. Carcasses of *C. glacialis* that had been cut in half were observed during only May–July. Their flux ranged 0–0.62 ind. m^{-2} day^{-1} (Fig. 23b), and various copepodid stages (C4–C6) were observed (Fig. 23c).

5–4. Discussion

5–4–1. Seasonal changes in the zooplankton community

Seasonal changes in the zooplankton community structure, the population structure and reproduction period of the dominant copepods and the other events are summarised in

Table 10. Mesozooplankton fluxes collected by the sediment trap moored at 180 m of St. NAP during 4 October 2010 to 28 September 2011. Values are means and standard deviations of the three groups identified by Bray-Curtis dissimilarity (cf. Fig. 20a). Differences between groups were tested by one-way ANOVA and post-hoc test by Fisher's PLSD. Any groups not connected by the underlines are significantly different ($p < 0.05$). Numbers in the parentheses indicate number of samples included in each group. *: $p < 0.05$, **: $p < 0.01$, ***: $p < 0.001$, NS: not significant.

Species	Flux (ind. m^{-2} day^{-1})			one-way ANOVA	Fisher's PLSD
	A (8)	B (6)	C (9)		
Copepoda					
Acartia longiremis	0.02±0.05	0	0	NS	
Aetideopsis multiserrata	0.23±0.32	0.33±0.25	0.24±0.17	NS	
Aetideopsis rostrata	0	0.27±0.37	0	NS	
Calanus glacialis	0.15±0.17	0.42±0.32	0.43±0.38	NS	
Calanus hyperboreus	0.91±0.54	0.27±0.27	2.72±1.96	**	B A C
Chiridius obtusifrons	0.27±0.31	0.56±0.86	0.09±0.16	NS	
Chiridiella reducta	0.08±0.16	0	0.02±0.05	NS	
Cyclopoida	0	0.04±0.11	0	NS	
Epilabidocera amphitrites	0.02±0.05	0.02±0.05	0	NS	
Gaidius brevispinus	0.39±0.33	0.07±0.11	0.09±0.21	*	B C A
Gaidius tenuispinus	0.36±0.36	0.87±0.70	0.58±0.32	NS	
Heterorhabdus compactus	0	0.02±0.05	0.03±0.10	NS	
Heterorhabdus norvegicus	1.60±1.16	3.27±1.22	3.42±2.23	NS	
Lucicutia anomala	0.02±0.05	0	0	NS	
Metridia longa	2.68±3.25	2.67±1.08	3.16±1.86	NS	
Metridia pacifica	0	0.02±0.05	0	NS	
Microcalanus pygmaeus	0.03±0.09	0	0.05±0.08	NS	
Neocalanus cristatus	0.26±0.30	0.02±0.05	0.09±0.11	NS	
Oncaea spp.	1.11±1.80	0.29±0.20	0.19±0.23	NS	
Paraeuchaeta glacialis	5.68±2.54	0.60±0.95	1.52±0.80	***	B C A
Pseudaetideus armatus	0	0	0.02±0.05	NS	
Pseudocalanus minutus	0.03±0.09	0.04±0.07	0.02±0.05	NS	
Pseudocalanus newmani	0.02±0.05	0	0	NS	
Scaphocalanus magnus	0.11±0.14	0.02±0.05	0.09±0.14	NS	
Spinocalanus longicornis	0.27±0.61	0.04±0.11	0.05±0.08	NS	
Tortanus discaudatus	0.02±0.05	0	0	NS	
Amphipoda					
Hyperia medusarum	0.42±0.50	0	0.27±0.43	NS	
Mimonecteola beebei	0.90±1.66	0.44±0.32	0	NS	
Mimonectes sp.	0.05±0.14	0.24±0.10	0.02±0.05	**	C A B
Proscina sp.	0.04±0.06	0	0	NS	
Themisto libellula	0.72±0.51	0.16±0.10	0.09±0.11	**	C B A
Appendicularia	0.76±0.83	0.27±0.33	0.19±0.17	NS	
Barnacle larva	0.37±0.51	0	0.02±0.05	*	C A
Bivalvia larva	0.05±0.15	0	0	NS	
Chaetognatha	0.06±0.11	0.11±0.10	0.14±0.18	NS	
Clione limacina	0.04±0.07	0.04±0.07	0	NS	
Decapoda	0.07±0.11	0	0	NS	
Echinoidermata larva	0.03±0.09	0.02±0.05	0.02±0.05	NS	
Eubrachyura zoea	0.24±0.45	0.02±0.05	0	NS	
Euphausiacea	0.02±0.05	0	0	NS	
Hydrozoa	0.12±0.19	0.13±0.15	0.14±0.12	NS	
Isopoda	0	0	0.02±0.05	NS	
Limacina helicina	0.25±0.28	0	0	NS	
Ostracoda	0.34±0.30	0.07±0.16	0.12±0.22	NS	
Polychaeta	0.52±0.31	0.22±0.14	1.25±0.50	***	B A C
Radiolaria	0.73±0.74	0.16±0.16	1.08±0.96	NS	
Total copepods	14.2±3.2	9.8±2.3	12.8±2.8	*	B C A
Total zooplankton	20.0±4.9	11.9±2.4	16.1±3.9	**	B C A

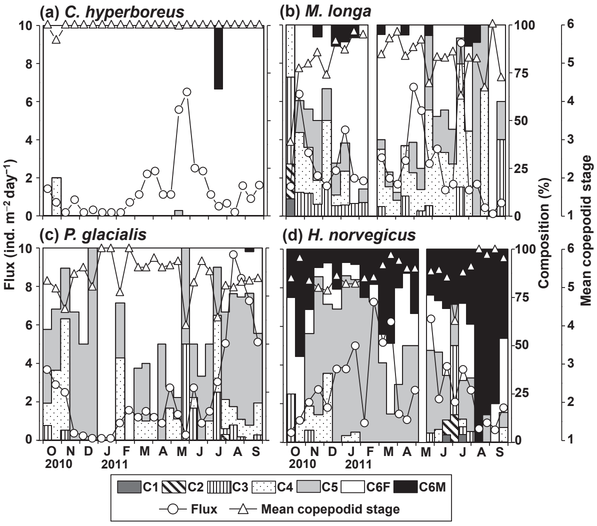

Fig. 21. Seasonal changes in the flux, copepodid stage composition and mean copepodid stage of the four dominant copepods: *Calanus hyperboreus* (a), *Metridia longa* (b), *Paraeuchaeta glacialis* (c), and *Heterorhabdus norvegicus* (d), at 180 m of St. NAP during 4 October 2010 to 28 September 2011.

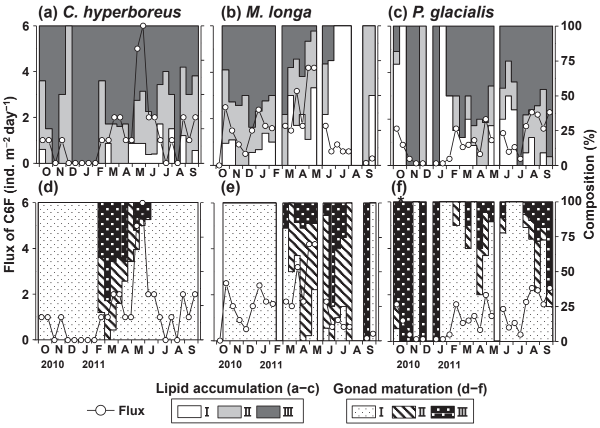

Fig. 22. Seasonal changes in the flux, lipid accumulation (upper panels) and gonad maturation (lower panels) compositions (stage I–III) of C6Fs of *Calanus hyperboreus* (a, d), *Metridia longa* (b, e) and *Paraeuchaeta glacialis* (c, f) at 180 m of St. NAP during 4 October 2010 to 28 September 2011. *: Egg sac attached to an individual.

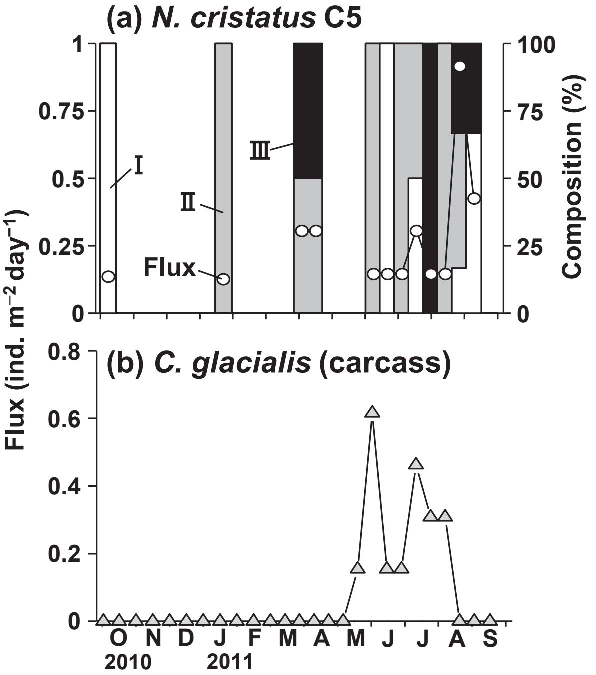

(c) *C. glacialis* (carcass)

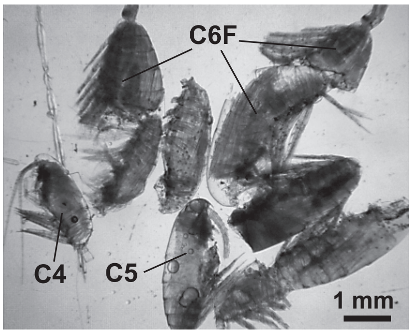

Fig. 23. Seasonal changes in the flux and lipid accumulation composition (I–III) of the Pacific *Neocalanus cristatus* C5 (a) and the carcass of the Arctic *Calanus glacialis* (b), as collected by a sediment trap that was moored at 180 m of St. NAP during 4 October 2010 to 28 September 2011. Picture on the carcasses of *C. glacialis* (c).

Fig. 24. The zooplankton community varied with the season: from July to October (group A), from November to January (group B), and from March to June (group C) (Fig. 24). Makabe et al. (2010) analysed zooplankton communities that were collected by a sediment trap that was moored at a 200 m depth in the southeast Beaufort Sea and reported that the communities varied during late autumn to winter and spring to early summer, and the changes in spring to early summer might have been related to the water temperature, salinity and sea ice concentration. In the present study, group A occurred during the no-ice period, which suggests that the presence or absence of ice coverage could affect the zooplankton community.

Group A was dominated by the carnivorous *P. glacialis* (3.7–9.4 times greater abundance than the other groups) (Table 10, Fig. 20c). This relationship could be related to the ice-edge bloom at the surface (Springer and McRoy, 1993), which induces the upward migration of Arctic copepods (e.g., *C. glacialis*) and reproduction in small copepods (e.g., *Pseudocalanus* spp.) (Conover and Huntley, 1991), which would provide the carnivorous *P. glacialis* food to grow and reproduce. For the dominant copepods, the reproduction season corresponded with their dominant season (Figs. 20b, 24).

During the ice coverage period (November–June), the zooplankton community changed from group B to C in February due to the drastic increase (ca. 10 times) of *C. hyperboreus* (Table 10). *Calanus hyperboreus* is known to perform sea-

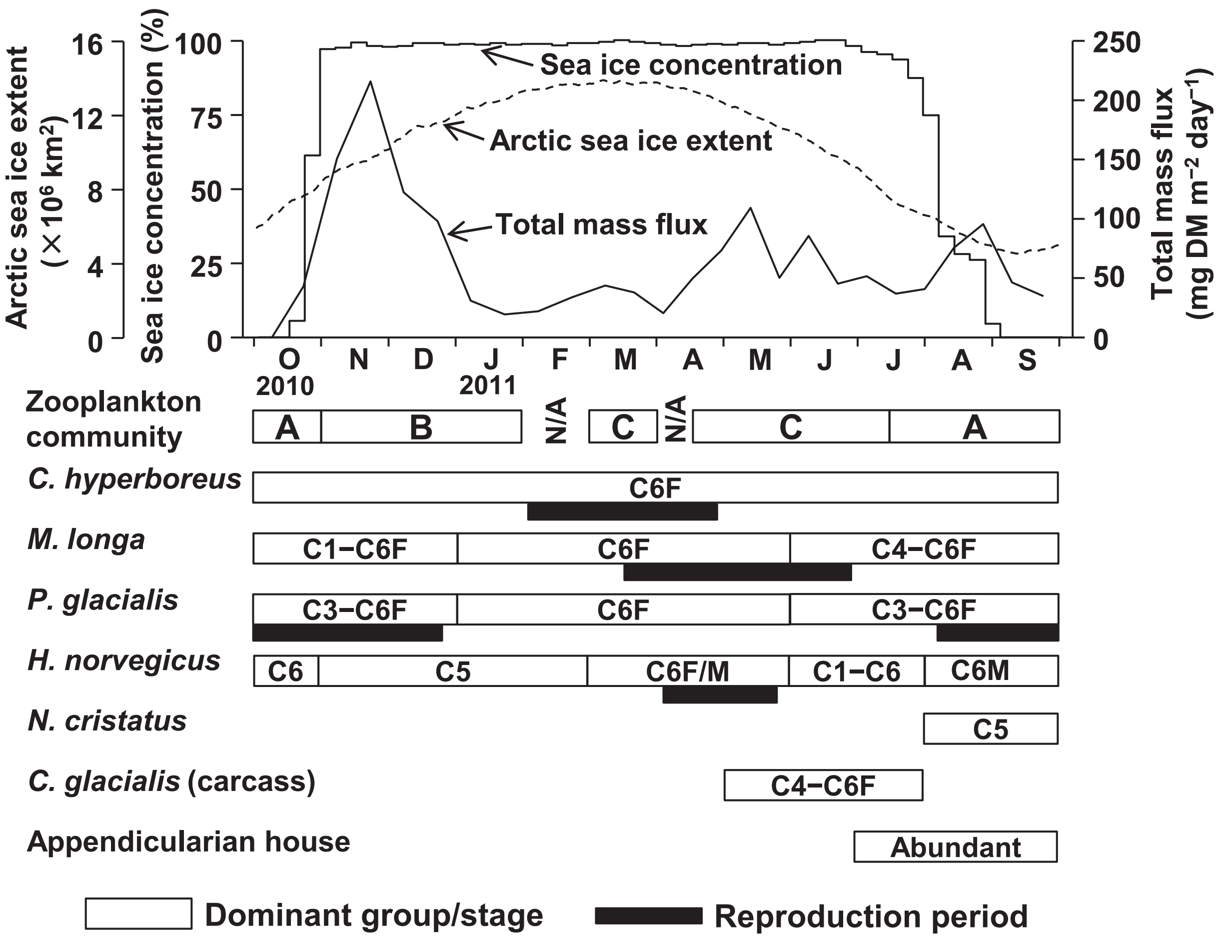

Fig. 24. Schematic diagram on the seasonal changes of the sea ice concentration, the total mass flux in a < 1 mm size fraction (upper panel), the zooplankton community, the population structure and the reproduction period of copepods (*C. hyperboreus*, *M. longa*, *P. glacialis* and *H. norvegicus*), and occurrences of the Pacific *N. cristatus*, carcass of the Arctic *C. glacialis* and appendicularian houses collected by a sediment trap at 180 m of St. NAP during 4 October 2010 to 28 September 2011 (lower panel). For *C. hyperboreus*, *M. longa* and *P. glacialis*, the reproduction period was evaluated by C6F gonad maturation (Fig. 22d–f). For *H. norvegicus*, their reproduction period was estimated by the occurrence of early copepodid stages (Fig. 21d).

sonal vertical migration (Hirche, 1997; Vinogradov, 1997), diapause at depths of (500–1,500 m) in winter, and make upward migration to the surface layer in April (Hirche and Niehoff, 1996). In the present chapter, it was shown that *C. hyperboreus* included only C6Fs, and their flux increased from February and peaked in May (Fig. 21a). This increase in the flux during February to May was presumably due to their upward migration from deep layers. Therefore, the change in the zooplankton community (from group B to C) during January–March might have been caused by the upward seasonal vertical migration of *C. hyperboreus*.

Three specialised seasonal events (i.e., the occurrence of appendicularian houses, Pacific copepods and carcasses of Arctic copepods) were observed. Appendicularian houses were abundant in the > 1 mm size class fraction during 10 July to 13 September (Fig. 19). A dominance of appendicularian houses in summer was also reported from the sediment trap samples collected in the Beaufort Sea (Forest et al., 2007). These facts suggest that appendicularian houses could have an important role in the vertical POC flux during the summer in the Arctic Ocean.

The Pacific copepod *N. cristatus* C5 was abundant during August–September when the sea ice coverage decreased (Fig. 24). This seasonal pattern suggests that the amount of the inflow Pacific Water could increase when the sea ice coverage decreases. While *N. cristatus* C5 is known to migrate to deep layers to diapause during late summer (Miller et al., 1984), the greater flux of *N. cristatus* C5 in August–September could also be caused by their ontogenetic vertical migration.

While *C. glacialis* is known to be the dominant copepod in the western Arctic Ocean (Hopcroft et al., 2010; Matsuno et al., 2012b), the only copepods that were collected by the sediment trap in this study (Table 10) were carcasses that had been cut in half during May to July (Fig. 24). *Calanus glacialis* is an important component of zooplankton biomass (Matsuno et al., 2012b) and feeds on various carnivorous zooplankton (Hobson et al., 2002). In the Arctic Ocean, Sampei et al. (2009) also observed the occurrence of many copepod carcasses in sediment trap samples. Before the dead copepods sink into a sediment trap, their swimming legs are reported to be pointed forward to the cephalosome (Sampei et al., 2009). Additionally in this study, the swimming legs of all of the half-cut carcasses of *C. glacialis* were pointed forward (Fig. 23c), and several carcasses were decomposed by bacteria. These facts suggest that the copepods were dead before entering the sediment trap. Because the flux of the carcasses reached a maximum at 91% of the POC flux in the Beaufort Sea, the flux of the carcasses is considered to have a significant role in the carbon cycle (Sampei et al., 2012). The large number of carcasses of *C. glacialis* could have been caused by a die off after reproduction (Sampei et al., 2012). However, this case might not have occurred in this study because the carcasses contained various stages from C4 to C6F. Presumably, the half-cut carcasses in this study were attacked by carnivorous zooplankton (*P. glacialis* or carnivorous amphipods). The carcasses were observed during only May–July (Fig. 24). After July, the abundance of carnivorous *P. glacialis* greatly increased by 3.7–9.4 times, and the species reproduces during August–December. Group A, which was observed during July to October, was characterised by the carnivorous amphipod *T. libellula* and the carnivorous copepod *P. glacialis* (Table 10). These facts suggest that these carnivorous zooplankton might have fed on *C. glacialis* near the surface layer before *C. glacialis* entered the sediment trap, to obtain sufficient energy for growth and reproduction.

5–4–2. Population structure of dominant copepods

The four dominant copepods that were collected in this study (*C. hyperboreus*, *M. longa*, *P. glacialis* and *H. norvegicus*) are dominant species in the basin of the Arctic Ocean (Ashjian et al., 2003; Matsuno et al., 2012b).

Calanus hyperboreus populations were composed of a substantial amount of C6F throughout the year (Fig. 21a). In the summer of the Greenland Sea and the central Arctic Ocean, C6F of *C. hyperboreus* are distributed at approximately 200 m in depth (Dawson, 1978; Hirche, 1997) and were collected by a sediment trap that is moored at 200 m depth in Amundsen Bay (Ota et al., 2008). Because our sediment trap was moored at 180 m, the results of this study (i.e., the predominance of C6F) correspond well with the results of previous studies. *Calanus hyperboreus* reproduces during November–April in Amundsen Bay (Ota et al., 2008), November–March in the Greenland Sea (Hirche and Niehoff, 1996), and February–March in the Norwegian Sea (Østvedt, 1955). In the present study, mature C6F were observed only from February to April, which suggests that this interval is the reproduction period (Fig. 24). This reproduction season (February–April) generally corresponds to previous studies that have slight seasonal variances. For the regional variability in the reproduction timing of *C. hyperboreus*, the timing of the phytoplankton bloom is reported to be the most important factor (Conover and Siferd, 1993; Hirche and Niehoff, 1996). Full-lipid individuals in stage C6F dominated in December–January, and the lipid accumulation decreased from February when the reproduction started (Fig. 22a). This seasonal correspondence between the reproduction period and the decrease in the lipid accumulation would be caused by the utilisation of the stored lipid for reproducing (Hirche and Niehoff, 1996; Vinogradov, 1997).

The *M. longa* population was dominated by C6F during January–May and by early copepodid stages (C1–C4) during June–October (Fig. 21b). *Metridia longa* is an omnivore, distributes in a deep layer (Ashjian et al., 2003), performs diel vertical migration (Conover and Huntley, 1991; Ashjian et al., 1995), and has no diapause phase (Båmstedt and Ervik, 1984; Grønvik and Hopkins, 1984). The main reproduction season shows regional variability: during April–May in the Balsfjorden (Tande and Grønvik, 1983), in winter under the sea ice in the Barents Sea (Hirche and Kosobokova, 2011), and in autumn in a polynya in the Beaufort Sea (Makabe et al., 2010). In this study, mature C6F occurred during only March–June (Fig. 22e), and early copepodid stages (C1–C4) dominated the population during June–October (Fig. 21b). These facts suggest that *M. longa* reproduces during March–June and that the new results appear during June–October. This reproduction season (March–June) in the western Arctic Ocean is slightly longer than that in the Balsfjorden (April–May) (Tande and Grønvik, 1983) and varies with those in the other regions. Full-lipid individuals dominated during October—December and decreased gradually over the winter, and no specimens had oil sacs in July (Fig. 22b). This season of decreasing lipids (March–June) parallel the gonad maturation season (March–June). These facts suggest that the stored lipids are used for gonad maturation of *M. longa,* as was observed in *C. hyperboreus*.

The *P. glacialis* population was dominated by C6F during January–May and contained early copepodid stages (C2–C4) during June–October (Fig. 21c). Carnivorous *Paraeuchaeta* spp. perform raptorial feeding throughout the year, accumulate a large amount of lipids, and have no diapause phase (Båmstedt, 1979; Øresland, 1991). For the lipid accumulation of *P. glacialis*, there was little seasonal variability (Fig. 22c). This pattern could occur because *P. glacialis* has no diapause phase. Because mature C6F *P. glacialis* dominated during August–December and egg-carrying C6F also occurred during the same period (Fig. 22f), this species is assumed to reproduce in this period. This reproduction season of *P. glacialis* (August–December) differs with those of *C. hyperboreus* (February–April) and *M. longa* (March–June). These differences could be related to differences in feeding modes, i.e., carnivory in *P. glacialis* and suspension feeding in *C. hyperboreus* and *M. longa*.

The *H. norvegicus* population was dominated by C5 during

November–February and C6F/M during March–May, and C1 and C2 were collected in June and July (Fig. 21d). Because lipid accumulation and gonad maturation could not be analysed for *H. norvegicus*, the reproduction season was estimated from the population structure data. Combining the dominance of early copepodid stages (June and July) and assuming the development time of *Heterorhabdus* spp. nauplii (1–2 months) (Yamaguchi and Ikeda, 2000), the reproduction season is thought to occur during April and May. Little comparable information is available for the life cycle of *H. norvegicus*. Thus, the reproduction seasons of the dominant four copepods differed (Fig. 24), and the possible causes of these differences include species-specific feeding modes, seasonal changes in food availability, and the presence/absence of ontogenetic vertical migration.

In conclusion, through the analyses on zooplankton swimmers collected by a sediment trap, zooplankton communities were clearly separated into three seasons (Fig. 24). The characterised species of each community varied with the season. The season when they dominated corresponded with the reproduction timing of each species. For the four dominant copepods, their reproduction timings varied with the species, which could be related to the feeding modes. In addition, the dominance of the appendicularian houses, the occurrence of the carcasses of various stages of *C. glacialis* and the occurrence of the Pacific copepods were observed. All three events occurred only during the period of low sea ice coverage (May–September), which suggests that the reduction in the sea ice has a large effect on the seasonal variability of zooplankton in the western Arctic Ocean.

6. Synthesis

6–1. Characteristics of the plankton community in the western Arctic Ocean

The characteristics of microplankton and mesozooplankton communities in the western Arctic Ocean during the summer are summarised in Fig. 25. The communities were divided into two regions (i.e., shelf and basin). In the shelf region, because of the inflow of the Pacific Water, which contains a high level of nutrients, the phytoplankton standing stock was high, and it was dominated by diatoms, and the mesozooplankton abundance was also high (Fig. 25).

Recently, in the shelf region (Chukchi Sea) of the western Arctic Ocean, the ice-free period has lengthened (Markus et al., 2009), and the primary production has been increasing (Arrigo et al., 2008). Previously, abundant ice algae attached on the sea-ice settled to the sea bottom and provided abundant food for the benthos community. However, in recent years, drastic sea-ice reduction has decreased the ice algae, and the zooplankton grazing impact on the phytoplankton in the water column has increased by a high temperature, which results in a decrease in the food supply to the benthos community (a change from a Pelagic-benthic coupling community to a pelagic-pelagic community: Grebmeier et al., 2006).

Additionally, in the NBSS analysis of the present study (Chapter 4), the zooplankton community in the southern Chukchi Sea was more productive in 2007 than in 1991/1992 (Fig. 17), which suggests that increased organic consumption by zooplankton grazing occurred in the water column during 2007. Thus, in the shelf region, an increased ice-free period and inflow of the Pacific Water are expected to result in increased primary production, while an increase in the zooplankton community and their feeding are expected to lead to a decrease in the material flux to the seafloor.

In the basin, the inflow of Pacific Water was severely limited, oligotrophic ice melt water covered the surface, a small Chl. *a* peak occurred in the sub-surface layer, dinoflagellates and ciliates were dominant, and the abundances of both microplankton and mesozooplankton community were extremely low (Fig. 25). In the Canada Basin, because the ice melt water increased at the surface layer, the halocline became stronger, the nutrient supply to the surface decreased, and the dominant-sized phytoplankton changed from nano-size to pico-size (Li et al., 2009). In addition, because of the increase in strength of the Beaufort Gyre, the halocline became deeper, and primary production was reported to decrease (Nishino et al., 2011b). Thus, in recent years in the basin of the western Arctic Ocean, primary production has been low. In such an environment, zooplankton standing stock will decrease.

In the basin, the Arctic copepod *C. hyperboreus* dominated the zooplankton biomass. Its generation length is long (usually 3 years) and has large regional flexibility (from 1 to 5 years) (Falk-Petersen et al., 2009). If primary production decreases in the basin of the western Arctic Ocean, the generation length of *C. hyperboreus* is expected to increase due to having more multiple diapauses at a high depth. In addition to changes in the life cycle, decreased primary production at the surface reduces the material flux that travels to the seafloor.

Thus, the recent changes in the plankton community could vary between the shelf and basin. In the shelf region, the primary production has increased, but organic consumption by zooplankton in the water column has also increased, and as a result, the vertical material flux to the bottom is thought to have decreased. While in the basin, a decrease in the primary production could induce lower vertical material flux to deep water. Thus, the mechanism varied between the regions, but decreases in the vertical material flux are expected to occur for both the shelf and basin regions of the western Arctic Ocean.

6–2. Fate of immigrant Pacific copepods in the Arctic Ocean

Increased transportation of the southern originating species

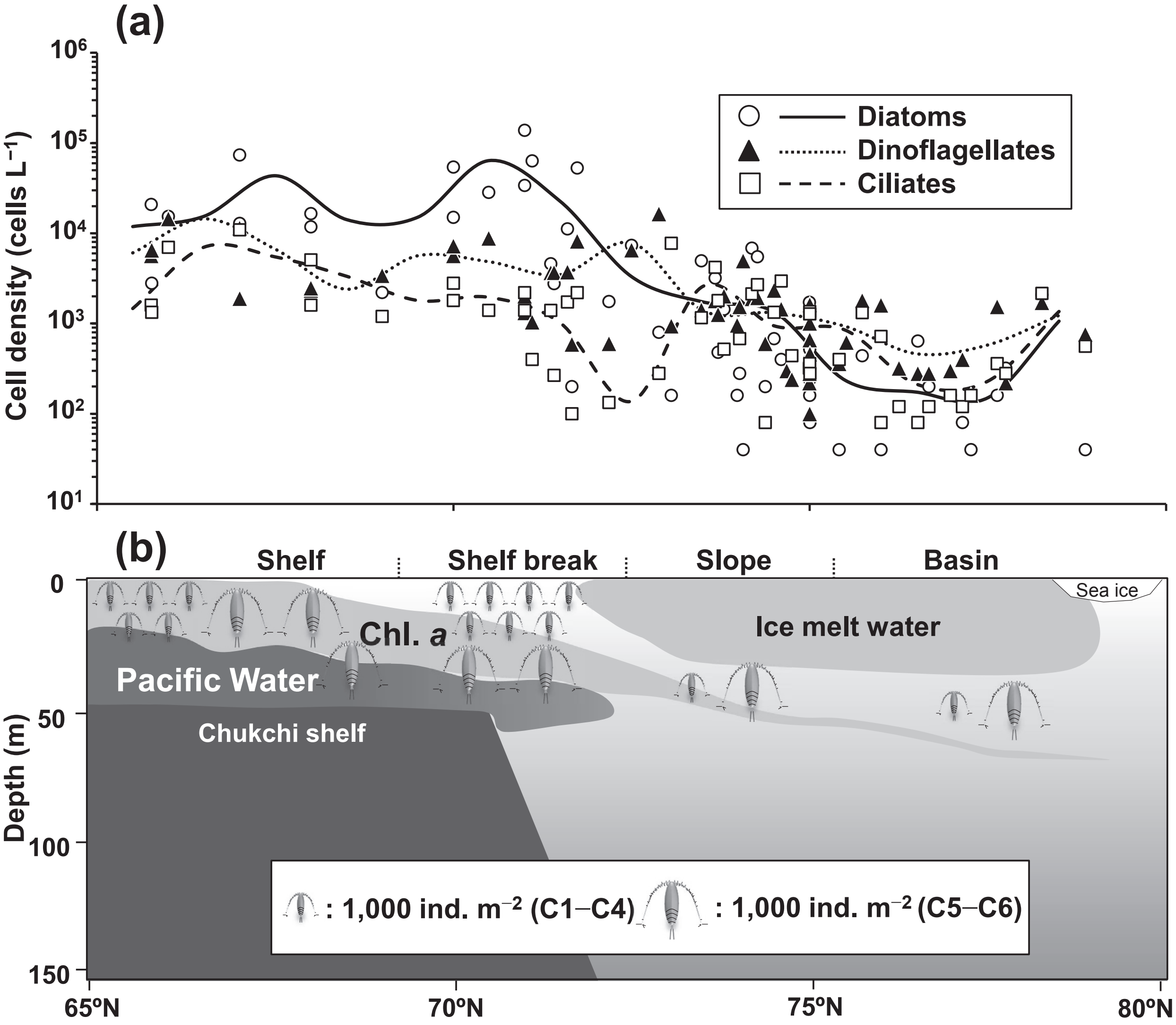

Fig. 25. Schematic diagram showing regional variation in microplankton community (a), copepod (*C. glacialis*) population structure (b) in the western Arctic Ocean during August–October. For microplankton, the mean cell densities are calculated with each taxon, and note that the density axis is on a log scale. For the copepod community, the numbers of small- and large-sized symbols indicate the amount of abundance (1,000 ind. m^{-2} per symbol) of early (C1–C4) and late (C5–C6) copepodid stages, respectively.

have been reported in the Arctic Ocean. According to Reid et al. (2007), the diatom *Neodenticula seminae* was first recorded in the Labrador Sea in the North Atlantic Ocean in May 1999, and this species is considered to have been transported by an increased inflow from the Pacific Ocean via the Arctic Ocean into the Atlantic Ocean. According to Heide-Jørgensen et al. (2011), because the sea ice around the Canadian archipelago melted in August 2010, the distribution of bowhead whale populations from the North Pacific and North Atlantic overlapped in the same region (Canadian archipelago) for 10 days. If these distributions continue in the future, then outbreeding between the Pacific and Atlantic populations could occur.

Additionally in the present study, the zooplankton community from the Pacific Water increased in 2007/2008, and the distribution of the Arctic zooplankton community shifted northward (Fig. 16). Next, I will discuss if the transported Pacific copepods will be able to maintain their immigrant population in the Arctic Ocean.

First, I will review the life cycle of the Arctic copepods. The Arctic copepod *C. glacialis* migrates to the surface in April under the sea ice (Kosobokova, 1999) and grazes on ice algae that is attached to the sea-ice (Campbell et al., 2009) (Fig. 26b). Adult females actively graze on both ice algae and ice-edge phytoplankton blooms that occur after the sea-ice melt to obtain energy for reproduction. Thus, the life cycle of the Arctic *C. glacialis* is well adapted to the sea ice. They obtain energy for reproduction by actively grazing both ice algae and ice-edge blooms near the surface layer. Afterward, they migrate to a deep layer in August,

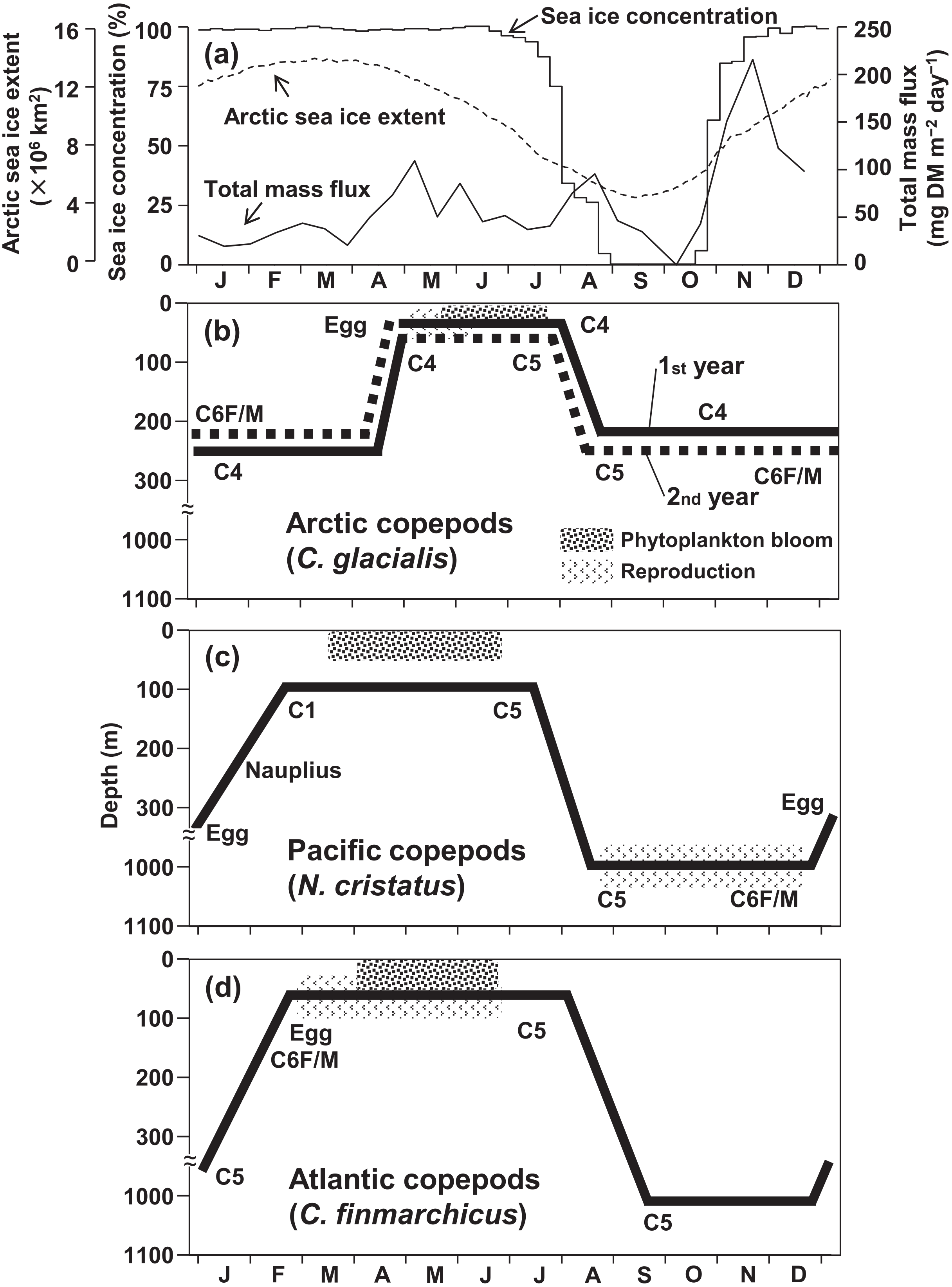

Fig. 26. Schematic diagram showing the seasonal changes in the environmental conditions (sea ice extent, concentration and total mass flux) (a) and the life cycle patterns of the Arctic (b), Pacific (c) and Atlantic (d) copepods in each region (cf. Miller, 1984; Conover, 1988; Kosobokova, 1999; Kobari and Ikeda, 2000; Falk-Petersen et al., 2009). The lines in (b)-(d) indicate the seasonal vertical distribution of the major populations.

during the oligotrophic season in the Arctic Ocean.

On the other hand, the life cycles of the Pacific and Atlantic copepods are considered to be adapted to ice-free conditions. They grow at the surface in April through July. The Pacific copepod *N. cristatus* reproduces in a deep layer in December through January (winter), and the newly born juveniles (C1) migrate to the surface in May (Fig. 26c). Because the new generation could have weak swimming and feeding abilities, they might not graze ice algae that is attached to the sea-ice as *C. glacialis* adults do. This circumstance is suggested by an example of the Sea of Okhotsk population, which is located at the southern end of the marginal ice zone of the Northern Hemisphere. The abundance of *N. cristatus* is much lower in the Sea of Okhotsk than in the adjacent Oyashio region (Yamaguchi, 2009). The transportation of Pacific copepods was recorded at 85°06′N 60 years ago (1953) (Johnson, 1963). Because Pacific copepods have not successfully immigrated to the Arctic Ocean, these migrations are thought to be abortive migrations to the Arctic Ocean.

The Atlantic copepod *C. finmarchicus* reproduces during April to June while grazing on phytoplankton blooms at the surface (Fig. 26d). Atlantic copepods have also been transported from the North Atlantic to the Arctic Ocean, but *C. finmarchicus* could not maintain a population in the Arctic Ocean because their reproduction timing does not match the timing of the ice edge bloom in the Arctic Ocean (Melle and Skjoldal, 1998). Thus, if the amount of transported copepods from the Pacific and Atlantic to the Arctic Ocean increase because their life cycle pattern (the seasonal timing of the migration to the surface and their feeding ability) might not match the seasonal ice coverage and food conditions (ice algae and ice edge bloom) in the Arctic Ocean the maintenance of their population as an immigrant in the Arctic Ocean is considered to be difficult in the future.

6-3. Future prospects

The effects of recent environmental changes on the plankton community in the Arctic Ocean are summarised in Table 11. The most common patterns of planktonic changes are found in the increasing primary production. For the primary production, various studies have been conducted using satellite data. Because the ice-free areas increased, the areas and periods of phytoplankton photosynthesis availability are considered to have increased (e.g., Arrigo et al., 2008). However, as mentioned above for the Canada Basin, a reverse pattern (a decrease in the primary production due to an increase in the oligotrophic ice melt water) was also observed in the basin of the western Arctic Ocean (Nishino et al., 2011b). These reverse results (increase/decrease in the primary production) are considered to be caused by the differences in spatial scales of the analysed areas. Thus, the primary production could increase for the whole Arctic Ocean, while the changes have regional differences, and the primary production in the basin of the western Arctic Ocean could decrease by increasing the ice melt water near the surface. To accurately evaluate the effects of sea-ice reduction, studies on the planktonic community should be made in each region, such as the Canada Basin and Chukchi Sea, among others.

For zooplankton community quantification, because of the difficulty of remote sensing on these taxa, field sampling by net towing is necessary. Thus, the long-term monitoring data are limited for zooplankton in the Arctic Ocean (cf. Astthorsson and Vilhjálmsson, 2002). As mentioned above, zooplankton fauna vary between the Arctic, Pacific and Atlantic Oceans, and their distributions correspond well with the water mass distribution (Conover, 1988). Thus, the variability in the zooplankton community is not directly related to climate change and instead is related to hydrographic changes (water mass, ocean current, and other factors) (Astthorsson and Vilhjálmsson, 2002; Pedersen and Rice, 2002). To evaluate the accurate effects of environmental changes on the planktonic community, clarification and specification of what parameters govern the variability of each taxon, flora and fauna are important.

Environmental parameters that could have affected the plankton communities include sea-ice reduction, changes in currents, water masses, warming temperature, increased freshwater and ocean acidification (lowered pH) (Table 11). Concerning the sea-ice reduction, the duration of ice-free water has gradually increased in the western Arctic Ocean (Markus et al., 2009). In the present study, seasonal changes in the timing of the zooplankton community was related to the sea-ice coverage (Fig. 24). This relationship suggests that changes in the sea-ice coverage timing could induce changes in the seasonal timing of the zooplankton community in the future. Thus, the application of mooring systems (such as a sediment trap) is a powerful tool to evaluate the seasonal changes in the zooplankton community in the Arctic Ocean.

Changes in the Beaufort Gyre or anticyclonic eddy affected both the microplankton and mesozooplankton communities (Figs. 5, 10). For the other environmental parameters, increased temperatures induced increased zooplankton respiration in the Fram Strait (Vaquer-Sunyer et al., 2010), and ocean acidification (lowered pH) could have a negative effect on the calcification of plankton that has $CaCO_3$ shells (e.g., coccolithophores, foraminiferans and pteropods) (Fabry et al., 2008).

The reported changes for the plankton community in the western Arctic Ocean are mainly attributed to the increased freshwater at the surface later or changes in the water masses (Table 11). In the future, the effects of the other environmental changes (e.g., the temperature and ocean acidification) on the planktonic community should be monitored. As another point of monitoring, because the plankton communi-

Table 11. Summary on recent changes reported for plankton community in the Arctic Ocean.

Subjects	Regions	Estimated causes	Observed period	Observed changes	References
Phytoplankton					
Diatoms	Labrador Sea	Changes in current	1999–2004	Occurence of *Neodenticula seminae*	Reid et al., (2007)
Coccolithophores	(Laboratory experiment)	Increased CO_2		Increased calcification and primary production	Iglesias–Rodriguez et al., (2008)
Phytoplankton size composition	Canada Basin	Increased freshwater	2004–2008	Increased small–sized phytoplankton composition	Li et al., (2009)
Primary production	Arctic Ocean	Changes in ice cover area	2003–2007	Increased annual primary production	Arrigo et al., (2008)
Primary production	Arctic Ocean	Ice cover, temperature	1998–2006	Increased primary production	Pabi et al., (2008)
Primary production	Iceland shelf	Changes in water masses	1958–1994	Increased primary production in spring	Gudmundsson, (1998)
Primary production	Canada Basin	Increased freshwater	2002–2009	Decreased primary production	Nishino et al., (2011)
Zooplankton					
Foraminiferans	(Laboratory experiment)	Lowered pH		Decreased calcification	Manno et al., (2012)
Pteropods	(Laboratory experiment)	Lowered pH		Decreased calcification	Comeau et al., (2009)
Amphipods	Kongsfjord, Svalbard	Changes in current	1996–2002	Changes in species composition	Hop et al., (2006)
Copepods	Kongsfjord, Svalbard	Changes in current	1996–2002	Increased contribution of smaller copepods	Hop et al., (2006)
Zooplankton community	West Greenland	Temperature	1950–1984	Increased/decreased in abundance and composition changes	Pedersen and Rice, (2002)
Zooplankton community	Chukchi/Beaufort Seas	Temperature?	1950–2002	Increased zooplankton abundance	Lane et al., (2008)
Zooplankton community	Iceland shelf	Changes in water masses	1961–1993	Increased/decreased in zooplankton abundance	Astthorsson and Vilhjálmsson, (2002)
Zooplankton community	Chukchi Sea	Changes in water masses	1991–2008	Increased in biomass and composition changes	Chapter 4 in this study
Zooplankton community	Western Arctic Ocean	Changes in current	2008–2010	Changes in distribution of zooplankton community	Chapter 3 in this study
Zooplankton respiration rate	Fram Strait	Warming temperature	2006–2007	Increased respiration rate of zooplankton	Vaquer–Sunyer et al., (2010)

ties greatly varied between the shelf and basin in the western Arctic Ocean (Fig. 25), the responses of the plankton community with the environmental changes are expected to vary between the regions. Thus, regional studies are needed for accurate evaluation of the effects of environmental changes on plankton in the western Arctic Ocean.

7. Summary

Recently, drastic reduction in the sea ice coverage area has been observed in the Pacific sector of the Arctic Ocean (the western Arctic Ocean). This reduction is considered to be caused by the increased inflow of the warm Pacific Water, and the effects on the marine ecosystem are of concern. Because of their short generation-to-generation length, the responses of plankton to environmental changes are expected to be rapid. From this point of view, it is important to evaluate the effects of environmental changes on plankton in the Arctic Ocean.

To reveal the spatial, interannual and seasonal changes in the microplankton and mesozooplankton communities in the western Arctic Ocean, I studied four topics: the horizontal distribution of microplankton, the horizontal distribution of mesozooplankton, the interannual changes in mesozooplankton, and the seasonal changes in mesozooplankton. Based on these results, the possible changes in plankton in response to the recent environmental changes in the Arctic Ocean are discussed.

1. Horizontal distribution of microplankton

To reveal the horizontal distribution of the microplankton, water samples were collected in the western Arctic Ocean during September–October 2010. The cell densities of diatoms, dinoflagellates and ciliates had the ranges of 0–138,640, 0–16,460 and 0–10,933 cells L^{-1}, respectively, and were higher on the shelf. For the diatoms, 50 species that belong to 25 genera were observed (*Pseudo-nitzschia* spp. and *Cylindrotheca closterium* dominated). Dinoflagellates also comprised 50 species, which belonged to 13 genera (with the dominance of *Prorocentrum* spp. and *Gymnodinium* spp.). Ciliates from 32 species that belonged to 21 genera were collected (*Strombidium* spp. dominated). Cluster analysis that was based on the cell density separated the microplankton community into five groups. The groups contained 25, 22, 6, 4 and 2 stations, respectively. The largest group was observed in the basin and was characterised by having a low cell density and a dominance of ciliates. The second group was observed in the shelf region and showed a high cell density that was dominated by diatoms. Because of the low cell density and the dominance of the ciliates, the former group is considered to be dominated by the microbial food web. Because of the high cell density and the predominance of diatoms, the latter group is characterised by eutrophication, which is enhanced by the continuous inflow of nutrient-rich Pacific Water through the Bering Strait. The remaining three small groups were located between the two large groups. Because the physical oceanography in the boundary area was complex, the horizontal distribution of these three groups can be reflected by complex physical structures, such as an anticyclonic eddy.

2. Horizontal distribution of mesozooplankton

To reveal the horizontal distribution of the mesozooplankton community, net samples were collected by vertical hauls using a NORPAC net in the western Arctic Ocean during September–October of 2008 and 2010. The zooplankton abundance and biomass range was 0.03–2.74 $\times 10^5$ ind. m^{-2} and 3–678 g WM m^{-2}, respectively, and they were higher in the shelf region. Copepods were the most dominant taxa and composed 8–95% of the zooplankton abundance. Based on the zooplankton abundance, the communities were classified into four groups, which had 30% and 36% dissimilarity. The horizontal distribution of each group was well synchronised with the bottom depth, and they were named Shelf, Shelf break, Slope and Basin. Neritic copepods (*Pseudocalanus* spp.) and benthos larvae were the dominant taxa in the Shelf region. Arctic copepods (*Calanus glacialis* and *Metridia longa*) with early copepodid stages were substantially greater at the Shelf break. Mesopelagic copepods were greater in the Slope and Basin regions. A comparison of the horizontal distributions between 2008 and 2010 revealed that the Shelf break group occurred further north in 2008, and the distributions of the Shelf break and Slope groups were more mixed and more complex in 2008 than in 2010. These facts could have been caused by a meandering or enhancement of the Beaufort Gyre due to the greater sea ice reduction in 2008.

3. Interannual changes in mesozooplankton

To examine the interannual changes in the mesozooplankton community, net samples were collected by vertical hauls using a NORPAC net in the Chukchi Sea during July–August in 1991, 1992, 2007 and 2008. Zooplankton abundance ranged 0.04–3.16$\times 10^5$ ind. m^{-2} and was greater in 2008. Zooplankton biomass ranged 0.07–286 g wet mass m^{-2} and was greater in 2007. Cluster analysis based on zooplankton abundance showed a division of the zooplankton community into four groups. The occurrence of each group was separated geographically and interannually, and the horizontal distributions of each group in 1991 and 1992 were similar, but those in 2007 and 2008 shifted northward. Especially in 2007, the group that was characterised by Pacific copepods (e.g., *Eucalanus bungii*) was observed near the Bering Strait. Because both the abundance and biomass were higher in 2007/08 than in 1991/92, the sea ice reduction would have a positive effect on the zooplankton standing stock and production. At the same time, the northern shift of the zooplankton community in 2007/08 indicated that the sea ice reduction would have a negative effect on the zooplankton fauna (a loss of characterised Arctic species from the shelf).

4. Seasonal changes in mesozooplankton

To examine seasonal changes in the mesozooplankton community, analyses were made on the swimmer samples (> 1 mm size) that were collected by a sediment trap mooring at 180 m depth at St. NAP (75°00′N, 162°00′W) in the western Arctic Ocean during October 2010 to September 2011. The zooplankton flux ranged 5-44 ind. m^{-2} day^{-1} and was greater from July to October; copepods were the dominant taxon. Based on the zooplankton flux, cluster analysis classified samples into three groups (A, B and C). The occurrence of each group showed clear seasonality; group A was observed during July to October, group B was observed in November to January, and group C was observed during March to June, and the change from B to C occurred under the sea ice. For the four dominant copepods (*C. hyperboreus*, *Metridia longa*, *Heterorhabdus norvegicus* and *P. glacialis*), their population structures varied with the species. Most *C. hyperboreus* were stage C6F throughout the year, and they matured from February through April. For *M. longa* and *P. glacialis*, C6Fs dominated from January through May, and the composition of early copepodid stages (C1-C4) increased from June through October. *Heterorhabdus norvegicus* was dominated by C5 from November through February and C6F/M from March through May. The Pacific copepod *Neocalanus cristatus* occurred throughout the year and was abundant especially during August to September, when the sea ice coverage was the lowest. Through the analysis of zooplankton swimmers that were collected by the sediment trap, this study revealed the presence of clear seasonality in the zooplankton community and the population structure of the dominant copepods in the western Arctic Ocean. This seasonality would be related to the seasonal changes in the sea ice coverage and the copepod life cycle.

5. Future prospects

In the western Arctic Ocean, both the microplankton and mesozooplankton communities during the summer were clearly divided into two regions: the shelf and the basin. In the future, in the shelf region, primary production is expected to increase, while organic consumption by zooplankton in the water column will also increase. The result will be that the vertical material flux to the seafloor is expected to decrease. In the basin, a decrease in the primary production is expected to occur by means of an increase in the oligotrophic ice melt water, which will induce lowered vertical material flux to the deep areas. The number of transported copepods from the Pacific and Atlantic to the Arctic Ocean should increase. However, because their life cycle pattern (the seasonal timing of the migration to the surface and their feeding ability) does not match the environment in the Arctic Ocean, the maintenance of their population as an immigrant in the Arctic Ocean is considered to be difficult. In the future, in detailed regional studies, it is important to evaluate accurately the effects of environmental changes on plankton in the western Arctic Ocean.

8. Acknowledgements

I wish to express my sincere thanks to Professor Yasunori Sakurai, Hokkaido University, for his kind advice and critical reading of this manuscript. I wish to thank Professors Kenshi Kuma and Ichiro Imai for their critical reading of the manuscript. Associate Professors Toru Hirawake and Atsushi Yamaguchi provided kind guidance and valuable discussion. I also thank Associate Professor John Richard Bower for correcting the English of this manuscript.

I am grateful to Associate Professor Koji Shimada (Tokyo University of Marine Science and Technology) and Drs. Motoyo Itoh and Takashi Kikuchi (JAMSTEC) for their valuable comments on this study and for helping with my plankton sampling during the cruises on the R/V *Mirai*. I also express my sincere thanks to Drs. Naomi Harada, Sanae Chiba, Shigeto Nishino, Jonaotaro Onodera and Yusuke Kawaguchi (JAMSTEC) for providing the sediment trap samples and hydrographic data and for offering valuable comments on this study.

This study was supported by Green Network of Excellence Program (GRENE Program); the Arctic Climate Change Research Project ‘Rapid Change of the Arctic Climate System and its Global Influences’; the Grant-in-Aid for Scientific Research (S) Catastrophic reduction of sea-ice in the Arctic Ocean–its impact on the marine ecosystems in the polar region–to Dr. Naomi Harada; and the Japan Society for the Promotion of Science (JSPS) Fellows (234167) to the author.

I wish to acknowledge the captains, officers and crew members of the T/S *Oshoro-Maru*, Hokkaido University, and the R/V *Mirai*, JAMSTEC, for their kind help in collecting the samples that were used for this study. Thanks are also due to all of the members of the Marine Biology Laboratory, Hokkaido University, for their support and kind help during this study. Finally, I express my sincere thanks to my parents and family for providing me the opportunity to study at Hokkaido University and for their continuous encouragement and support throughout my study.

9. References

Acuña, J.L., Deibel, D. and Morris, C.C. (1996) Particle capture mechanism of the pelagic tunicate *Oikopleura vanhoeffeni*. *Limnol. Oceanogr.*, **41**, 1800-1814.

Acuña, J.L., Deibel, D., Bochdansky, A.B. and Hatfield, E. (1999)

In situ ingestion rates of appendicularian tunicates in the northeast water Polynya (NE Greenland). *Mar. Ecol. Prog. Ser.*, **186**, 149-160.

Ambrose, W.G.Jr. and Renaud, P.E. (1997) Does a pulsed food supply to the benthos affect polychaete recruitment patterns in the northeast water Polynya?. *J. Mar. Syst.*, **10**, 483–495.

Arrigo, K.R., Dijken, G. and Pabi, S. (2008) Impact of a shrinking Arctic ice cover on marine primary production. *Geophys. Res. Lett.*, **35**, L19603, doi: 10.1029/2008GL035028.

Ashjian, C.J., Gallager, S.M. and Plourde, S. (2005) Transport of plankton and particles between the Chukchi and Beaufort Seas during summer 2002, described using a Video Plankton Recorder. *Deep-Sea Res. II*, **52**, 3259-3280.

Ashjian, C.J., Smith, S.L. and Lane, P.V.Z. (1995) The Northeast Water Polynya during summer 1992: distribution and aspects of secondary production of copepods. *J. Geophys. Res.*, **100**, 4371–4388.

Ashjian, C.J., Campbell, R.G., Welch, H.E., Butler, M. and Keuren, D.V. (2003) Annual cycle in abundance, distribution, and size in relation to hydrography of important copepod species in the western Arctic Ocean. *Deep-Sea Res. I*, **50**, 1235-1261.

Ashjian, C.J., Braund, S.R., Campbell, R.G., George, J.C.C., Kruse, J., Maslowski, W., Moore, S.E., Nicolson, C.R., Okkonen, S.R., Sherr, B.F., Sherr, E.B. and Spitz, Y.H. (2010) Climate variability, oceanography, bowhead whale distribution, and Iñupiat subsistence whaling near Barrow, Alaska. *Arctic*, **63**, 179-194.

Astthorsson, O.S. and Vilhja´lmsson, H. (2002) Iceland Shelf LME: Decadal assessment and resource sustainability. pp. 219-243, Sherman, K. and Skjoldal, H.R. (eds), *Large Marine Ecosystems of the North Atlantic: Changing States and Sustainability*, Elsevier, Amsterdam, The Netherlands.

Baird, M.E., Timko, P.G., Middleton, J.H., Mullaney, T.J., Cox, D.R. and Suthers, I.M. (2008) Biological properties across the Tasman front off southeast Australia. *Deep-Sea Res. I*, **55**, 1438-1455.

Båmstedt, U. (1979) Reproduction bioenergetics within the summer and winter generations of *Euchaeta norvegica* (Copepoda). *Mar. Biol.*, **54**, 135-142.

Båmstedt, U. and Ervik, A. (1984) Local variations in size and activity among *Calanus finmarchicus* and *Metridia longa* (Copepoda, Calanoida) overwintering on the west coast of Norway. *J. Plankton Res.*, **6**, 843-857.

Barnes, H. (1957) Processes of restoration and synchronization in marine ecology. The spring diatom increase and spawning of the common barnacle *Balanus balanoides* (L). *Annee Biol.*, **33**, 67-85.

Basedow, S.L., Tande, K.S. and Zhou, M. (2010) Biovolume spectrum theories applied: spatial patterns of trophic levels within a mesozooplankton community at the polar front. *J. Plankton Res.*, **32**, 1105-1119.

Bray, J.B. and Curtis, J.T. (1957) An ordination of the upland forest communities of southern Wisconsin. *Ecol. Monogr.*, **27**, 325-349.

Brodeur, R.D., Decker, M.B., Ciannelli, L., Purcell, J.E., Bond, N.A., Stabeno, P.J., Acuna, E. and Hunt, Jr.G.L. (2008) Rise and fall of jellyfish in the eastern Bering Sea in relation to climate regime shifts. *Prog. Oceanogr.*, **77**, 103-111.

Brodsky, K.A. (1967) *Calanoida of the far-eastern seas and polar basin of the USSR.* Israel Program Scientific Translation, Jerusalem.

Campbell, R.G., Sherr, E.B., Ashjian, C.J., Plourde, S., Sherr, B.F., Hill, V. and Stockwell, D.A. (2009) Mesozooplankton prey preference and grazing impact in the western Arctic Ocean. *Deep-Sea Res. II*, **56**, 1274-1289.

Capriulo, G.M. and Carpenter, E.J. (1983) Abundance, species composition and feeding impact of tintinnid micro-zooplankton in central long island sound. *Mar. Ecol. Prog. Ser.*, **10**, 277-288.

Clare, A.S. and Walker, G. (1986) Further studies on the control of the hatching process in Balanus balanoides (L). *J. Exp. Mar. Biol. Ecol.*, **97**, 295-304.

Clare, A.S., Walker, G., Holland, D.L. and Crisp, D.J. (1984) Nature of the barnacle hatching substance and the role of dopamine in the egg hatching process. pp. 569, Engels, W. (ed), *Advances in invertebrate reproduction, Volume 3*, Elsevier Science Publishers B.V., Amsterdam.

Coachman, L.K. and Aagaard, K. (1966) On the water exchange through Bering Strait. *Limnol. Oceanogr.*, **11**, 44-59.

Codispoti, L.A., Flagg, C., Kelly, V. and Swift, J.H. (2005) Hydrographic conditions during the 2002 SBI process experiments. *Deep-Sea Res. II*, **52**, 3199-3226.

Comeau, S., Gorsky, G., Jeffree, R., Teyssie, J.-L. and Gattuso, J.-P. (2009) Impact of ocean acidification on a key Arctic pelagic mollusk (*Limacina helicina*). *Biogeosciences*, **6**, 1877-1882.

Comiso, J.C., Parkinson, C.L., Gersten, R., and Stock, L. (2008) Accelerated decline in the Arctic sea ice cover. *Geophys. Res. Lett.*, **35**, L01703. doi: 10.1029/2007GL031972.

Conover, R.J. (1988) Comparative life histories in the genera Calanus and Neocalanus in high latitudes of the northern hemisphere. pp. 127-142, Boxshall, G.A. and Schminke, H.K. (eds), *Biology of Copepods*, Kluwer Academic Publishers, Dordrecht.

Conover, R.J. and Huntley, M. (1991) Copepods in ice-covered seas-Distribution, adaptations to seasonally limited food, metabolism, growth patterns and life cycle strategies in polar seas. *J. Mar. Syst.*, **2**, 1-41.

Conover, R.J. and Siferd, T.D. (1993) Dark-season survival strategies of coastal zone zooplankton in the Canadian Arctic. *Arctic*, **46**, 303-311.

Corkett, C.J. and McLaren, I.A. (1978) The biology of *Pseudocalanus*. *Adv. Mar. Biol.*, **15**, 1-563.

Cota, G.F., Pomeroy, L.R., Harrison, W.G., Jones, E.P., Peters, F., Sheldon, W.M.Jr. and Weingartner, T.R. (1996) Nutrients, primary production and microbial heterotrophy in the southeastern Chukchi Sea: Arctic summer nutrient depletion and heterotrophy. *Mar. Ecol. Prog. Ser.*, **135**, 247-258.

Crisp, D.J. (1962) Release of larvae by barnacles in response to the available food supply. *Anim. Behav.*, **10**, 382-383.

Darnis, G., Barber, D.G. and Fortier, L. (2008) Sea ice and the onshore-offshore gradient in pre-winter zooplankton assemblages in southeastern Beaufort Sea. *J. Mar. Syst.*, **74**, 994-1011.

Dawson, J.K. (1978) Vertical distribution of *Calanus hyperboreus* in the central Arctic Ocean. *Limnol. Oceanogr.*, **23**, 950-957.

Degerlund, M. and Eilertsen, H.C. (2010) Main species characteristics of phytoplankton spring blooms in NE Atlantic and Arctic waters (68-80°N). *Estuar. Coast.*, **33**, 242-269.

Fabry, V.J., Seibel, B.A., Feely, R.A. and Orr, J.C. (2008) Impacts of ocean acidification on marine fauna and ecosystem processes. *ICES J. Mar. Sci.*, **65**, 414-432.

Falk-Petersen, S., Mayzaud, P., Kattner, G. and Sargent, J.R. (2009) Lipids and life strategy of Arctic *Calanus.* *Mar. Biol. Res.*, **5**, 18-39.

Field, J.G., Clarke, K.R. and Warwick, R.M. (1982) A practical strategy for analyzing multispecies distribution patterns. *Mar. Ecol. Prog. Ser.*, **8**, 37-52.

Finlay, K., Beisner, B.E., Patoine, A. and Pinel-Alloul, B. (2007) Regional ecosystem variability drives the relative importance of bottom-up and top-down factors for zooplankton size spectra. *Can. J. Fish. Aquat. Sci.*, **64**, 516-529.

Forbes, J.R., Macdonald, R.W., Carmack, E.C., Iseki, K. and O'Brien, M.C. (1992) Zooplankton retained in sequential sediment traps along the Beaufort Sea shelf break during winter. *Can. J. Fish. Aquat. Sci.*, **49**, 663-670.

Forest, A., Sampei, M., Hattori, H., Makabe, R., Sasaki, H., Fukuchi, M., Wassmann, P. and Fortier, L. (2007) Particulate organic carbon fluxes on the slope of the Mackenzie Shelf (Beaufort Sea): Physical and biological forcing of shelf-basin exchanges. *J. Mar. Syst.*, **68**, 39-54.

Fritz, L. and Triemer, R.E. (1985) A rapid simple technique utilizing Calcofluor white M2R for the visualization of dinoflagellate thecal plates. *J. Phycol.*, **21**, 662-664.

Frost, B.W. (1974) *Calanus marshallae*, a new species of calanoid copepod closely allied to the sibling species *C. finmarchicus* and *C. glacialis*. *Mar. Biol.*, **26**, 77-99.

Frost, B.W. (1989) A taxonomy of the marine calanoid copepod genus *Pseudocalanus*. *Can. J. Zool.*, **67**, 525-551.

Fukuyo, Y., Inoue, H. and Takayama, H. (1997) Class Dinophyceae. pp. 31-112, Chihara, M. and Murano, M. (eds), *An Illustrated Guide to Marine Plankton in Japan*, Tokai University Press, Tokyo.

Gaines, G. and Elbrächter, M. (1987) Heterotrophic nutrition. pp. 224-268, Taylor, F.J.R. (ed), *The Biology of Dinoflagellates*, Blackwell, Oxford.

Gast, V. (1985) Bacteria as a food source for microzooplankton in the Schlei Fjord and Baltic Sea with special reference to ciliates. *Mar. Ecol. Prog. Ser.*, **22**, 107-120.

Grebmeier, J.M. (2012) Shfting patterns of life in the Pacific Arctic and sub-Arctic Seas. *Annu. Rev. Marine. Sci.*, **4**, 63-78.

Grebmeier, J.M., Cooper, L.W., Feder, H.M. and Sirenko, B.I. (2006) Ecosystem dynamics of the Pacific-influenced northern Bering and Chukchi Seas in the Amerasian Arctic. *Prog. Oceanogr.*, **71**, 331-361.

Grebmeier, J.M., Feder, H.M. and McRoy, C.P. (1989) Pelagic-benthic coupling on the shelf of the northern Bering and Chukchi Seas. II. Benthic community structure. *Mar. Ecol. Prog. Ser.*, **51**, 253-268.

Grønvik, S. and Hopkins, C.C.E. (1984) Ecological investigations of the zooplankton community of Balsfjorden, northern Norway: generation cycle, seasonal vertical distribution, and seasonal variations in body weight and carbon and nitrogen content of the copepod *Metridia longa* (Lubbock). *J. Exp. Mar. Biol. Ecol.*, **80**, 93-107.

Gudmundsson, K. (1998) Long-term variation in phytoplankton productivity during spring in Iceland waters. *ICES J. Mar. Sci.*, **55**, 635-643.

Hansen, B.W. and Jensen, F. (2000) Species growth rates of protozooplankton in the marginal ice zone of the central Barents Sea during spring. *J. Mar. Biol. Ass. UK.*, **80**, 37-44.

Hasle, G.R. and Syvertsen, E.E. (1997) Marine Diatoms. pp. 5-385, Tomas, C.R. (ed), *Identifying Marine Phytoplankton*, Academic Press, San Diego.

Heide-Jørgensen, M.P., Laidre, K.L., Quakenbush, L.T. and Citta, J.J. (2011) The northwest passage opens for bowhead whales. *Biol. Lett.*, **8**, 270-273.

Herman, A.W. (1988) Simultaneous measurement of zooplankton and light attenuance with a new optical plankton counter. *Cont. Shelf Res.*, **8**, 205-221.

Herman, A.W. (1992) Design and calibration of a new optical plankton counter capable of sizing small zooplankton. *Deep-Sea Res. A*, **39**, 395-415.

Herman, A.W. and Harvey, M. (2006) Application of normalized biomass size spectra to laser optical plankton counter net intercomparisons of zooplankton distributions. *J. Geophys. Res.*, **111**, C05S05, doi: 10.1029/2005JC002948.

Hill, V. and Cota, G. (2005) Spatial patterns of primary production on the shelf, slope and basin of the western Arctic in 2002. *Deep-Sea Res. II*, **52**, 3344-3354.

Hill, V., Cota, G. and Stockwell, D. (2005) Spring and summer phytoplankton communities in the Chukchi and eastern Beaufort Seas. *Deep-Sea Res. II*, **52**, 3369-3385.

Hirche, H.-J. (1997) Life cycle of the copepod *Calanus hyperboreus* in the Greenland Sea. *Mar. Biol.*, **128**, 607-618.

Hirche, H.-J. and Kosobokova, K.N. (2011) Winter studies on zooplankton in Arctic seas: the Storfjord (Svalbard) and adjacent ice-covered Barents Sea. *Mar. Biol.*, **158**, 2359-2376.

Hirche, H.-J. and Niehoff, B. (1996) Reproduction of the Arctic copepods *Calanus hyperboreus* in the Greenland sea-field and laboratory observations. *Polar Biol.*, **16**, 209-219.

Hobson, K.A., Fisk, A., Karnovsky, N., Holst, M., Gagnon, J.-M. and Fortier, M. (2002) A stable isotope (δ^{13}C, δ^{15}N) model for the North Water food web: implications for evaluating trophodynamics and the flow of energy and contaminants. *Deep-Sea Res. II*, **49**, 5131-5150.

Hokkaido University. (1992) *Data Record of Oceanographic Observation and Exploratory Fishing, No. 35.* The Faculty of Fisheries, Hokkaido University, Hakodate.

Hokkaido University. (1993) *Data Record of Oceanographic Observation and Exploratory Fishing, No. 36.* The Faculty of Fisheries, Hokkaido University, Hakodate.

Hokkaido University. (2008) *Data Record of Oceanographic Observation and Exploratory Fishing, No. 51.* The Faculty of Fisheries, Hokkaido University, Hakodate.

Hokkaido University. (2009) *Data Record of Oceanographic Observation and Exploratory Fishing, No. 52.* The Faculty of Fisheries, Hokkaido University, Hakodate.

Hop, H., Falk-Petersen, S., Svendsen, H., Kwasnievski, S., Pavlov, V., Pavlova, O. and Søreide, J.A. (2006) Physical and biological characteristics of the pelagic system across Fram Strait to Kongsfjorden. *Prog. Oceanogr.*, **71**, 182-231.

Hopcroft, R.R., Kosobokova, K.N. and Pinchuk, A.I. (2010) Zooplankton community patterns in the Chukchi Sea during summer 2004. *Deep-Sea Res. II*, **57**, 27-39.

Hoppenrath, M. and Drebes, G. (2009) *Marine Phytoplankton*, E. Schweizerbart'sche Verlagsbuchhandlung, Stuttgart.

Hunt, Jr.G.L. and Drinkwater, K. (2007) Introduction to the proceedings of the GLOBEC symposium on effects of climate variability on sub-Arctic marine ecosystems. *Deep-Sea Res. II*, **54**, 2453-2455.

Huntley, M.E., Zhou, M. and Nordhausen, W. (1995) Mesoscale distribution of zooplankton in the California current in late spring, observed by optical plankton counter. *J. Mar. Res.*, **53**, 647-674.

Iglesias-Rodriguez, M.D., Halloran, P.R., Rickaby, R.E.M., Hall, I.R., Colmenero-Hidalgo, E., Gittins, J.R., Green, D.R.H., Tyrrell, T., Gibbs, S.J., von Dassow, P., Rehm, E., Armbrust, E.V. and Boessenkool, K.P. (2008) Phytoplankton calcification in a high-CO_2 world. *Science*, **320**, 336-340.

Johnson, M.W. (1963) Zooplankton collections from the high polar basin with special reference to the copepoda. *Limnol. Oceanogr.*, **8**, 89–102.

Kerr, S.R. (1974) Theory of size distribution in ecological communities. *J. Fish. Res. Board Can.*, **31**, 1859–1862.

Kobari, T. and Ikeda, T. (2000) Life cycle of *Neocalanus* species in the Oyashio region. *Bull. Plankton Soc. Japan*, **47**, 129–135.

Kosobokova, K.N. (1999) The reproduction cycle and life history of the Arctic copepod *Calanus glacialis* in the White Sea. *Polar Biol.*, **22**, 254–263.

Lane, P.V.Z., Llinás, L., Smith, S.L. and Pilz, D. (2008) Zooplankton distribution in the western Arctic during summer 2002: Hydrographic habitats and implications for food chain dynamics. *J. Mar. Syst.*, **70**, 97–133.

Li, W.K.W., McLaughlin, F.A., Lovejoy, C. and Carmack, E.C. (2009) Smallest algal thrive as the Arctic Ocean freshens. *Science*, **326**, 539.

Lowry, L.F., Sheffield, G. and George, C. (2004) Bowhead whale feeding in the Alaskan Beaufort Sea, based on stomach contents analyses. *J. Cetacean Res. Manage.*, **6**, 215–223.

Maeda, M. (1997) Suborder Oligotrichida. pp. 397–420, Chihara, M. and Murano, M. (eds), *An Illustrated Guide to Marine Plankton in Japan*, Tokai University Press, Tokyo.

Makabe, R., Hattori, H., Sampei, M., Ota, Y., Fukuchi, M., Fortier, L. and Sasaki, H. (2010) Regional and seasonal variability of zooplankton collected using sediment trap in the southeastern Beaufort Sea, Canadian Arctic. *Polar Biol.*, **33**, 257–270.

Manno, C., Morata, N. and Bellerby, R. (2012) Effects of ocean acidification and temperature increase on the plankton foraminifer *Neogloboquadrina pachyderma* (sinistral). *Polar Biol.*, **35**, 1311–1319.

Margalef, R. (1979) Life–forms of phytoplankton as survival alternatives in an unstable environment. *Oceanol. Acta.*, **1**, 493–509.

Marin, V. (1987) The oceanographic structure of eastern Scotia Sea–IV. Distribution of copepod species in relation to hydrography in 1981. *Deep–Sea Res. A*, **34**, 105–121.

Markus, T., Stroeve, J.C. and Miller, J. (2009) Recent changes in Arctic sea ice melt onset, freezeup, and melt season length. *J. Geophys. Res.*, **114**, C12024. doi: 10.1029/2009JC005436.

Matsuno, K., Yamaguchi, A., Hirawake, T. and Imai, I. (2011) Year–toyear changes of the mesozooplankton community in the Chukchi Sea during summers of 1991, 1992 and 2007, 2008. *Polar Biol.*, **34**, 1349–1360.

Matsuno, K., Yamaguchi, A. and Imai, I. (2012a) Biomass size spectra of mesozooplankton in the Chukchi Sea during the summers of 1991/1992 and 2007/2008: an analysis using optical plankton counter data. *ICES J. Mar. Sci.*, **69**, 1205–1217.

Matsuno, K., Yamaguchi, A., Shimada, K. and Imai, I. (2012b) Horizontal distribution of calanoid copepods in the western Arctic Ocean during the summer of 2008. *Polar Sci.*, **6**, 105–119.

McLaren, I.A., Laberge, E., Corkett, C.J. and Sevigny, J.M. (1989) Life cycle of four species of *Pseudocalanus* in Nova Scotia. *Can. J. Zool.*, **67**, 552–558.

Melle, W. and Skjoldal, H.R. (1998) Reproduction and development of *Calanus finmarchicus*, *C. glacialis* and *C. hyperboreus* in the Barents Sea. *Mar. Ecol. Prog. Ser.*, **169**, 211–228.

Miller, C.B. (1988) *Neocalanus flemingeri*, a new species of calanidae (copepoda: calanoida) from the subarctic Pacific Ocean, with a comparative redescription of *Neocalanus plumchrus* (Marukawa) 1921. *Prog. Oceanog.*, **20**, 223–273.

Miller, C.B., Frost, B.W., Batchelder, H.P., Clemons, M.J. and Conway, R.E. (1984) Life histories of large, grazing copepods in the subarctic ocean gyre: *Neocalanus plumchrus*, *Neocalanus cristatus* and *Eucalanus bungii* in the Northeast Pacific. *Prog. Oceanogr.*, **13**, 201–243.

Mizobata, K., Shimada, K., Woodgate, R., Saitoh, S.–I. and Wang, J. (2010) Estimation of heat flux through the eastern Bering Strait. *J. Oceanogr.*, **66**, 405–424.

Moore, S.K. and Suthers, I.M. (2006) Evaluation and correction of subresolved particles by the optical plankton counter in three Australian estuaries with pristine to highly modified catchments. *J. Geophys. Res.*, **111**, C05S04, doi: 10.1029/2005JC002920.

Motoda, S. (1959) Devices of simple plankton apparatus. *Mem. Fac. Fish. Hokkaido Univ.*, **7**, 73–94.

Mullin, M.M., Goetze, E., Beaulieu, S.E. and Lasker, J.M. (2000) Comparisons within and between years resulting in contrasting recruitment of Pacific hake (*Merluccius productus*) in the California current system. *Can. J. Fish. Aquat. Sci.*, **57**, 1434–1447.

Niemi, A., Michel, C., Hille, K. and Poulin, M. (2011) Protist assemblages in winter sea ice: setting the stage for the spring ice algae bloom. *Polar Biol.*, **34**, 1803–1817.

Nishino, S., Itoh, M., Kawaguchi, Y., Kikuchi, T. and Aoyama, M. (2011a) Impact of an unusually large warm–core eddy on distributions of nutrients and phytoplankton in the southwestern Canada Basin late summer/early fall 2010. *Geophys. Res. Lett.*, **38**, L16602. doi: 10.1029/2011GL047885.

Nishino, S., Kikuchi, T., Yamamoto–Kawai, M., Kawaguchi, Y., Hirawake, T. and Itoh, M. (2011b) Enhancement/reduction of biological pump depends on ocean circulation in the sea–ice reduction regions of the Arctic Ocean. *J. Oceanogr.*, **67**, 305–314.

Nogueira, E., González–Nuevo, G., Bode, A., Varela, M., Morán, X.A.G. and Valdés, L. (2004) Comparison of biomass and size spectra derived from optical plankton counter data and net samples: application to the assessment of mesoplankton distribution along the northwest and north Iberian Shelf. *ICES J. Mar. Sci.*, **61**, 508–517.

Norrbin, M.F. (1994) Seasonal patterns in gonad maturation, sex ratio and size in some small, high latitude copepods: implications for overwintering tactics. *J. Plankton Res.*, **16**, 115–131.

Norrbin, M.F. (1996) Timing of diapauses in relation to the onset of winter in the high–latitude copepods *Pseudocalanus acuspes* and *Acartia longiremis*. *Mar. Ecol. Prog. Ser.*, **142**, 99–109.

Øresland, V. (1991) Feeding of the carnivorous copepod *Euchaeta antarctica* in Antarctic waters. *Mar. Ecol. Prog. Ser.*, **78**, 41–47.

Østvedt, O.J. (1955) Zooplankton investigations from weathership "M" in the Norwegian Sea, 1948–49. *Hvalrad. Skr.*, **40**, 1–93.

Ota, Y., Hattori, H., Makabe, R., Sampei, M., Tanimura, A. and Sasaki, H. (2008) Seasonal changes in nauplii and adults of *Calanus hyperboreus* (Copepoda) captured in sediment trap, Amundsen Gulf, Canadian Arctic. *Polar Sci.*, **2**, 215–222.

Pabi, S., van Dijken, G.L. and Arrigo, K.R. (2008) Primary production in the Arctic Ocean, 1998–2006. *J. Geophys. Res.*, **113**, C08005, doi: 10.1029/2007JC004578.

Paffenhöfer, G.A. (1973) The cultivation of an appendicularian through numerous generations. *Mar. Biol.*, **22**, 183–185.

Paranjape, M.A. (1987) Grazing by microzooplankton in the eastern Canadian arctic in summer 1983. *Mar. Ecol. Prog. Ser.*, **40**, 239–246.

Pedersen, S.A. and Rice, J.C. (2002) Dynamics of fish larvae, zooplankton, and hydrographical characteristics in the West

Greenland Large marine Ecosystem, 1950–1984. pp. 151–193, Sherman, K. and Skjoldal, H.R. (eds), *Large Marine Ecosystems of the North Atlantic: Changing States and Sustainability*, Elsevier, Amsterdam, The Netherlands.

Pertsova, N.M., Kosobokova, K.N. and Prudkovsky, A.A. (2006) Population size structure, spatial distribution, and life cycle of the Hydromedusa *Aglantha digitale* (O.F. Müller, 1766) in the White Sea. *Oceanology*, **46**, 228–237.

Platt, T. and Denman, K. (1977) Organization in the pelagic ecosystem. *Helgoländer Wiss. Meeresunters.*, **30**, 575–581.

Platt, T. and Denman, K. (1978) The structure of pelagic marine ecosystems. *Rapp. P.-V. Réun. Cons. Int. Explor. Mer*, **173**, 60–65.

Pomeroy, L.R. (1974) The ocean's food web: a changing paradigm. *Bioscience*, **24**, 499–503.

Poulsen, L.K. and Kiørboe, T. (2006) Vertical flux and degradation rates of copepod fecal pellets in a zooplankton community dominated by small copepods. *Mar. Ecol. Prog. Ser.*, **323**, 195–204.

Quinones, R.A., Platt, T. and Rodriguez, J. (2003) Patterns of biomass-size spectra from oligotrophic waters of the northwest Atlantic. *Prog. Oceanogr.*, **57**, 405–427.

Reid, P.C., Johns, D.G., Edwards, M., Starr, M., Poulins, M. and Snoeijs, P. (2007) A biological consequence of reducing Arctic ice cover: arrival of the Pacific diatom *Neodenticula seminae* in the north Atlantic for the first time in 800000 years. *Global Change Biol.*, **13**, 1910–1921.

Renz, J. and Hirche, H.-J. (2006) Life cycle of *Pseudocalanus acuspes* Giesbrecht (Copepoda, Calanoida) in the Central Baltic Sea: I. Seasonal and spatial distribution. *Mar. Biol.*, **148**, 567–580.

Renz, J., Peters, J. and Hirche, H.-J. (2007) Life cycle of *Pseudocalanus acuspes* Giesbrecht (Copepoda, Calanoida) in the Central Baltic Sea: II. Reproduction, growth and secondary production. *Mar. Biol.*, **151**, 515–527.

Reynolds, R.W., Rayner, N.A., Smith, T.M., Stokes, D.C. and Wang, W. (2002) An improved in situ and satellite SST analysis for climate. *J. Climate*, **15**, 1609–1625.

Richter, C. (1995) Seasonal changes in the vertical distribution of mesozooplankton in the Greenland Sea Gyre (75°N): distribution strategies of calanoid copepods. *ICES J. Mar. Sci.*, **52**, 533–539.

Rodriguez, J. and Mullin, M.M. (1986) Relation between biomass and body weight of plankton in a steady state oceanic ecosystem. *Limnol. Oceanogr.*, **31**, 361–370.

Sambrotto, R.N., Goering, J.J. and McRoy, C.P. (1984) Large yearly production of phytoplankton in the western Bering Strait. *Science*, **225**, 1147–1150.

Sampei, M., Sasaki, H., Forest, A. and Fortier, L. (2012) A substantial export flux of particulate organic carbon linked to sinking dead copepods during winter 2007–2008 in the Amundsen Gulf (southeastern Beaufort Sea, Arctic Ocean). *Limnol. Oceanogr.*, **57**, 90–96.

Sampei, M., Sasaki, H., Hattori, H., Forest, A. and Fortier, L. (2009) Significant contribution of passively sinking copepods to the downward export flux in Arctic waters. *Limnol. Oceanogr.*, **54**, 1894–1900.

Sergeeva, V.M., Sukhanova, I.N., Flint, M.V., Pautova, L.A., Grebmeier, J.M. and Cooper, L.W. (2010) Phytoplankton community in the western Arctic in July–August 2003. *Oceanology*, **50**, 184–197.

Shannon, C.E. and Weaver, W. (1949) *The Mathematical Theory of Communication.* The University of Illinois Press, Urbana.

Sheldon, R.W., Prakash, A. and Sutcliffe, W.H.Jr. (1972) The size distribution of particles in the ocean. *Limnol. Oceanogr.*, **17**, 327–340.

Shimada, K., Carmack, E.C., Hatakeyama, K. and Takizawa, T. (2001) Varieties of shallow temperature maximum waters in the western Canadian Basin of the Arctic. *Geophys. Res. Lett.*, **28**, 3441–3444.

Shimada, K., Kamoshida, T., Itoh, M., Nishino, S., Carmack, E., McLaughlin, F., Zimmermann, S. and Proshutinsky, A. (2006) Pacific Ocean inflow: Influence on catastrophic reduction of sea ice cover in the Arctic Ocean. *Geophys. Res. Lett.*, **33**, L08605. doi: 10.1029/2005GL0256254.

Shoden, S., Ikeda, T. and Yamaguchi, A. (2005) Vertical distribution, population structure and life cycle of *Eucalanus bungii* (Copepoda: Calanoida) in the Oyashio region, with notes on its regional variations. *Mar. Biol.*, **146**, 497–511.

Splures, W.G. and Munawar, M. (1986) Plankton size spectra in relation to ecosystem productivity, size, and perturbation. *Can. J. Fish. Aquat. Sci.*, **43**, 1789–1794.

Springer, A.M. and McRoy, C.P. (1993) The paradox of pelagic food webs in the northern Bering Sea–III. Patterns of primary production. *Cont. Shelf Res.*, **13**, 575–599.

Springer, A.M., McRoy, C.P. and Turco, K.R. (1989) The paradox of pelagic food web in the northern Bering Sea–II. Zooplankton communities. *Cont. Shelf Res.*, **9**, 359–386.

Stroeve, J., Holland, M.M., Meier, W., Scambos, T. and Serreze, M. (2007) Arctic sea ice decline: Faster than forecast. *Geophys. Res. Lett.*, **34**, L09501. doi: 10.1029/2007GL029703.

Sukhanova, I.N., Flint, M.V., Pautova, L.A., Stockwell, D.A., Grebmeier, J.M. and Sergeeva, V.M. (2009) Phytoplankton of the western Arctic in the spring and summer of 2002: Structure and seasonal changes. *Deep-Sea Res. II*, **56**, 1223–1236.

Sullivan, B.K., Garcia, J.R. and Klein-MacPhee, G. (1994) Prey selection by the scyphomedusan predator *Aurelia aurita*. *Mar. Biol.*, **121**, 335–341.

Suthers, I.M., Taggart, C.T., Rissik, D. and Baird, M.E. (2006) Day and night ichthyoplankton assemblages and zooplankton biomass size spectrum in a deep ocean island wake. *Mar. Ecol. Prog. Ser.*, **322**, 225–238.

Svensen, C. and Nejstgaard, J.C. (2003) Is sedimentation of copepod faecal pellets determined by cyclopoids? Evidence from enclosed ecosystems. *J. Plankton Res.*, **25**, 917–926.

Tande, K.S. and Grønvik, S. (1983) Ecological investigations on the zooplankton community of Balsfjorden, northern Norway: sex ratio and gonad maturation cycle in the copepod *Metridia longa* (Lubbock). *J. Exp. Mar. Biol. Ecol.*, **71**, 43–54.

Taniguchi, A. (1997) Suborder Tintinnina. pp. 421–483, Chihara, M. and Murano, M. (eds), *An Illustrated Guide to Marine Plankton in Japan*, Tokai University Press, Tokyo.

Thibault, D., Head, E.J.H. and Wheeler, P.A. (1999) Mesozooplankton in the Arctic Ocean in summer. *Deep-Sea Res. I*, **46**, 1391–1415.

Throndsen, J. (1997) The Planktonic Marine Flagellates. pp. 591–729, Tomas, C.R. (ed), *Identifying Marine Phytoplankton*, Academic Press, San Diego.

Toriumi, S. (1997) Class Chrysophyceae. pp. 147–156, Chihara, M. and Murano, M. (eds), *An Illustrated Guide to Marine Plankton in Japan*, Tokai University Press, Tokyo.

Tsuda, A., Saito, H. and Kasai, H. (2004) Life histories of *Eucalanus bungii* and *Neocalanus cristatus* (Copepoda: Calanoida) in the western subarctic Pacific Ocean. *Fish. Oceanogr.*, **13** (supplement), 10–20.

Vanin, N.S. (2010) Thermohaline water structure on the southwestern Chukchi Sea shelf under conditions of opposite regimes of atmospheric circulation in summer periods of 2003 and 2007. *Russ. Meteorol. Hydrol.*, **35**, 468–475.

Vaquer-Sunyer, R., Duarte, C.M., Santiago, R., Wassmann, P. and Reigstad, M. (2010) Experimental evaluation of plankton respiration response to warming in the European Arctic Sector. *Polar Biol.*, **33**, 1661–1671.

Vinogradov, M.E. (1997) Some problems of vertical distribution of meso-macroplankton in the ocean. *Adv. Mar. Biol.*, **32**, 1–92.

Vinogradov, M.E., Volkov, A.F. and Semenova, T.N. (1996) *Hyperiid amphipods (Amphipoda, Hyperiidea) of the world oceans*. Science publishers, Inc., Labanon.

von Oertzen, J.-A. (1972) Cycle and rates of reproduction of six Baltic Sea bivalves of different zoogeographical origin. *Mar. Biol.*, **14**, 143–149.

Wassmann, P., Reigstad, M., Haug, T., Rudels, B., Carroll, M.L., Hop, H., Gabrielsen, G.W., Falk-Petersen, S., Denisenko, S.G., Arashkevich, E., Slagstad, D. and Pavlova, O. (2006) Food webs and carbon flux in the Barents Sea. *Prog. Oceanogr.*, **71**, 232–287.

Woodgate, R.A., Weingartner, T. and Lindsay, R. (2010) The 2007 Bering Strait oceanic heat flux and anomalous Arctic sea-ice retreat. *Geophys. Res. Lett.*, **37**, L01602. doi: 10.1029/2009GL041621.

Yamaguchi, A. (2009) Characteristics of the zooplankton community in the Okhotsk Sea in autumn: A comparison with the Oyashio region. pp. 240–242, Kashiwai, M. and Kantakov, G.A. (eds), *Proceedings of the Fourth Workshop on the Okhotsk Sea and Adjacent Areas*, *PICES Scientific Report No. 36*, North Pacific Marine Science Organization (PICES), Sidney.

Yamaguchi, A. and Ikeda, T. (2000) Vertical distribution, life cycle, and body allometry of two oceanic calanoid copepods (*Pleuromamma scutullata* and *Heterorhabdus tanneri*) in the Oyashio region, western North Pacific Ocean. *J. Plankton Res.*, **22**, 29–46.

Yokoi, Y., Yamaguchi, A. and Ikeda, T. (2008) Regional and inter-annual changes in the abundance, biomass and community structure of mesozooplankton in the western North Pacific in early summer; as analyzed with an optical plankton counter. *Bull. Plankton Soc. Japan*, **55**, 79–88.